

Di(benzothiazol-2-yl)phosphane

– Studies on a *Janus Head* Ligand –

Dissertation zur Erlangung des
naturwissenschaftlichen Doktorgrades
der Bayerischen Julius-Maximilians-Universität Würzburg

vorgelegt von
Thomas Josef Stey
aus Fulda

Würzburg 2004

Eingereicht am:
bei der Fakultät für Chemie und Pharmazie

1. Gutachter:
2. Gutachter:

1. Prüfer:
2. Prüfer:
3. Prüfer:
des Öffentlichen Promotionskolloquiums

Tag des öffentlichen Promotionskolloquiums:

Doktorurkunde ausgehändigt am:

Nehmt Neuland unter den Pflug!

Hosea

Danksagung

Die vorliegende Arbeit wurde in der Zeit von März 2001 bis Dezember 2004 im Arbeitskreis von Prof. Dr. D. Stalke am Institut für Anorganische Chemie der Universität Würzburg angefertigt. Hier soll all jenen Dank ausgesprochen werden, die zum Gelingen dieser Arbeit beigetragen haben.

An erster Stelle gilt mein Dank Herrn Professor Dr. D. Stalke für die Möglichkeit, die vorliegende Arbeit anzufertigen. Für die gewährten wissenschaftlichen Freiheiten, das hervorragende Arbeitsklima und seine stete Diskussionsbereitschaft bin ich sehr dankbar.

Ich danke Herrn Dr. Dirk Leusser für seine engelsgleiche Geduld, wenn es darum ging, mir die Geheimnisse der Kristallographie näher zu bringen, und für seine väterlichen Ratschläge in allen Bereichen des menschlichen Miteinanders. Viel Spaß mit den restlichen 40%!!!

Herrn Dr. Matthias Pfeiffer danke ich für die hervorragende Einführung in das Gebiet der Phosphorchemie und dafür, dass er mir noch etwas zum Forschen übrig gelassen hat.

Herrn Dr. Bernhard Walfort danke ich für viele gute Ratschläge und seine praktische Hilfe.

Frau Dr. Carola Selinka danke ich für die hervorragende Zusammenarbeit, ihre mütterliche Fürsorge im Arbeitskreis und die besten Schokomuffins der Welt.

Herrn Dr. Nikolaus Kocher danke ich für die hervorragende Zusammenarbeit und seine bemerkenswerten Beiträge zu den Themen *Studierende*, *Frauen* und *das beklagenswerte Dasein eines Menschen als Lehrkraft*.

Herrn Dr. Alexander Murso danke ich für das Teilen des Schicksals eines Phosphorchemikers.

Herrn Dipl. Chemiker St. Deuerlein (Stephan) danke ich für seine stets gute Laune, die sehr fruchtbaren Diskussionen, diverse Abendveranstaltungen und das Lösen meiner Computerprobleme (Es waren bei weitem mehr als genug!).

Frau Ulrike Flierler danke ich dafür, dass sie sich nicht von uns hat abschrecken lassen. Ich danke ihr für die geleisteten Hilfestellungen, ihren hervorragenden Humor und ihr stets offenes Ohr.

Herrn Dipl. Chem. Gerald Schwab sei dafür gedankt, dass er es mit mir in einem Labor ausgehalten hat und den Laboralltag durch das Mitbringen diverser CDs wahrlich bereicherte.

Ulli, Stephan und Gerald danke ich für das Korrekturlesen dieser Arbeit. Ohne Euch wären einige ‚mayor mistakes‘ übrig geblieben. Besonders bedanke ich mich bei Ulli und Stephan für ihren unermüdlichen Einsatz gegen Ende des Zusammenschreibens.

Frau Veronika Duchnik danke ich für ihr sonniges Gemüt, unzählige Überstunden, die sie im Labor verbrachte und nicht zuletzt für die Erfahrung des „Beubelns“ (oder so). Natürlich darf hier auch die Entwicklung der ‚*Duchnik-Stey-Phosphanapparille*‘ nicht unerwähnt bleiben.

Herrn Dr. Julian Henn bin ich für viele Kaffeepausen und seine Bemühungen um die theoretische Chemie zu Dank verpflichtet.

Allen, die bei der Entstehung des LiBooks mitgewirkt haben sei gesagt, dass mich der gezeigte Einsatz enorm beeindruckt hat.

Herrn Berthold Fertig danke ich dafür, dass er aus Scherben immer wieder brauchbare Glasware schuf. Besonders bedanken möchte ich mich für die Hilfe bei der Entwicklung von Spezialanfertigungen und die Herstellung derselben in erstaunlich kurzer Zeit.

Herrn Alfred Schertzer danke ich für seine Unterstützung des Laborgeschäfts, besonders danke ich für die Ausweitungen seiner „Sprechzeiten“.

Frau Schäfer danke ich für das Kurbeln von NMR-Spektren, Frau Schedl für die Durchführung von Thermodifferenzialmessungen und CHN-Analysen, Herrn Kneis für CHN-Analysen, Herrn Ruf für diverse Schlosserarbeiten, Herrn Reinhardt für seine Mechanikertätigkeiten und Herrn Obert für Elektroarbeiten.

Besonders danke ich Herrn Kai Ofenstein für seine treue Freundschaft und Hilfe, wenn es darum geht, mein Leben zu bewältigen.

Der SMJ danke ich, dass sie versucht hat, eine ordentlichen Menschen aus mir zu machen.

Den Jungs und Mädels vom TLV Eichenzell danke ich für viele tausend Kalorien, die ich nun doch nicht mit mir rumtragen muss und geniale Stunden rund um den Handball.

Frau Silvia Schwarz danke ich für das gemeinsame Kaba-Trinken und alles was darauf folgte.

Mein ganz besonderer Dank gilt meinen Eltern und Geschwistern, die mich von Kindesbeinen an unterstützt haben, wo sie nur konnten.

1	INTRODUCTION.....	1
2	DI(BENZOTHAZOL-2-YL)PHOSPHANE (1).....	7
	2.1 Preparation of Di(benzothiazol-2-yl)phosphane	7
	2.2 Structure of Di(benzothiazol-2-yl)phosphane (1).....	9
	2.3 Properties and Reactivity of Di(benzothiazol-2-yl)phosphane (1).....	13
3	DI(BENZOTHAZOL-2-YL)PHOSPHANIDES.....	19
	3.1 Synthesis and Structure of $[(Et_2O)_2Li(bth)_2P]$ (2).....	19
	3.2 Synthesis and Structure of $[Me_2Al(bth)_2P]$ (3)	23
	3.3 Synthesis and Structure of $[(Me_3Si)_2NZn(bth)_2P]_2 \cdot 2(THF)$ (4)	27
	3.4 Synthesis and Structure of $[(Me_3Si)_2NCd(bth)_2P]_2 \cdot (THF)$ (5)	33
	3.5 Synthesis and Structure of $[(Me_3Si)_2NSn(bth)_2P] \cdot 0.49(Et_2O)$ (6).....	38
	3.6 Synthesis and Structure of $[Fe\{(bth)_2P\}_2] \cdot 0.5(Tol)$ (7).....	43
	3.7 Synthesis and Structure of $[Cs(bth)_2P]_\infty$ (8).....	46
	3.8 Synthesis and Structure of $[Li(bth)_2P\{Mn(CO)_2Cp\}_2]_\infty \cdot 2.5(Tol)$ (9).....	51
	3.9 Syntheses and Structure of $[(OC)_4W(bth)_2P(H)W(CO)_5] \cdot C_6D_6$ (10).....	57
	3.10 Comparison of Compounds 1 to 10	63
	3.11 Prospects	66
4	THE (BENZOTHAZOL-2-YL)PHENYLPHOSPHANIDE SYSTEM	67
	4.1 Crystal Structure and Reaction of $(bth)PPh_2$ (11) with Elemental Lithium	67
	4.2 Synthesis and Structure of $[(THF)_3Li(bth)PPh]$ (12).....	69
	4.3 Prospects	71
5	COUPLING OF DI(BENZOTHAZOL-2-YL)METHANE.....	73

6	CONCLUSION AND PROSPECTS	77
6.1	Conclusion.....	77
6.2	Prospects	81
7	ZUSAMMENFASSUNG UND AUSBLICK	82
7.1	Zusammenfassung.....	82
7.2	Ausblick.....	86
8	EXPERIMENTAL SECTION.....	87
8.1	General.....	87
8.2	Syntheses and Characterisation of Compounds 1 to 14.....	88
9	CRYSTALLOGRAPHIC SECTION.....	97
9.1	Crystal application	97
9.2	Data collection	97
9.3	Absorption correction	97
9.4	Structure solution and refinement.....	98
9.5	Crystallographic Data for Compounds 1 to 14.....	99
10	LITERATURE	120

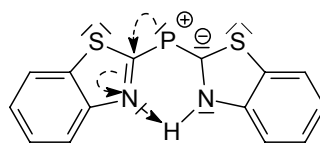
Abbreviations

approx.	approximately
av.	averaged
bth	benzothiazol-2-yl
Bu	butyl
<i>c</i>	cyclo
calc.	calculated
Cp	cyclopentadienyl
CSD	Cambridge Structural Database
C ₆ D ₆	deutero benzene
d	day(s)/doublet
decomp.	decomposition
e.g.	exempla gratia; for example
Et ₂ O	diethylether
h	hour(s)
IR	infrared
L	liter
m	multiplatt
m.p.	melting point
[M]	metal fragment

m.p.	melting point
MAO	methylaluminoxane
<i>n</i>	neo
NMR	nuclear magnetic resonance
p.d.	per definitionem
Ph	phenyl
py	2-pyridyl
r.t.	room temperature
s	singulett
sof	site occupation factor
t	triplet
<i>t</i>	tertiary
THF	tetrahydrofuran
Tol	toluene
vs	versus

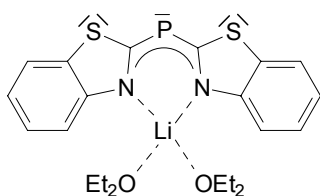
Compounds

Stellberg



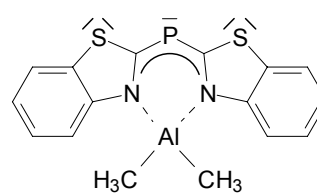
(bth)(bthH)P (1)

Bubenbader Steine



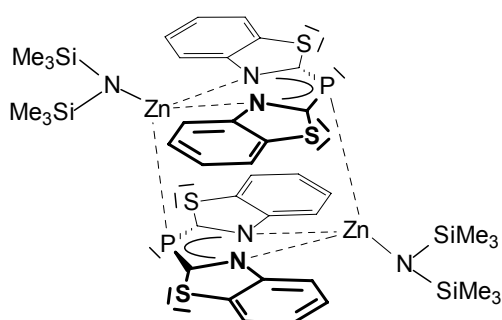
[(Et₂O)₂Li(bth)₂P] (2)

Soffi



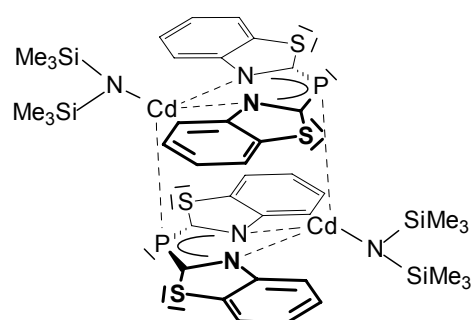
[Me₂Al(bth)₂P] (3)

Teufelstein



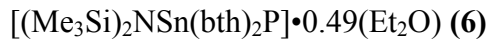
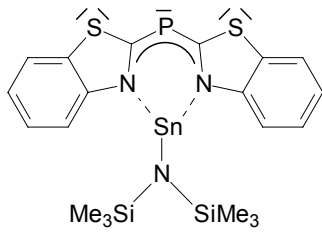
[(Me₃Si)₂NZn(bth)₂P]₂•2(THF) (4)

Maulkuppe

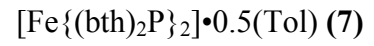
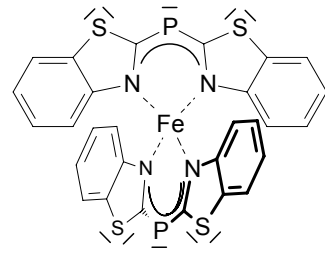


[(Me₃Si)₂NCd(bth)₂P]₂•(THF) (5)

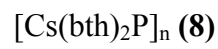
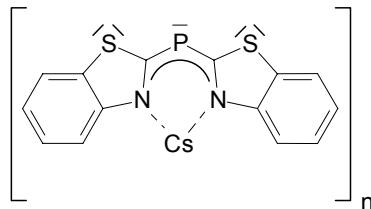
Kleinsassen



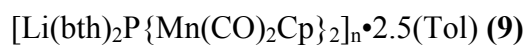
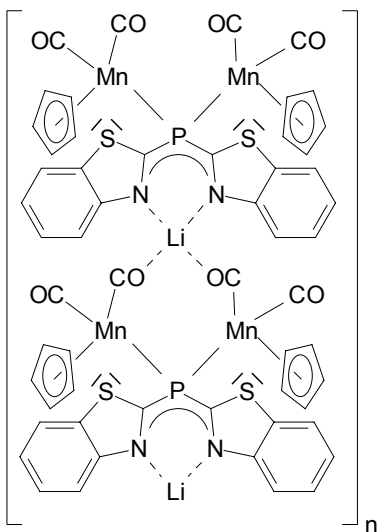
Steinwand



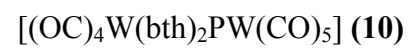
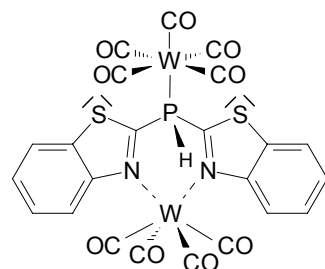
Schackau



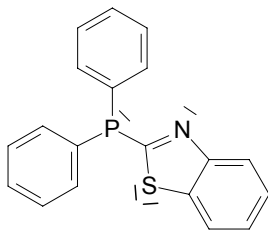
Schafstein



Heidelstein

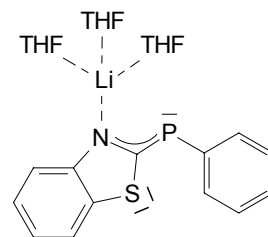


Pferdskopf



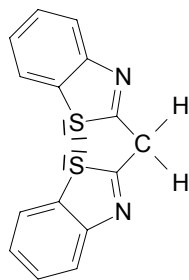
$\text{Ph}_2\text{P}(\text{bth})$ (11)

Milseburg



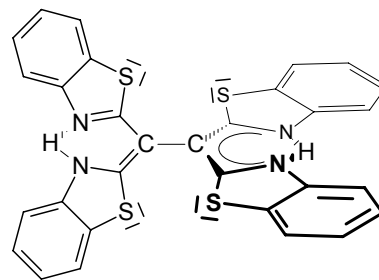
$[(\text{THF})_3\text{Li}(\text{bth})\text{PPh}]$ (12)

Wasserkuppe



$(\text{bth})_2\text{CH}_2$ (13)

Ziegenstein



$[\{(\text{bth})(\text{bthH})\text{C}\}_2\{\text{LiCl}\cdot(\text{THF})_2\}_2]$ (14)

1 Introduction

The design of ligands is one of the most important and simultaneously challenging fields of research in modern inorganic chemistry. The aim is to synthesise ligands that can serve as coordination units for a broad variety of metal fragments and different purposes. The ligands have to be very flexible concerning their donating behaviour and geometrical prerequisites in order to correspond to the required metal fragments.

Basic or non-functionalised ligands like water, ammonia, or phosphanes have only one *Lewis*-basic donor centre. The electron density at the central atoms, often residing in lone pairs, is donated to unoccupied orbitals of the coordinated metal.

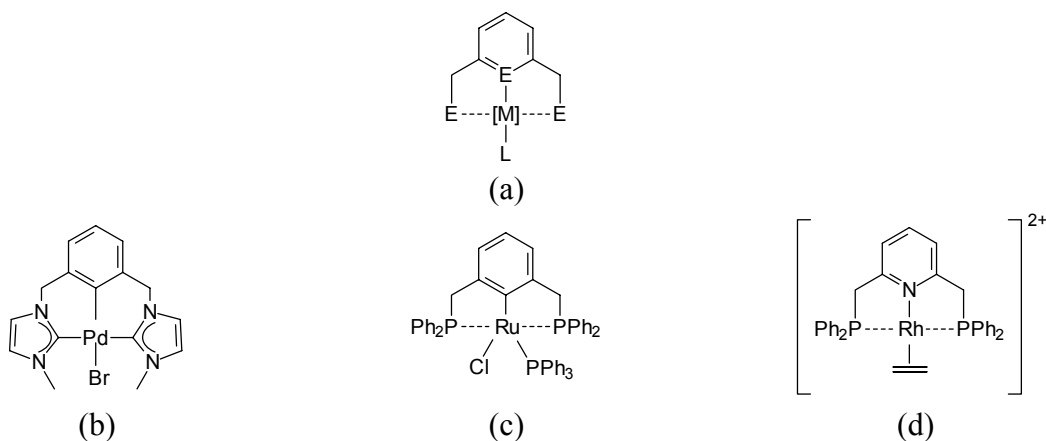
More sophisticated chelating ligands with at least two donor sites in general yield more stable complexes, mainly due to entropic effects. This is referred to as the chelate effect.^[1]

Classical chelate ligands consist of donor centres that are connected via a bridge. The spacer between the coordinating atoms determines the size of the ring that is made up of the metal centre, the first donor atom, the spacer, and the second donor atom. By changing the number of atoms within the bridge, not only ring strain can be tuned but also the bite distance can be varied to fit different metals. In another class of chelate ligands the additional periphery has two main functions: a) to provide steric bulk, increasing the solubility and inhibiting oligomerisation and b) to carry stereochemical information providing stereoselectivity in reactions. Hence, there are numerous parameters to tailor ligands for a certain reaction regarding solubility, size of the metal to be coordinated and stereochemical determination of the catalytical pathway of reactions.

The topic of pincer ligands^[2] attracted more and more attention during the last decades.^[3] Pincer ligands are usually formed by a central anionic phenyl or pyridyl ring (XCX-type and XNX-type) that is heteroatom substituted in 2- and 6-position. As the name already suggests, they pick metal fragments like a pincer. Later the standard motif was modified and pincer ligands e.g. of the following types were synthesised: CCC,^[4] NCN,^[5] OCO,^[6] PCP,^[7] SCS,^[8] CNC,^[9] NNN,^[10] PNP,^[11] SNS,^[12] PPP,^[13] SPS,^[14] and mixed substituted derivatives (*Scheme 1.1*).^[15]

These ligands proved to be versatile tools for many reactions such as alkane dehydrogenation,^[16] cyclometallation,^[17] cross-coupling,^[18] and organic transformation.^[19]

Moreover, complexes containing pincer ligands are employed for a broad variety of applications (e.g. catalyst recovery,^[20] and antimicrobial agent^[21]) and promising results were obtained for their light emitting properties. Probably pincer ligand based LEDs and other electrophosphorescent devices can be designed.^[8a,c; 22]

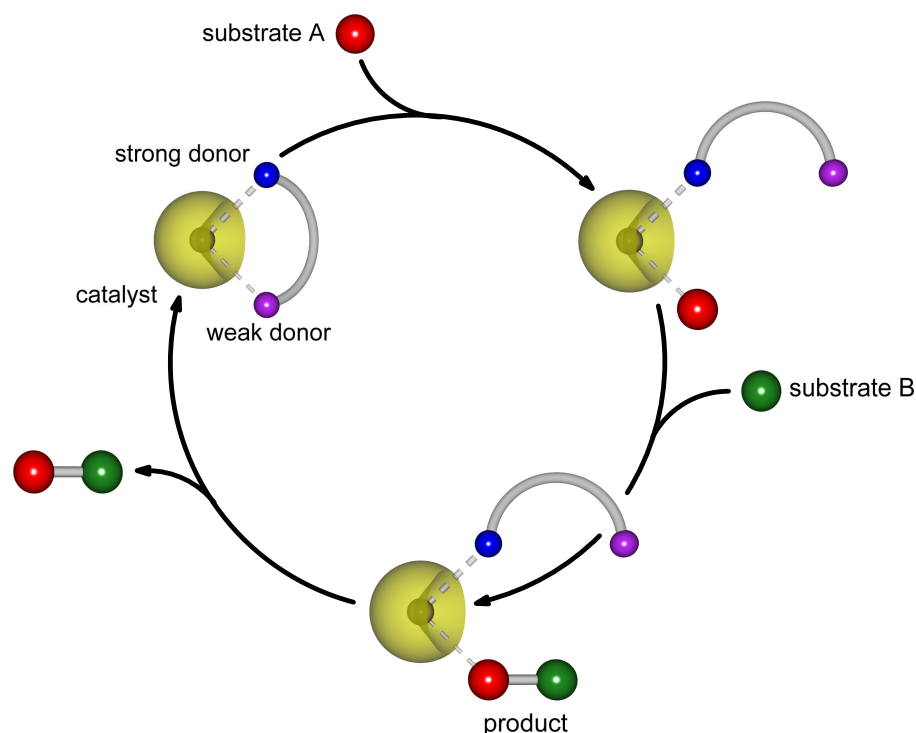


Scheme 1.1: Pincer ligands; (a) general design; (b) CCC pincer ligand complex;^[4] (c) PCP pincer ligand complex;^[3] (d) PNP pincer ligand complex^[13]

Coordinative bonds formed in the abovementioned systems are quite stable so that such a bond, once formed, is kept for the lifetime of the complex.

It seems feasible to unify different coordination sites in one coordinating molecule. Those ligands do not only bear coordination sites for either hard or soft metal centres – in terms of the HSAB concept by *Pearson*^[23] – but for both. Due to the fact that there is only one type of metal fragment offered, one donor centre suits the metal better than the other. This results in qualitatively different coordinative bonds between the different donor sites and the metal fragment.

The resulting hemilabile ligands offer at least two donor centres, one of which is quite strongly bonded to the active metal while the other only temporarily occupies a metal coordination site.^[24] Hemilabile or hybrid ligands proved their utility in oxidative addition and reductive elimination reactions as well as in many catalytic reactions in organometallic chemistry.^[25] Within a catalytic cycle their coordination behaviour is of fundamental importance: The highly reactive, coordinatively unsaturated metal centre forms two bonds to the ligand until the substrate of the reaction replaces the labile part of the ligand. Then the product is formed. The coordination gap at the metal centre is occupied by the substrate until the product leaves the complex and the cycle starts again (**Scheme 1.2**).



Scheme 1.2: Hemilabile ligands in catalysis

This reversible coordination behaviour may prolong the lifetime of the catalyst^[26] and have an influence on the product formation due to interactions such as H-bridging.^[27]

In many cases in catalysis, the alleged catalyst is indeed a catalyst precursor that has to be turned into the active catalyst by a co-catalyst, e.g. in olefin polymerisation reactions. A mixture of di(cyclopentadienyl)dimethyl zirconium and trimethyl aluminium for example turns from a poor to a very active catalytic system for ethylene polymerisation if the trimethyl aluminium is partially hydrolysed to yield the well established methylaluminumoxane (MAO).^[28] The development of catalytic systems being highly active even at room temperature and low pressure paved the way for the very profitable large-scale production of olefin-based polymers. Therefore, it is not astonishing that structure and function of MAO in catalytic reactions have been studied very intensively.^[29]

In nucleophile-electrophile reactions one can discriminate simple *Lewis* acid catalysts from cooperative intermolecular homobimetallic catalysts, cooperative intermolecular heterobimetallic catalysts, and cooperative intramolecular heterobimetallic catalysts.

The first class of the named catalysts is traditionally used to activate the electrophilic reactant for asymmetric additions^[30] while cooperative intermolecular homobimetallic catalysts promote addition reactions by the simultaneous activation of the electrophile and the

nucleophile by the same ligand system. The complexes for cooperative intermolecular heterobimetallic catalysis are designed in a way, that one metal fragment activates the electrophile while the other one facilitates the reaction of the nucleophile. Finally, cooperative intramolecular heterobimetallic catalysts are to unite the features of the former types in just one complex.

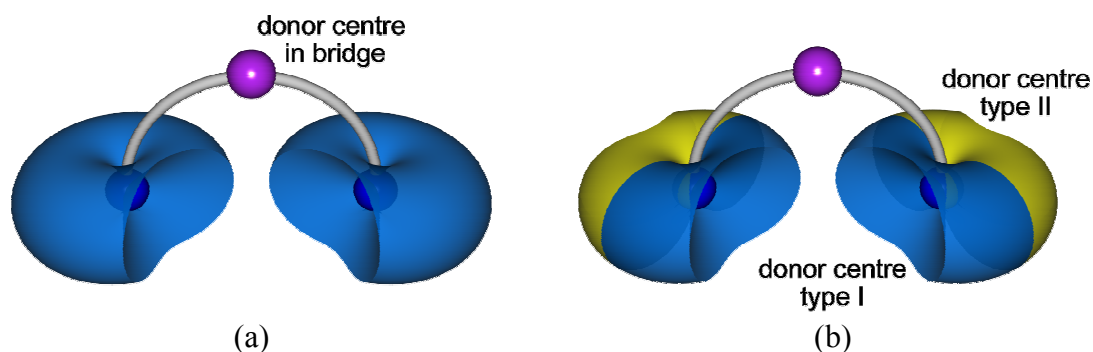
Besides olefin polymerisation and nucleophile-electrophile reactions, various reactions with the active catalyst containing at least two metal centres are known. Examples are CO insertion reactions catalysed by rhodium-iron clusters,^[31] asymmetric Michael reactions,^[32] and the activation of carbon-halide bonds.^[33] There are biological systems, too, in which the catalytic unit of the active centre is made up of at least two metal atoms. Examples for this are carbon monoxide dehydrogenase/Acetyl-CoA synthetases,^[34] purple acid phosphatases,^[35] and superoxide dismutases.^[36]

The abovementioned examples prove that the design of ligands for catalysis which bring the catalytically active atom and the activator or co-catalyst in close proximity is an advantageous aim.

To get heterobimetallic complexes it is useful to incorporate additional, qualitatively different coordination centres into the periphery of phosphane ligands. This leads to the so-called *Janus head* ligands (**Scheme 1.3a**). The name is derived from *Janus*, the Roman god of doors and all beginnings. Roman statues often present him with two faces looking in diametrically opposite directions.^[37] An advantage of these ligands is the combination of soft and hard coordination sites in the same molecule. For example di(pyrid-2-yl)phosphane is able to coordinate metals as different in size and hardness as aluminium and caesium. Depending on the metal fragment offered, the ligand acts as an N,N-chelating ligand, as a P,N-chelating ligand, or as P-coordinating ligand exclusively.^[38] It was shown that these systems can be modified to get even more flexible ligands by insertion of a methylene unit into the bridge which leads to 2-picolylyl substituted phosphanes.^[39] After deprotonation, these ligands contain a carbanionic centre which is able to donate electron density to metal fragments.

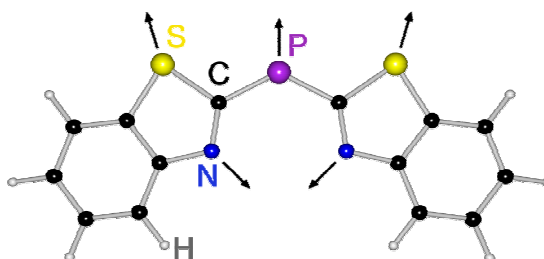
Another way to alter and augment the coordination behaviour of this class of ligands is to change the heteroaromatic substituents at the ligand periphery in order to improve the coordinative flexibility and to get to advanced *Janus head* ligands (**Scheme 1.3b**).

The latter do not just carry the hard centres in the aromatic ring systems and the soft centre in the bridge but additional soft centres in the aromatic ligand periphery, supplying electron density to coordinate a soft metal fragment while a hard metal fragment is already bonded.



Scheme 1.3: (a) Janus head ligands; (b) advanced Janus head ligand

The scope of this work was to synthesise an advanced *Janus head* ligand system and to investigate its reactivity as well as its coordination ability. Di(benzothiazol-2-yl)-phosphane was chosen as a model system. Benzothiazol is a heteroaromatic system derived from thiazol. In thiazol additionally to a sulfur atom a pyridine-like nitrogen atom is present. Thiazol is an electron-rich heteroaromat, with the π -electron excess mainly located at the nitrogen atom. Equipped with this heteroaromatic substituents a secondary phosphanide should prove a rich coordination site selectivity to various metal fragments (**Scheme 1.4**).



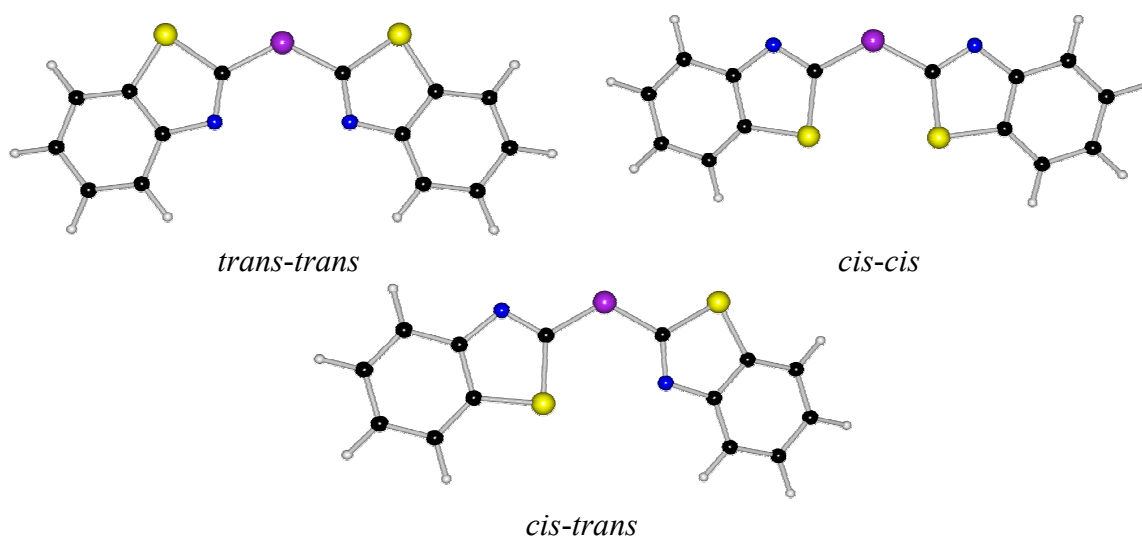
Scheme 1.4: Potential donating sites in di(benzothiazol-2-yl)phosphanide

In the coordination, the heteroaromatic rings should be able to rotate about the P–C bonds. This adjusts the distance between the donor centres and facilitates metals different in size to be coordinated. In principal the substituents can adopt different conformations by rotating the heteroaromatic rings about the P–C bonds (**Scheme 1.5**).

They can e.g. be *trans-trans* arranged with both nitrogen atoms in close proximity. This is a conformation in which the ligand should be able to function as an NPN pincer ligand.

In a hypothetical *cis-cis* arrangement the ligand could act as an SPS pincer ligand. Employing the phosphorus centre in metal coordination might lead to heterobimetallic compounds in both cases.

In the *cis-trans* arrangement, a behaviour resembling a hemilabile ligand is possible. One of the active donor centres would represent the strong donor, while the other active donor centre would act as the weak donor.



Scheme 1.5: Different conformations of the di(benzothiazol-2-yl)phosphanide unit

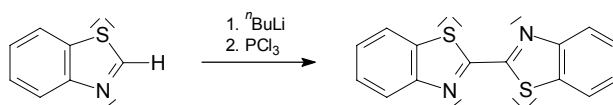
Additionally, haptotropic donation can be envisaged. This coordination mode could lead to an open hetero pentadienide analogue. As there are phenyl and thiazol fragments present, both types of aromatic subunits could act as parts of sandwich complexes in organometallic compounds. Hence, a very broad variety of coordination geometries and modes can be expected if using di(benzothiazol-2-yl)phosphane or di(benzothiazol-2-yl)phosphanide as ligand for metal fragments.

2 Di(benzothiazol-2-yl)phosphane (1)

2.1 Preparation of Di(benzothiazol-2-yl)phosphane

Only a few benzothiazol-2-yl substituted phosphanes have been characterised structurally, for example 1,2-bis(di(benzothiazol-2-yl)phosphanyl)ethane,^[40] 1,1-bis(di(benzothiazol-2-yl)phosphanyl)methane,^[41] and tri(benzothiazol-2-yl)phosphane.^[42]

The already mentioned di(pyrid-2-yl)phosphane is synthesised by reacting pyrid-2-yl lithium with phosphorus trichloride which leads to the formation of the parent tertiary phosphane. This compound is treated with elemental lithium yielding the secondary phosphane and 2,2'-bipyridine as a by-product after hydrolysis.^[43] The traditional way to prepare heteroaromatic substituted phosphanes is resumed.^[44] In the case of the tri(benzothiazol-2-yl)phosphane the reaction of the lithiated benzothiazol-2-ide with phosphorus trichloride gives mainly the coupling product (**Scheme 2.1**).^[45]

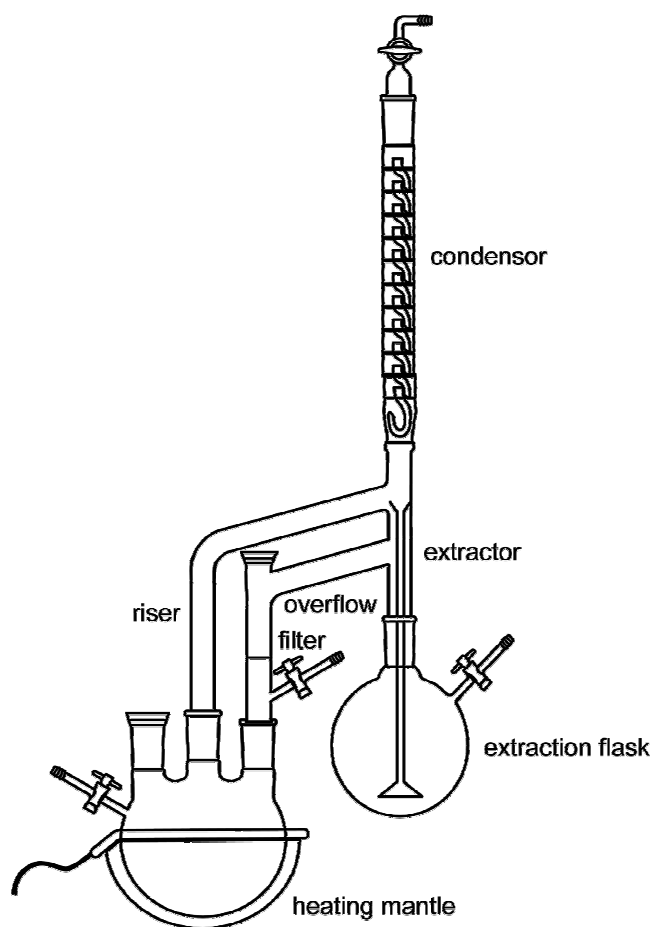


Scheme 2.1: Formation of the coupling product

The preparation of di(benzothiazol-2-yl)phosphane starts with the lithiation of benzothiazol in diethylether at -78 °C. This is followed by reacting the solution with chlorotrimethylsilane at the same temperature. The generated benzothiazol-2-yl trimethylsilane can be purified by distillation.^[46] The C_{ipso}-Si bond is cleaved electrophilically, when treating the silane is treated with phosphorus trichloride yielding tri(benzothiazol-2-yl)phosphane.^[42]

The tertiary phosphane is dissolved in THF and elemental lithium is added at room temperature. After the removal of excessive metal and hydrolysis the secondary phosphane can be isolated.

Due to the very poor yields obtained in the beginning (about 10% based on the employed benzothiazol) the 'Duchnik-Stey-Phosphanapparille' - based on the idea of perforators - was developed (**Scheme 2.2**). The use of this apparatus resulted in by far improved yields of approx. 60% based on the employed benzothiazol.



Scheme 2.2: The 'Duchnik-Stey-Phosphanapparille'

The hydrolysis mixture is filled into the extraction flask with the extractor in the centre. Diethylether is heated to reflux in the left flask and gaseous diethylether passes the riser and condenses at the cooling unit. From there the diethylether drops into the extractor, which has a porous basis to force the solvent to get in contact with the mixture in the extraction flask. The diethylether containing the phosphane rises in the extraction flask up to the overflow and runs back into the left flask after being dried over magnesium sulfate. The phosphane stays in the left flask while the diethylether starts off the cycle again.

Already during the extraction crystals of the phosphane in form of yellow needles start to grow in the left flask.

2.2 Structure of Di(benzothiazol-2-yl)phosphane (1)

Di(benzothiazol-2-yl)phosphane (**1**) crystallises in the orthorhombic space group *Pbca* with the whole molecule in the asymmetric unit. The solid state structure of **1** (*Figure 2-1*) was determined by a single crystal X-ray diffraction experiment.

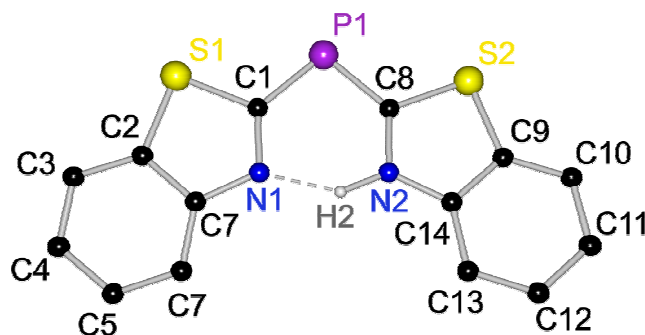


Figure 2-1: Solid state structure of di(benzothiazol-2-yl)phosphane (1)

The phosphorus atom in this secondary phosphane is divalent as a hydrogen atom is located at a ring nitrogen atom. The position of the hydrogen atom was taken from the difference Fourier map and refined freely. A standard N–H bond distance determined by X-ray diffraction experiments is anticipated to be about 89 pm.^[47] This value is valid for room temperature data. Using low temperature (100 K) data sets leads to about two pm longer N–H bond distances. As the discussed X-ray diffraction experiment was carried out at low temperatures (100 K) the N–H bond distance of 85(5) pm has to be regarded remarkably short.

The hydrogen atom H2 is additionally linked to the second nitrogen atom via a hydrogen bond. The bond distance of 192(5) pm for the hydrogen bond N1...H2 is rather short.^[48] The atoms N1...H2–N2 include an angle of 140(4)°. The C8–N2–H2 angle is 119(3)° and the C14–N2–H2 angle is 124(3)°. The sum of the angles around the nitrogen atom N2 is 358°. These data are in accordance with an sp^2 hybridisation of N2. The sum of the angles around N1 is 360°. The C1–N1...H2 angle is 104(1)° and the C7–N1...H2 angle is 143(1)°. They differ significantly from the expected 120° for an sp^2 hybridised nitrogen atom.

Although, divalent phosphorus(III) compounds are known, for example in di(ketonato)phosphanes,^[49] the connectivity in **1** shows a difference between the classical *Janus head* ligands and this improved one. The discrepancy must be ascribed to a significant alteration of the electronic situation within the ligand. The electron density at the nitrogen

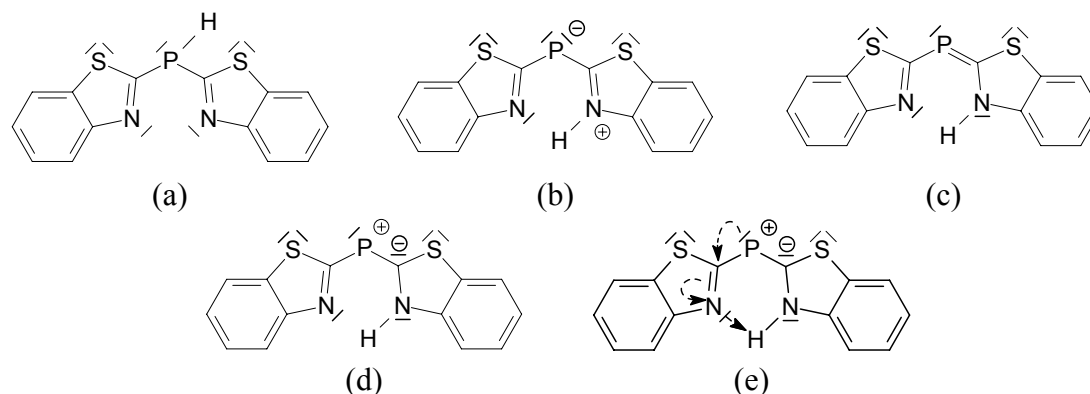
atom suits the hydrogen atom better than the one at the phosphorus atom. The bonding situation explains why a $^1J_{\text{P-H}}$ coupling, analogous to the spectra of the di(pyrid-2-yl) phosphane, could not be observed in the NMR spectra.^[43] The abovementioned asymmetry in the structure contrasts the symmetry observed for the other structural features in the molecule. The P–C bonds distances are equal within their estimated standard deviations as well as the C_{ipso} –N bond distances. Both bonds are half-way between a single and a double bond, regarding the bond distances (**Table 2-1**).^[50]

Table 2-1: Selected bond lengths [pm] and angles [°] of **1**

	bond length [pm]		bond angle [°]
P1–C1	178.4(5)	C1–P1–C8	98.7(2)
P1–C8	177.8(4)	N2–H2...N1	140(4)
N1...H2	192(5)	C8–N2–H2	119(3)
N2–H2	85(5)	C14–N2–H2	124(3)
C1–N1	133.1(6)	C1–N1...H2	104(1)
C8–N2	133.4(5)	C7–N1...H2	143(1)
N1...N2	262.3(5)		
			angle between planes [°]
		(bth)...(bth')	10.6

These structural parameters lead to difficulties in formulating an adequate *Lewis* diagram. **Scheme 2.3** displays various *Lewis* diagrams for **1**. The first approach starts from a *Lewis* diagram showing the connectivity anticipated for a secondary phosphane (a). Next the proton is transferred to the right ring nitrogen atom, leaving the phosphorus atom negatively and the protonated nitrogen atom positively charged (b). The electron density in the right hetero-aromatic ring is reduced by the protonation of the nitrogen atom. This depletion is partly compensated by electron density at the phosphorus centre coupling into the ring system. This interaction is visualised by the formulation of an ylenic phosphorus centre (c). In a formulation analogue to *Wittig* ylides this phosphorus carbon single bond is shortened by electrostatics (d). Electron density is shifted from the lone pair at the non-protonated nitrogen

atom to the hydrogen atom that is located at the other ring nitrogen atom. This causes an electron density loss in the left heteroaromatic ring. The electron density left at the phosphorus centre interacts with the non-protonated ring system and partly compensates the electron density loss which is due to the formation of the hydrogen bridge (e). Therefore, the P–C bond distances are equal within their estimated standard deviations. They are 178.4(5) pm for the P1–C1 bond and 177.8(4) pm for the P1–C8 bond. They are shorter than in the parent tri(benzothiazol-2-yl)phosphane (182.0(2) pm).^[51] This electronic situation is also responsible for the bond elongation of the C_{ipso} –N bonds. The bond distances are 133.1(6) pm for the C1–N1 bond and 133.4(5) pm for the C8–N2 bond. In tri(benzothiazol-2-yl)phosphane the C_{ipso} –N bond distance is 129.3(2) pm.



Scheme 2.3: Deduction of a Lewis diagram for **1**

The structure of this divalent secondary phosphane is another striking example for the lack of possibilities of *Lewis* diagrams to reflect the real geometrical, not to mention the electronic structure of a molecule.^[52]

Different to the parent tertiary phosphane, where the heteroaromatic rings are arranged with a nitrogen atom next to a sulfur atom,^[51] in **1** the benzothiazol-2-yl rings are *trans-trans* arranged. Therefore, the two hard donor centres get close to each other. The N1...N2 distance is 262.3(5) pm. The C1–P1–C8 angle is 98.7(2)°. It can be assumed that the phosphorus atom is either sp^3 hybridised with a deviation of 10.7° to the anticipated 109° or not hybridised with a deviation of 8.7° to the expected 90°.

The two best planes defined by the atoms of the ring systems in the ligand molecule include an angle of 10.6°. This leads to an almost planar molecule, with the phosphorus atom in plane. The C1–P1–C8 angle and the angle between the two benzothiazol-2-yl rings reflect the compromise between keeping the optimum angle at the central atom, holding up planarity as

known for fully conjugated aromatic systems, and keeping an appropriate hydrogen bond. The other bond distances in **1** can be compared to those of tri(benzothiazol-2-yl)phosphane^[51] showing no significant differences.

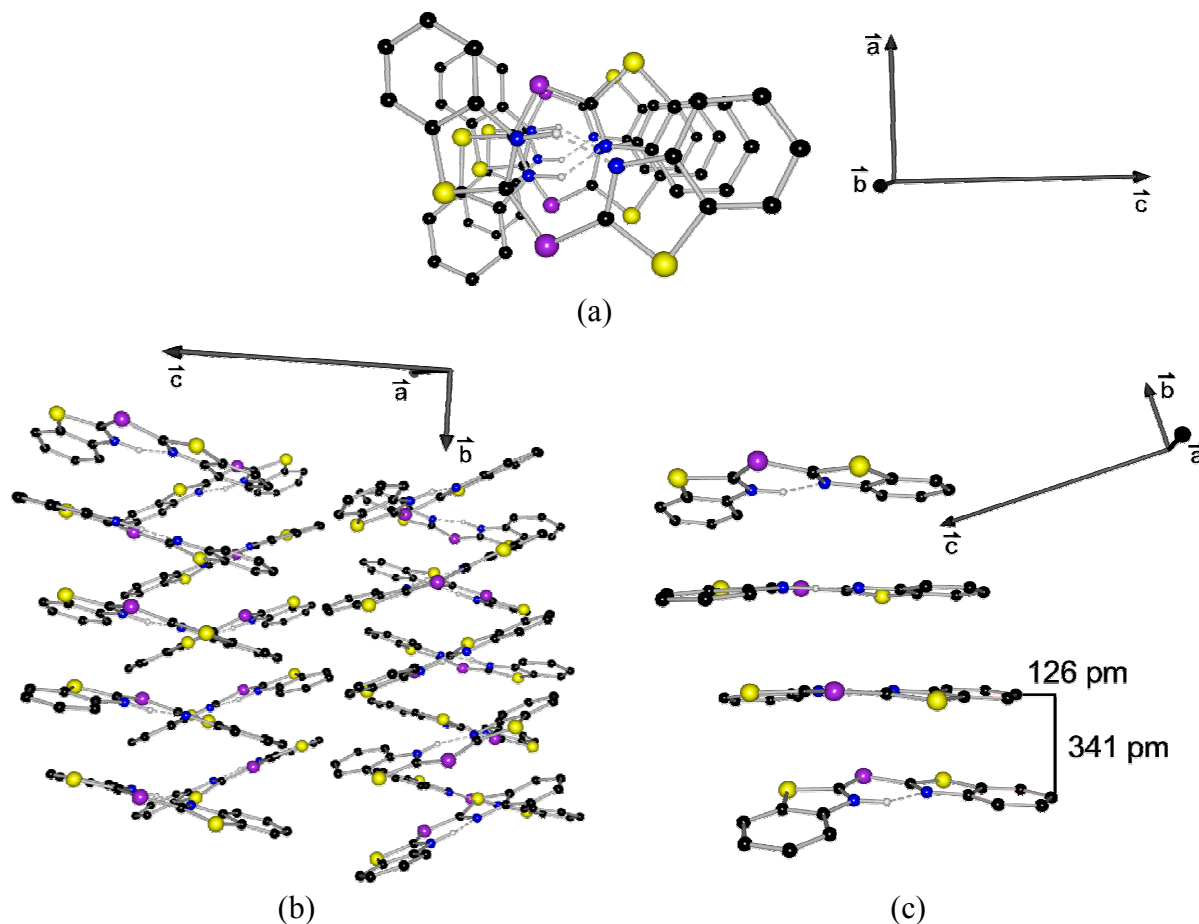


Figure 2-2: (a) Rod of di(benzothiazol-2-yl)phosphane in solid state (phosphorus atoms of layer A pointing up and those of layer B pointing down); (b) arrangement of rods in solid state; (c) interlayer distances

In solid state the molecules form rods along the \vec{b} vector which are parallel by crystallographic requirements of the orthorhombic space group. Although the rods are parallel, the planes of corresponding molecules in adjacent rods intersect at an angle of 38.8° . The rods do not interlock. Within a single rod the molecules are stacked with every second molecule turned along the C4...C7 vector by 180° giving an A/B pattern, in which the C₆ perimeter of the non-protonated benzothiazol-2-yl rings are approximately above each other. The shearing angle between a layer A and a layer B molecule is approx. 42° . The distance between adjacent non-protonated benzothiazol-2-yl rings of a rod is approx. 341 pm with the molecules being shifted by about 126 pm sideways from an A to a B layer (**Figure 2-2**).

2.3 Properties and Reactivity of Di(benzothiazol-2-yl)phosphane (1)

The solid state structure of di(benzothiazol-2-yl)phosphane (**1**) is the N–H tautomer of the expected P–H form, anticipated for secondary phosphanes. Therefore, it was of great interest to get information about the stability of the solid state tautomer compared to the P–H tautomer. Theoretical calculations are an excellent tool to determine the relative energies of various conformers. Geometries were optimized at the B3LYP/6-311++G** level of theory and the total energies were calculated (*Table 2-2*).⁵³

The structure determined by an X-ray diffraction experiment was used as starting geometry. As reference geometries the P–H tautomer of di(benzothiazol-2-yl)phosphane (**1**) was calculated in *trans-trans*, *cis-trans*, and *cis-cis* arrangement. Each geometry was optimised for a planar and a non-planar adjustment (*Figure 2-3*).

The optimised structure derived from the experimentally determined geometry turned out to be the energetically most favourable one. Although bond distances and angles in this structure differ from those found in di(benzothiazol-2-yl)phosphane (**1**), the experimental geometry is almost reproduced. Differences are found for the P–C bond distances which are 178.4(5) pm (P1–C1) and 177.8(4) pm (P1–C8) in **1** but 181.6 pm (P1–C1 bond) and 175.5 pm (P1–C8) for the calculated geometry. The latter two distances differ but are still between those for P–C double and single bonds.^[50] The average bond distance of 178.6 pm matches the one of the experimentally determined structure (178.1 pm on average) quite well. Similarly, the *C_{ipso}*–N bond distances differ more significantly in the calculated structure (131.2 pm (C1–N1) and 135.4 pm (C8–N2)) than in the experimental (133.1(6) pm (C1–N1) and 133.4(5) pm (C8–N2)). Both heteroaromatic rings in the calculated geometry are coplanar due to the geometrical constraint used.

To simplify the comparison, the total energy of the optimised X-ray structure was defined to be zero. Except for the optimised N–H tautomer, the pyramidal compounds are more stable than the planar ones. The energies of the planar geometries range from 137.44 kJ/mol for the *cis-trans* arrangement to 152 kJ/mol for the *trans-trans* arrangement. The total energies decrease by more than 100 kJ/mol if the phosphorus atom is permitted to adopt a pyramidal environment. The energies for the non-planar arrangements span a range from 22.54 kJ/mol for the *cis-trans* arrangement to 28.65 kJ/mol for the *cis-cis* conformation. In all non-planar geometries the heteroaromatic rings are rotated about the P–C bonds. The angles included by the ring systems range from 33.4° (*cis-cis* conformer) via 102.4° (*trans-trans* conformer) to 104.1° (*cis-trans* conformer).

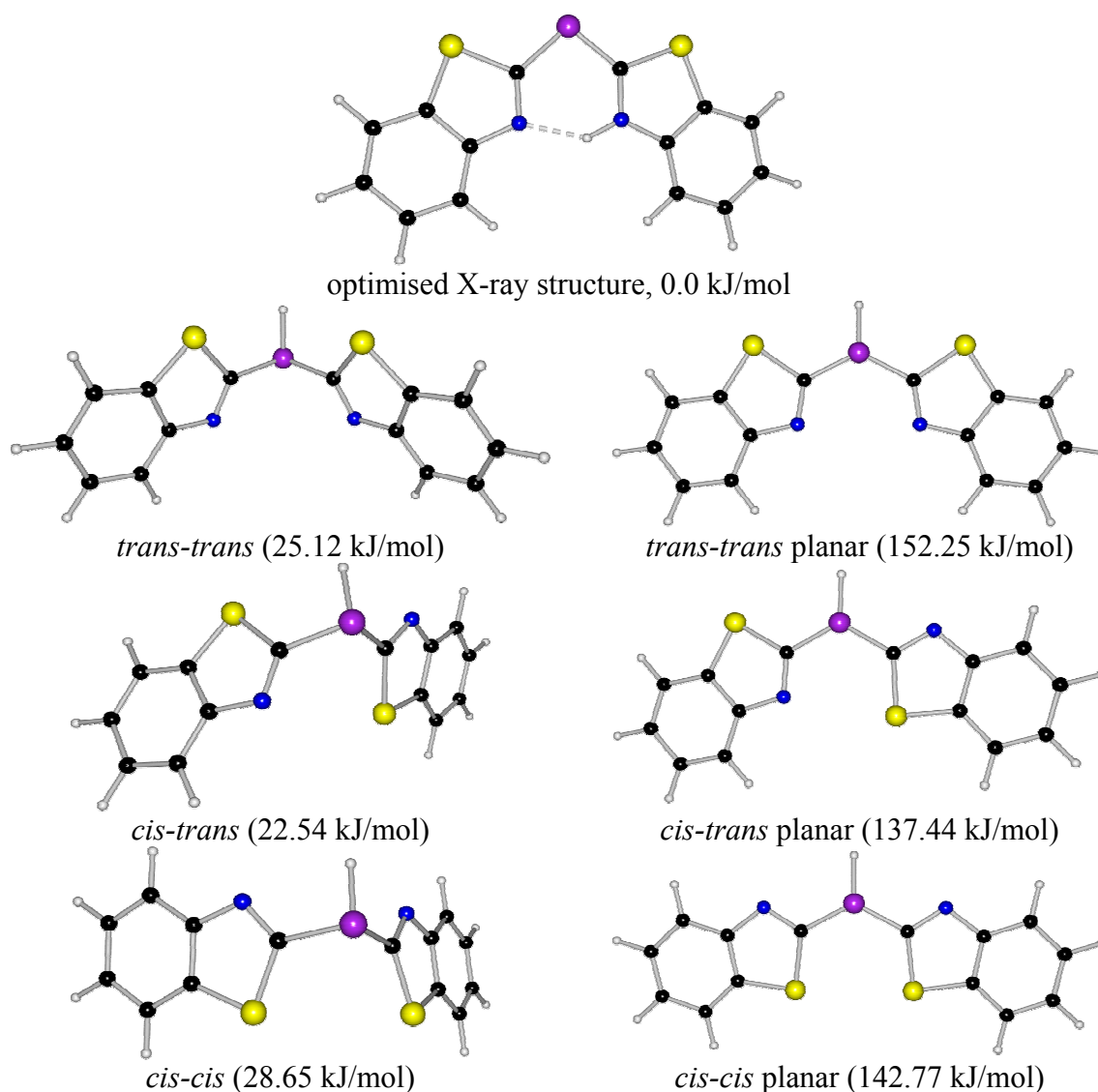


Figure 2-3: Optimised geometries for the tautomeric forms of di(benzothiazol-2-yl)phosphane (1)

Although non-planar P–H molecules are generally more stable than planar ones, the crystal structure of di(benzothiazol-2-yl)phosphane (1) displays an almost planar molecule. The total energy of the system decreases by the formation of a strong N–H...N hydrogen bond. Obviously, this energy gain overcompensates the energy required for the planar conformation.

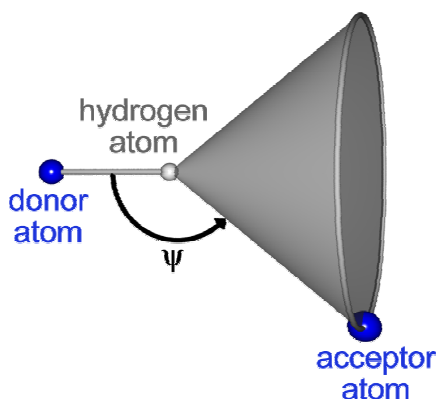
The inspection of the calculated Laplacian $-\nabla^2\rho$ shows four (3, -3) critical points around the phosphorus atom. These prove the existence of four valence shell charge concentrations (VSCC). VSCC are the physical expression for *Lewis* electron pairs, no matter whether they are bonding or non bonding.^[54] Therefore, the phosphorus centre has to be regarded as sp^3 hybridised with two lone pairs.

Table 2-2: Bond distances [pm], angles [°] and total energies [kJ/mol] for the tautomeric forms of di(benzothiazol-2-yl)phosphane (1)

	P1-C1	P1-C8	C1-N1	C8-N2	C-P-C	(bth) ... (bth')	sum of the angles around P	ΔE (absolute energy)
optimised X-ray structure	181.6	175.5	131.2	135.4	99.5	0.0	360.0	0.0 (p. d.)
<i>trans-trans</i>	185.0	184.9	129.2	129.1	100.1	102.4	291.1	25.12
<i>trans-trans</i> planar	176.8	176.8	129.1	129.1	125.8	0.0	360.0	152.25
<i>cis-trans</i>	185.0	184.4	129.3	129.2	100.3	104.1	291.4	22.54
<i>cis-trans</i> planar	176.1	176.8	129.7	129.8	121.3	0.0	360.0	137.44
<i>cis-cis</i>	185.3	185.2	129.0	129.0	101.0	33.4	289.9	28.65
<i>cis-cis</i> planar	176.7	176.7	129.8	129.8	125.1	0.0	360.0	142.77

Hydrogen bonds can be classified as weak or strong, according to their bond energies. For strong hydrogen bonds the estimated energy is 60 to 170 kJ/mol.^[55] Very often hydrogen bonds are classified by means of bond distances, not taking into account, that the geometry is a main argument to distinguish them from *Van der Waals* interactions. Hydrogen bonds have a distinct preference for linearity. Statistical analyses showed, that most strong hydrogen bonds are nearly linear. The angle ψ between the donor atom, the hydrogen atom and the acceptor atom is between 160° and 170° for most of the examined compounds. Theoretical calculations on water dimer interactions indicate that the energy reaches its minimum with linear hydrogen bonds. The values found in crystal structures seem to contradict this.

For geometric reasons, the number of possible hydrogen positions at a donor–H...acceptor angle ψ is proportional to $\sin \psi$ (**Scheme 2.4**).^[56] For more reliable values the cone correction has to be applied. The cone correction weighs the frequency of occurrence values with $1/\sin \psi$. Doing so, the statistics has its maximum approximately at 180° .

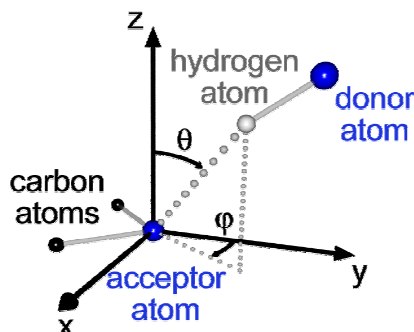


Scheme 2.4: Cone of opening angle $360^\circ - 2\psi$

However, the $N1\cdots H2-N2$ angle, being ψ , is $140(4)^\circ$. The deviation from 180° is caused by restrictions in the ligand geometry. It is impossible to have the $N2-H2$ bond in line with the lone pair at $N1$ without breaking at least one carbon phosphorus bond.

Not only for the donor atom but also for the acceptor atom linearity is preferred. For the pyridine nitrogen atom as acceptor, the preference of linearity has been shown.^[57] The hydrogen atom has to be in plane with the pyridine ring and the maximum of electron density of the lone pair at the pyridine nitrogen atom. **Scheme 2.5** visualises the geometrical requirements. θ shows the deviation of the hydrogen atom from the normal to the pyridine plane, while φ shows the deviation of the hydrogen atom from the C–N–C bisector.

The hydrogen bonds are most stable if θ is 90° , and hence the hydrogen atom is in-plane with the pyridine ring, and φ is 0° , i.e. the hydrogen atom is positioned at the C–N–C bisector. This situation can be compared directly to the situation in di(benzothiazol-2-yl)phosphane (1).



Scheme 2.5: *Geometry of a hydrogen bond: The acceptor atom is located at the origin of the Cartesian coordinate system, the y-axis shows the C–N–C bisector at the ring heteroatom acceptor and the z-axis shows the normal to the pyridine plane*

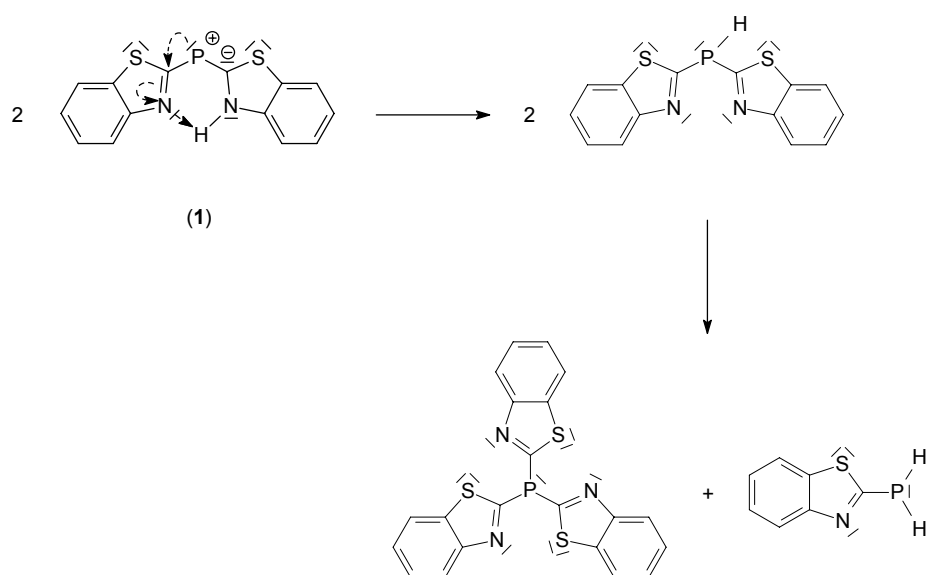
The angles around N2 are $115.4(4)^\circ$ (C8–N2–C14), $119.3(31)^\circ$ (C8–N2–H2), and $124.4(31)^\circ$ (C8–N2–H2). The sum of the angles is approx. 359° . Thus, the nitrogen atom N2 is sp^2 hybridised. The hydrogen atom H2 is only 8.2 pm displaced from the best plane defined by the atoms of the heteroaromatic ring containing N2. However, the planes defined by the heteroaromatic rings intersect at an angle of 10.6° . Therefore, the hydrogen atom H2 cannot be in plane with the second heteroaromatic ring and an angle θ of 83° is observed.

The C1–N1–C7 angle is $113.1(4)^\circ$. The sum of the angles around N1 of approx. 359° proves an almost planar environment around the sp^2 hybridised nitrogen atom N1. Both angles including the hydrogen involved in hydrogen bonding (C1–N1–H2 and C7–N1–H2) ought to be 123.5° to give the ideal value of 0° for φ . However, those angles are $103.5(14)^\circ$ and $142.7(14)^\circ$. They differ considerably more from the 120° anticipated for an sp^2 hybridised atom than those at N2. Hence the deviation from 0° for φ is much more pronounced.

The discrepancy of φ from 0° and the deviation from 90° for θ is due to the geometrical limitations of the ligand. The determined structure results from many factors, such as the tendency, to keep θ at 90° and φ at 0° , to reduce steric interactions between the heteroaromatic ring systems and not to strain the P–C bonds.

The N–H tautomer is stable in diethylether showing a signal in the ^{31}P NMR spectrum at 6.81 ppm with a $^3J_{\text{P-H}}$ coupling constant of 8 Hz. If tetrahydrofuran is used as solvent a second signal at -65.77 ppm appears which can be assigned to the P–H tautomer.

The $^1\text{J}_{\text{P-H}}$ coupling constant is 226 Hz and therefore close to the one of di(pyrid-2-yl)phosphane (225 Hz).^[43] Surprisingly, the P–H tautomer is not stable and a transformation of the P–H tautomer to tri(benzothiazol-2-yl)phosphane and a primary phosphane, is observed. Presumably, the primary phosphane is the (benzo-thiazol-2-yl)phosphane (**Scheme 2.6**), which is up to now solely characterised by NMR data. The absence of any organic solvent other than diethylether seems to be of vital importance for the stability of **1**. In any other solvent tested so far, the rearrangement takes place.



Scheme 2.6: Reaction of di(benzothiazol-2-yl)phosphane (**1**) in tetrahydrofuran

Up to now it was not possible to determine the reaction mechanism unambiguously, but it seems plausible to deduce from NMR data that the first step has to be the equilibration between the N–H and the P–H form of the molecule, followed by a substituent exchange reaction.

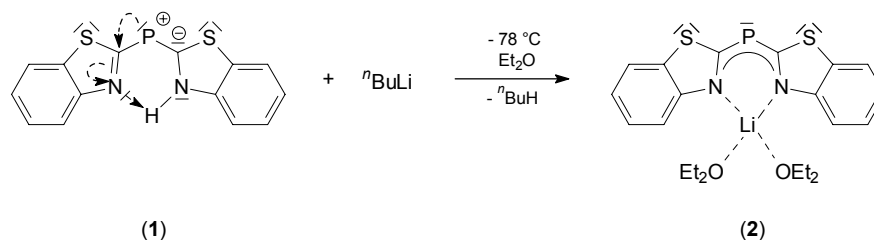
Consequently, all reactions starting from di(benzothiazol-2-yl)phosphane (**1**) were carried out in diethylether. The solid parent phosphane **1** decomposes gradually, indicated by a colour change from bright yellow to orange. Simultaneously the consistency changes from powder to paste, the latter shows reduced solubility and reactivity. Therefore, the starting material needs to be stored in a sealed flask at $-38\text{ }^\circ\text{C}$ under a dry inert gas atmosphere.

3 Di(benzothiazol-2-yl)phosphanides

A conclusion which can be drawn from the NMR spectra of di(benzothiazol-2-yl)phosphane (**1**) is, that the proton at the nitrogen atom is quite acidic and should be easily removed by almost any base added, leading to a negatively charged di(benzothiazol-2-yl)phosphanide. The monoanionic system should show the coordination behaviour expected for advanced *Janus head* ligands, such as a high flexibility regarding the size of metals, different donating sites for different metal centres, the ability to coordinate two different metal fragments simultaneously, and to act as hemilabile ligand.

3.1 Synthesis and Structure of $[(Et_2O)_2Li(bth)_2P]$ (**2**)

It was shown for the di(pyrid-2-yl)amine and di(pyrid-2-yl)phosphane that they can be readily deprotonated by organolithium compounds.^[58] The crystal structures of these compounds show that the hard metal fragment is coordinated by the ring nitrogen atoms exclusively. An analogue reaction of **1** with *n*-butyl lithium in diethylether leads to the expected product (*Scheme 3.1*).



Scheme 3.1: Preparation of $[(Et_2O)_2Li(bth)_2P]$ (**2**)

$[(Et_2O)_2Li(bth)_2P]$ (**2**) crystallises in the orthorhombic space group $Pca2_1$ with one formula unit in the asymmetric unit. The ligand adopts the *trans-trans* conformation with the two hard donor centres in close proximity. The cationic lithium atom is coordinated by the two nitrogen atoms of the deprotonated di(benzothiazol-2-yl)phosphane (**1**) almost symmetrically. Therefore, the asymmetry in the lithiated species is not as pronounced as the one found in **1**. The coordination sphere of the metal atom is completed by two diethylether molecules, one of which is disordered over two positions, which are almost equally occupied (52% vs. 48%) (*Figure 3-1*).

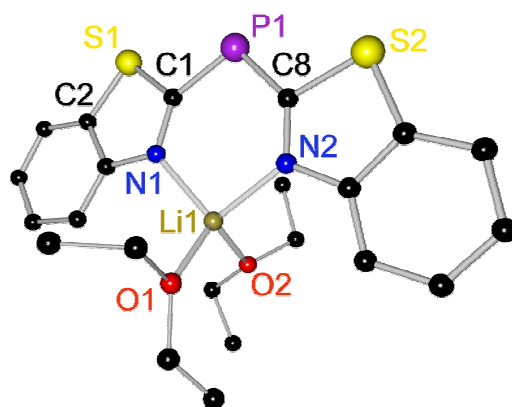


Figure 3-1: Crystal structure of $[(Et_2O)_2Li(bth)_2P]$ (**2**) (only one position of the disordered diethylether molecule depicted for clarity)

The distance between the two nitrogen atoms is 308.5 pm and therefore considerably longer than the corresponding N...N distance in **1** (262.2 pm). This can be ascribed to the larger radius of the lithium ion. The whole ligand is almost planar, the best planes of the heteroaromatic rings intersect at an angle of 9.9°. The benzothiazol-2-yl rings are marginally rotated about the P–C bonds in opposite directions. The ligand system is not planar as the nitrogen atoms have to coordinate the lithium cation properly, the lithium cation is located in plane with the benzothiazol-2-yl ring containing the nitrogen atom N1. At the same time, it is placed 45.1 pm above the other heteroaromatic ring system. The C_{ipso} –N bond distances of 131.0(2) pm for the C1–N1 bond and 131.3(2) pm for the C8–N2 bond are equal and do not differ from the corresponding bond lengths in di(benzothiazol-2-yl)phosphane (**1**). They are longer than double bonds between sp^2 hybridised carbon and nitrogen atoms (129 pm).^[50] The elongation of these bonds results from the electron density transfer from the formally negatively charged phosphorus centre to the heteroaromatic rings (**Table 3-1**).

The phosphorus atom is not involved in metal coordination, not even in long-range interactions to a second molecule. The P–C bonds of 177.9(2) pm for the P1–C1 bond and 177.9(2) pm for the P1–C8 bond are equal within their estimated standard deviations and resemble those found in **1**.

Table 3-1: Selected bond lengths [pm] and angles [°] of **2**

	bond length [pm]		bond angle [°]
P1–C1	177.9(2)	C1–P1–C8	104.2(1)
P1–C8	177.9(2)	N–Li–N	99.0(1)
C1–N1	131.0(2)	O1–Li–O2	106.2(2)
C8–N2	131.3(2)	O1–Li–O2'	116.4(2)
N1–Li1	202.4(3)	N–Li–O	107.5(5) to 118.3(2)
N2–Li1	203.7(3)		
N1...N2	308.7(2)		angle between planes [°]
		(bth)...(bth')	9.9

The C1–P1–C8 bond angle is 104.2(1)°. It is about 5.5° widened compared to that in **1**. The coordination of the lithium atom results in the wider angle as the bite of the ligand is forced to open to coordinate this cation. Nevertheless, the phosphorus atom is sp³ hybridised. The angle is a little more acute than the ideal tetrahedral angle of 109.4° because both heteroaromatic rings are tied together by metal coordination.

The plane containing the atoms O1, Li1, and O2 intersects the best plane defined by N1, C1, P1, C8, and N2 at an angle of 89.7°. This means the diethylether molecules completing the coordination sphere of the lithium atom are arranged in a way that steric interactions are minimised. The environment around the cationic centre is a distorted tetrahedron. The differences between the ideal angle of 109.4° and the actual angles are due to the geometric restrictions within the ligand system.

In solid state the molecules of **2** form rods along the \vec{a} vector that do not interlock. The molecules of a single rod are parallel keeping a distance of approx. 724 pm. This distance is by far larger than the distance between the molecules in di(benzothiazol-2-yl)phosphane (**1**) (341 pm). This can be explained by the steric demand of the diethylether molecules that act as spacers between the single molecules (*Figure 3-2b*).

All phosphorus atoms in one rod point in the same direction. The molecules of neighbouring rods along the b-axis are arranged in a head-to-tail manner. They point in opposite directions

along the *c*-axis. As in **1** the molecules are not located exactly above each other but shifted approx. 572 pm sideways. The best planes of single molecules of adjacent rods intersect at an angle of 68.1°.

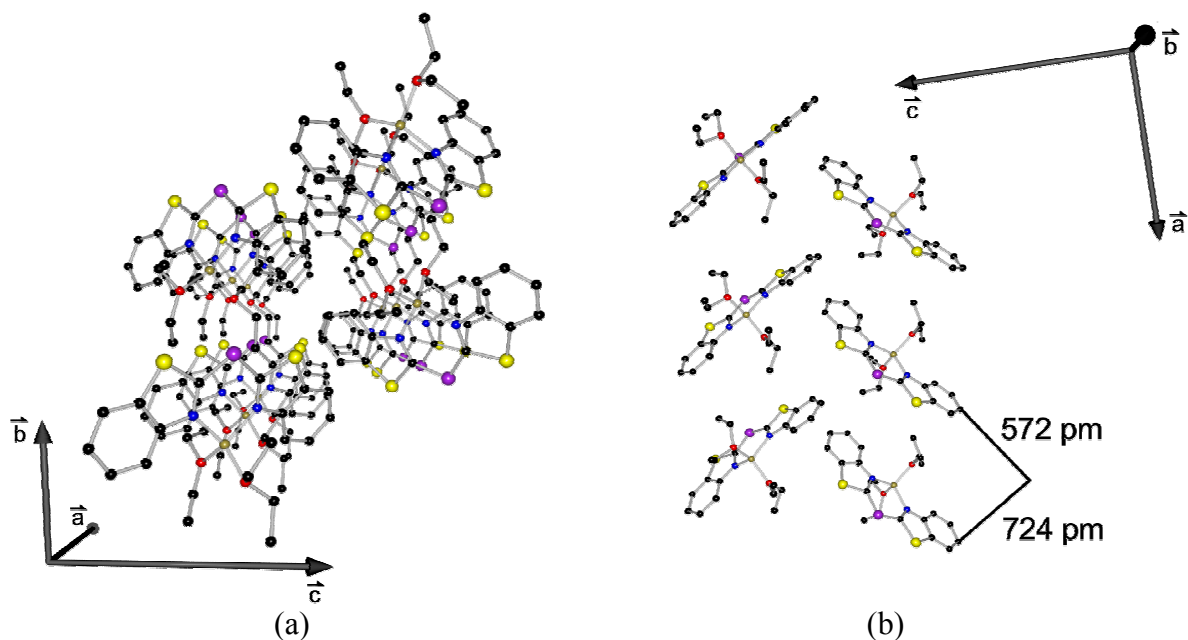


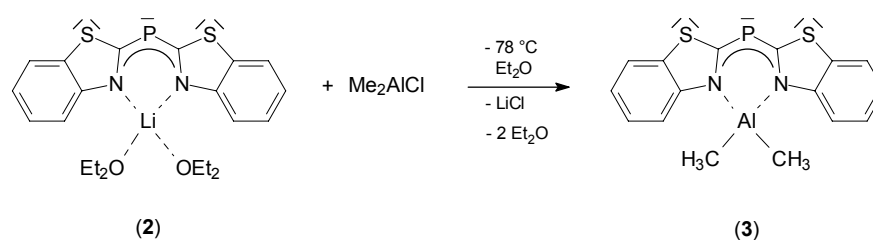
Figure 3-2: (a) View along the *a*-axis in **2**; (b) view along the *b*-axis in **2**

The crystal structure of **2** is similar to the one of lithium di(pyrid-2-yl)phosphanide.^[43] The N–Li distances of 202.4(3) pm for the N1–Li1 bond and 203.7(3) pm for the N2–Li1 bond are longer than the N–Li bonds in the (pyrid-2-yl)phosphanide (196.9(8) pm and 196.9(7) pm). Dative N→Li bond distances are approx. 200 to 240 pm.^[59] In contrast, amidic N–Li bond distances range from approx. 190 to 205 pm.^[60] Compounds in which bonds can not clearly be assigned as amidic or dative bonds are known as well. In these compounds the N–Li bond distances range from approx. 197 to 207 pm.^[58b,c;61] The N–Li bonds in **2** should be included in the latter group. The relatively long N–Li bonds together with the short P–C and elongated C_{ipso} –N bonds indicate a charge delocalisation over the whole ligand system.

The differences in N–Li bond distances between **2** and lithium di(pyrid-2-yl)phosphanide indicate, that the N–Li bonds in lithium di(benzothiazol-2-yl)phosphanide have a more dative character than the ones in lithium di(pyrid-2-yl)phosphanide. Consequently, the electron density at the phosphorus centre ought to be higher in **2** compared to the one in the pyrid-2-yl compound. Therefore, it is probably possible to involve the phosphorus centre directly in the coordination of additional metal fragments.

3.2 Synthesis and Structure of $[\text{Me}_2\text{Al}(\text{bth})_2\text{P}]$ (**3**)

In the previous section it was shown that di(benzothiazol-2-yl)phosphane (**1**) is readily deprotonated by *n*-butyl lithium to form the corresponding phosphanide. The analogue reaction with trimethyl aluminium yielded not a single product to be characterised unambiguously. Therefore, a salt elimination reaction was employed to get aluminium coordinated to the phosphanide ligand. $[(\text{Et}_2\text{O})_2\text{Li}(\text{bth})_2\text{P}]$ (**2**) was reacted with dimethyl aluminium chloride in tetrahydrofuran at $-78\text{ }^\circ\text{C}$ (**Scheme 3.2**).



Scheme 3.2: Synthesis of $[\text{Me}_2\text{Al}(\text{bth})_2\text{P}]$ (**3**)

Storage of the reaction mixture at $-38\text{ }^\circ\text{C}$ yielded crystals suitable for an X-ray diffraction experiment.

$[\text{Me}_2\text{Al}(\text{bth})_2\text{P}]$ (**3**) crystallises in the monoclinic space group $\text{P}2_1/\text{c}$ with a complete molecule in the asymmetric unit. **3** is isomorphous to the molecular assembly of the previous two compounds in the crystal (**Figure 3-3**). The two heteroaromatic rings are *trans-trans* arranged. The benzothiazol-2-yl rings are almost coplanar, they intersect at an angle of only 2.1° . The aluminium centre is obviously small enough to be coordinated by the two ring nitrogen atoms of the ligand without forcing the heteroaromatic rings to rotate about the P–C bonds in order to enlarge the bite distance. The assumed negative charge at the phosphorus atom, which is almost in plane with the heteroaromatic rings, participates in the π -electron system. The P1–C bond distances are equal within their estimated standard deviations (177.5(4) pm for the P1–C1 bond and 175.4(5) pm for the P1–C8 bond) (**Table 3-2**). Again, the values are between that of a P–C single bond (185 pm) and a double bond (167 pm).^[50] In the pyrid-2-yl analogue $[\text{Me}_2\text{Al}(\text{py})_2\text{P}]$ the P–C bonds are marginally longer and equal as well (178.6(2) pm and 178.2(2) pm).^[43]

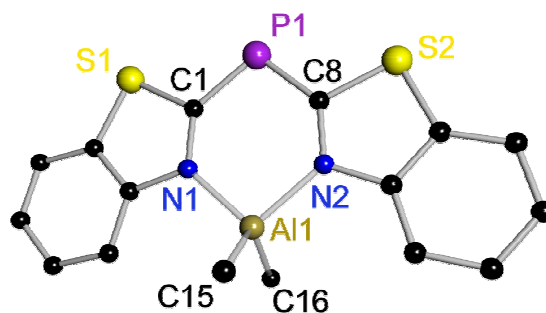


Figure 3-3: Crystal structure of $[Me_2Al(bth)_2P]$ (3)

Table 3-2: Selected bond lengths [pm] and angles [$^\circ$] of 3

	bond length [pm]		bond angle [$^\circ$]	
P1–C1	177.5(4)	C1–P1–C8	102.3(2)	
P1–C8	175.4(5)	N–Al–N	98.8(2)	
C1–N1	132.9(5)	C–Al–C	120.7(2)	
C8–N2	134.7(6)	N–Al–C (av.)	108.8(16)	
N1–Al1	192.3(4)			
N2–Al1	193.0(4)			angle between planes [$^\circ$]
N1...N2	292.4(5)	(bth)...(bth')	2.1	

The C_{ipso} –N bond distances, which are 132.9(5) pm for the C1–N1 bond and 134.7(6) pm for the C8–N2 bond, are similar and between those of a single and a double bond.^[50] Although slightly shorter, they are in the same range as the corresponding distances in dimethyl aluminium di(pyrid-2-yl)phosphanide (av. 135.7(6) pm). The elongation of the C–N bond, compared to a standard double bond, is a consequence of the electron density transferred from the phosphorus atom to the heteroaromatic rings.

The phosphorus atom is not directly involved in metal complexation. The hard aluminium fragment prefers the hard donating sites of the ligand.

The N1–Al1 bond distance is 192.3(4) pm and the N2–Al1 bond distance is 193.0(4) pm. Amidic N–Al bond distances span a range from approx. 172 to 188 pm.^[62] Dative N→Li bond distances range in length from approx. 192 to 214 pm.^[58b; 63] In compounds with

N–Al bonds classified between amidic and dative bonds, the bond distances are approx. 192 pm.^[58; 61b;64] The values found in [Me₂Al(bth)₂P] (**3**) match those of the latter class. This further substantiates a charge delocalisation over the whole ligand system.

As the aluminium cation is smaller than the lithium cation but bigger than a hydrogen atom, it is not surprising that the N1...N2 distance of 292.4(5) pm is between those found in di(benzothiazol-2-yl)phosphane (**1**) (262.2 pm) and lithium di(benzothiazol-2-yl)phosphanide (**2**) (308.5 pm). The N1...N2 distance in [Me₂Al(py)₂P] is 292.2 pm, yet another similarity to compound **3**.

The size of the aluminium cation is also responsible for the C1–P1–C8 angle (102.3(2)°) being between those found in **1** (98.7(2)°) and **2** (104.2(1)°).

The aluminium cation is only 0.8 pm above the best plane defined by the atoms N1, C1, P1, C8, and N2. The angles at the aluminium atom in **3** range from 98.8(2)° (N1–Al1–N2) to 120.7(2)° (C15–Al1–C16) and prove a distorted tetrahedral environment around the cationic centre. The rather acute angle of 98.8(2)° is due to the ligand geometry. The N–Al–C angles range from 107.9(2)° to 110.2(2)°. These values are very close to the standard tetrahedral angle of 109.4°. The C15–Al1–C16 angle of 120.7(2)° is widened compared to the ideal tetrahedral angle. This reflects the greater amount of space available for the methyl groups.

The N–Al bond distances and the N1...N2 distances in **3** do not differ remarkably from those found in [Me₂Al(py)₂P] (**Figure 3-4a**).^[43] Apparently the N–Al distances have to be in a quite narrow range around 292 pm for these compounds. The ligand has to adopt a certain conformation to fit the requirements of the metal. A tailored coordination can be achieved mainly by varying the C–P–C and C–N–C angles and by rotating the heteroaromatic rings about the P–C bonds. The latter is on the expense of the ligands conjugation and changes the C_{ipso}–N bond distances. The C–P–C angles are 102.3(2)° in **3** and 106.6(1)° in the pyrid-2-yl compound. The P–C–N angles are 137.7° on average in **3** and 127.0° on average in the pyridyl compound. The two heteroaromatic rings are almost coplanar in **3**, but include an angle of 25.1° in the butterfly arrangement of [Me₂Al(py)₂P]. Different to [(Et₂O)₂Li(bth)₂P] (**2**) the pyrid-2-yl rings in [Me₂Al(py)₂P] are rotated about the P–C bonds in the same direction. As a consequence the aluminium atom is dislocated from the N–C...C–N plane by 72.4 pm. Di(benzothiazol-2-yl)phosphanide coordinates the aluminium atom without giving up planarity. This might be important for the preparation of cooperative intramolecular heterobimetallic catalysts, in which the frequently used co-catalytic metal aluminium is employed.

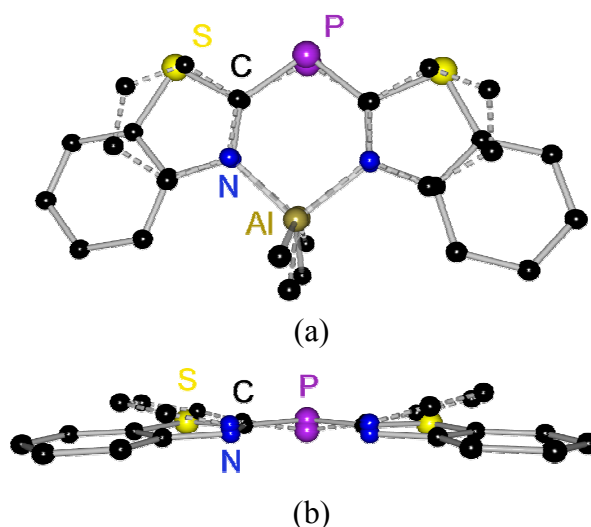


Figure 3-4: (a) Superposition of $[Me_2Al(bth)_2P]$ (3) (solid lines) and dimethyl aluminium di(pyrid-2-yl)phosphanide (dashed lines) (Me_2Al fragment omitted for clarity in (b))

In solid state the molecules form rods along the crystallographic *c*-axis (**Figure 3-5**). The molecules in the whole crystal are aligned parallelly. Within a rod the molecules are stacked in a way, that the straight line through the phosphorus and the aluminium atom of one molecule intersects that of a neighbouring molecule at a shearing angle of 83.7° . This results in rods built up of two different layers (A and B). The molecules of one layer are laterally shifted by approx. 51 pm. The molecules of one layer are laterally shifted by approx. 51 pm. The distance between adjacent layers is 366 pm. The rods build strands along the \vec{a} vector with a head-to-tail arrangement. Neighbouring strands are pointing in opposite directions and interlock in a zip-like manner. The interlock is asymmetric with the distances between interlocking planes of 360.1 and 373.6 pm.

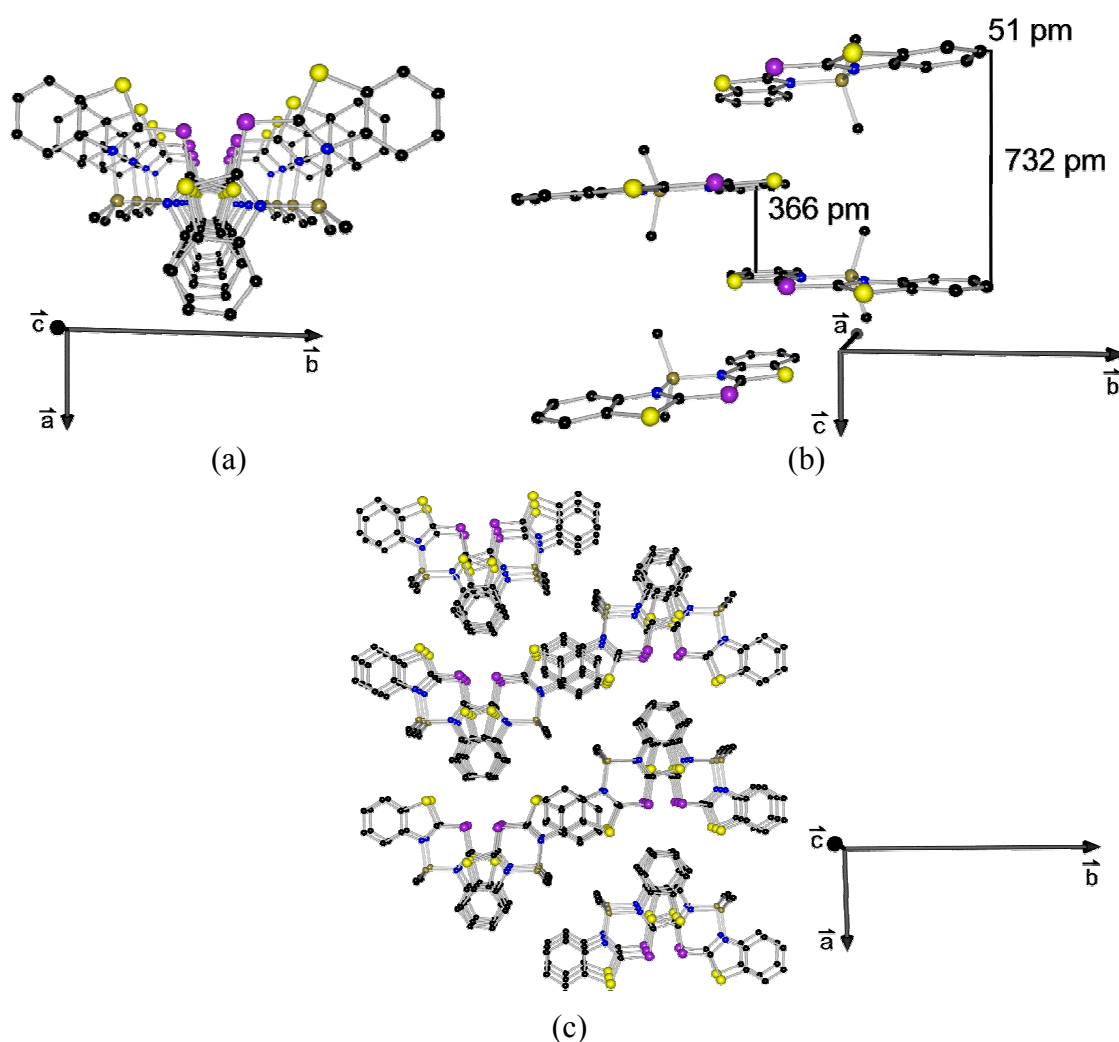


Figure 3-5: Solid state structure of $[\text{Me}_2\text{Al}(\text{bth})_2\text{P}]$ (3): (a) and (c) view along the a-axis; (b) view along the b-axis

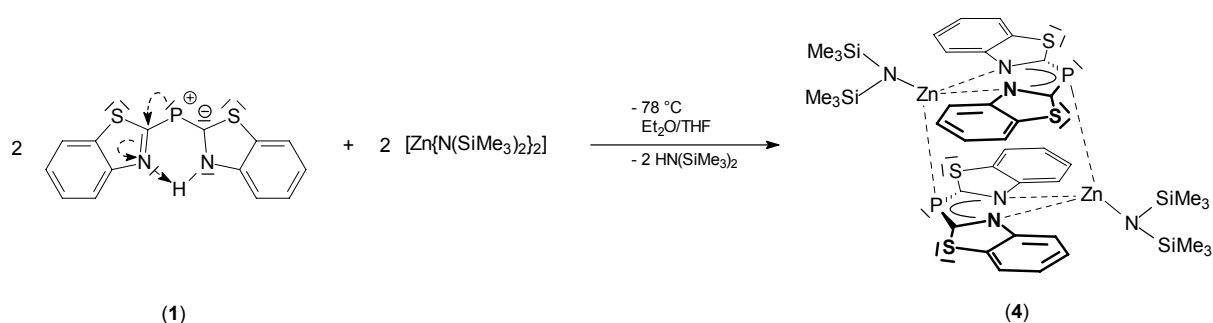
3.3 Synthesis and Structure of $[(\text{Me}_3\text{Si})_2\text{NZn}(\text{bth})_2\text{P}]_2 \cdot 2(\text{THF})$ (4)

The bulky bis(trimethylsilyl)amide group is well known in organometallic and coordination chemistry as it stabilises low coordination numbers in main group and transition metal compounds. From a synthetic point of view this substituent can readily be synthesised by salt metathesis reactions employing the lithium or sodium derivative of bis(trimethylsilyl)amine and an anhydrous metal halide. There are various ways to prepare the lithium and sodium compounds.^[65] The alkaline earth metal compounds are best prepared by reacting tin(II) or mercury(II) bis(bis(trimethylsilyl)amide) with the elemental metals.^[66] Amides of many main group and transition metals have been synthesised and structurally characterised.^[67]

Some of the amides are used in the MOCVD (metal organic chemical vapour deposition) process for growing lanthanum silicate thin films^[68] or for synthesising crystalline lanthanide nitride.^[69] Another field of research in which these amides and their derivatives are employed is catalysis, e.g. hydroamination reactions or the Claisen-Tishchenko reaction.^[70]

The amides can also be used to metallate compounds with protons more acidic than the N–H proton of bis(trimethylsilyl)amine. As di(benzothiazol-2-yl)phosphane (**1**) shows a quite acidic proton the amides were utilised to serve as a metal source for the ligand system.

To a suspension of di(benzothiazol-2-yl)phosphane (**1**) in diethylether, cooled down to $-78\text{ }^{\circ}\text{C}$, zinc bis(bis(trimethylsilyl)amide)^[71] was added in a 1:1 ratio over a period of 0.5 h (**Scheme 3.3**). After stirring the reaction mixture for four hours, the temperature was allowed to rise to room temperature. The solvent was removed in vacuo and the solid residue dissolved in 25 mL tetrahydrofuran. Storage of the red solution at $-35\text{ }^{\circ}\text{C}$ for two weeks yielded yellow crystals suitable for a single crystal X-ray diffraction experiment.



Scheme 3.3: Synthesis of $[(\text{Me}_3\text{Si})_2\text{NZn}(\text{bth})_2\text{P}]_2 \cdot 2(\text{THF})$ (**4**)

In the reaction the employed di(benzothiazol-2-yl)phosphane (**1**) is deprotonated to form the anionic di(benzothiazol-2-yl)phosphanide and bis(trimethylsilyl) amine.

$[(\text{Me}_3\text{Si})_2\text{NZn}(\text{bth})_2\text{P}]_2 \cdot 2(\text{THF})$ (**4**) crystallises in the triclinic space group $\text{P}\bar{1}$. The asymmetric unit consists of two independent phosphanide units and two non-coordinating tetrahydrofuran molecules one of which is disordered over three positions. The whole dimer is generated by a centre of inversion at 0, 0, 0 followed by the translation 0, 1, 0. The other dimer results from inversion at 0.5, 0.5, 0.5 and the successive translation 1, 1, 1. As there are only slight differences between the two independent units, the values for bond distances and bond angles given below are average values.

The results of the single crystal X-ray diffraction experiment show that the ligand is again arranged in a *trans-trans* manner. The zinc atom is coordinated by the two ring nitrogen atoms, similar to the metal coordination in $[(Et_2O)_2Li(bth)_2P]$ (**2**) and $[Me_2Al(bth)_2P]$ (**3**), and additionally by a nitrogen atom of a single remaining bis(trimethylsilyl)amide group (**Figure 3-6**).

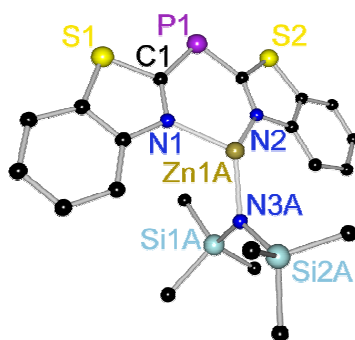


Figure 3-6: Asymmetric unit of $[(Me_3Si)_2NZn(bth)_2P]_2$ (**4**)

Again the coordination of the cationic metal centre causes a *trans-trans* arrangement of the ligand. The $N_{bth}-Zn$ bond distances are 205.9(5) pm on average (**Table 3-3**). N–Zn distances found in the CSD range from 182 to 255 pm.^[72] Amidic N–Zn bonds span a range from approx. 182 to 200 pm.^[73] Dative N–Zn bond distances range from approx. 197 to 255 pm.^[74] In **4** the $N_{bth}-Zn$ bonds are to be classified as bonds between classical amidic and classical dative bonds.

Table 3-3: Selected bond lengths [pm] and angles [°] of **4** (average values)

bond length [pm]		bond angle [°]	
P1–C1	180.5(3)	C1–P1–C8	103.8(2)
P1–C8	180.6(4)	$N_{bth}-Zn-N_{bth'}$	96.4(1)
P1–Zn1	248.7(3)		
C1–N1	131.2(4)		angle between planes [°]
C8–N2	131.5(4)	(bth)⋯(bth')	11.3
N1–Zn1A	205.9(3)		
N2–Zn1A	205.8(4)		
N3A–Zn1A	192.5(3)		
N1...N2	307.0(5)		

The bite distance N1...N2 is 307.0(5) pm. Thus, the ring nitrogen atoms in **4** have the same distance as the ones in [(Et₂O)₂Li(bth)₂P] (**2**) (308.7(2) pm). This is not surprising as the fourfold coordinated Zn²⁺ ion, with a radius of 60 pm, is negligibly bigger than a fourfold coordinated Li⁺ cation with a radius of 59 pm.^[75] The best planes defined by the two heteroaromatic rings include an angle of 11.3° in **4** while the corresponding angle in **2** is just 9.9°.

In contrast to [(Et₂O)₂Li(bth)₂P] (**2**), in [(Me₃Si)₂NZn(bth)₂P]₂•2(THF) (**4**) both heteroaromatic rings are rotated about the P–C bonds in the same direction. The dislocation of the cation from the ligand plane is more pronounced. While the lithium atom in **2** is in plane with one benzothiazol-2-yl ring but 45.1 pm out of the plane defined by the atoms of the other heteroaromatic ring, the zinc atom in **4** is av. 37.6 pm above the planes defined by the heteroaromatic rings. Relative to the best plane spanned by the atoms N_{bth}–C_{ipso}...C_{ipso}–N_{bth}, the cation is 53.8 pm on average out of plane. As the radius of a fourfold coordinated Zn²⁺ ion is just about 1 pm larger than the one of a fourfold coordinated Li⁺ ion, ion size can be ruled out to be the crucial factor for these changes.

The P–C bond distances are 180.5(3) pm (P1–C1) and 180.6(4) pm (P1–C8). They are a bit longer than the analogue distances in [(Et₂O)₂Li(bth)₂P] (**2**) (177.9(2) pm on average) and [Me₂Al(bth)₂P] (**3**) (176.5(16) pm on average). The C_{ipso}–N bond distances are 131.2(4) pm (C1–N1) and 131.5(4) pm (C8–N2), in **2** the C_{ipso}–N bond distances are almost the same (av. 131.2(4) pm) but tend to be a bit longer in **3** (av. 133.8(15) pm).

The C–P–C angle with an average value of 103.8(2)° is between those in the abovementioned complexes (104.2(1)° in **2** and 102.3(2)° in **3**).

(Me₃Si)₂N–Zn distances listed in the CSD range from 185 pm to 199 pm.^[72] The corresponding bond distances in **4** are 192.5(3) pm on average. Apparently, even without the contribution of electron density from the bis(trimethylsilyl)amide unit, the metal seems quite saturated so that the amide residue does not have to be bonded tightly.

Although, there are significant alterations concerning size and hardness of the cations coordinated, it is just the arrangement of the subunits in the ligand system that is affected by these changes. The bond distances do not differ that much from the ones found in compounds **1** to **3**.

In solid state **4** forms dimers. The zinc atom already coordinated to both nitrogen atoms of one anionic ligand is additionally bound to the phosphorus atom of another phosphanide ligand. (*Figure 3-7*).

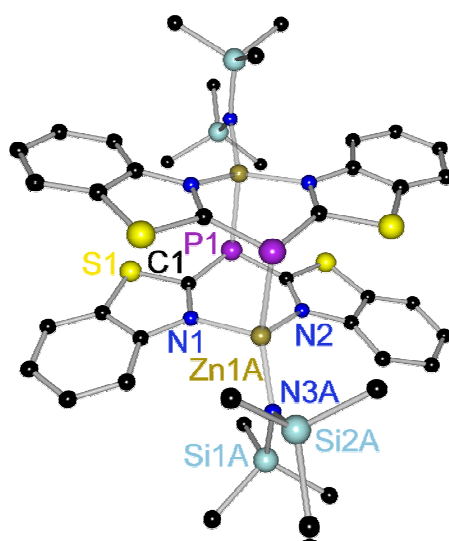


Figure 3-7: Solid state structure of $[(\text{Me}_3\text{Si})_2\text{NZn}(\text{bth})_2\text{P}] \cdot 2(\text{THF})$ (**4**) (THF molecules omitted for clarity)

The CSD lists phosphorus–zinc contacts within a range of 223 to 286 pm.^[72] The P–Zn distances are 248.7(3) pm on average in $[(\text{Me}_3\text{Si})_2\text{NZn}(\text{bth})_2\text{P}] \cdot 2(\text{THF})$ (**4**). Although the lone pairs at the phosphorus centre do not point in the direction of the metal centre, the electron density at the zinc atom is increased by this contact. The additional P–Zn contact is another reason for the relatively long $\text{Me}_3\text{SiN–Zn}$ bond distance.

Moreover, the P–[M] interaction is responsible for geometric changes in the ligand system. Charge distribution throughout the whole ligand is hindered. This causes relatively long P–C bond distances. The $C_{\text{ipso}}\text{–N}$ bond distances are only marginally affected.

As a consequence of the benzothiazol-2-yl ring rotations the phosphorus atom is displaced from the best plane defined by the $\text{N}_{\text{bth}}\text{–C}_{\text{ipso}}\cdots\text{C}_{\text{ipso}}\text{–N}_{\text{bth}}$ atoms. The abovementioned P–Zn interaction in $[(\text{Me}_3\text{Si})_2\text{NZn}(\text{bth})_2\text{P}] \cdot 2(\text{THF})$ (**4**) increases this displacement, so that the phosphorus atom is 20.0 pm on average out of plane. Simultaneously, the phosphorus atom attracts the metal ion and dislocates it from the anions plane. The attraction between the metal and the phosphorus atom forces the heteroaromatic rings to rotate about the P–C bonds. By this synergetic effect the phosphorus centres and the zinc atoms get in close contact (**Figure 3-8**).

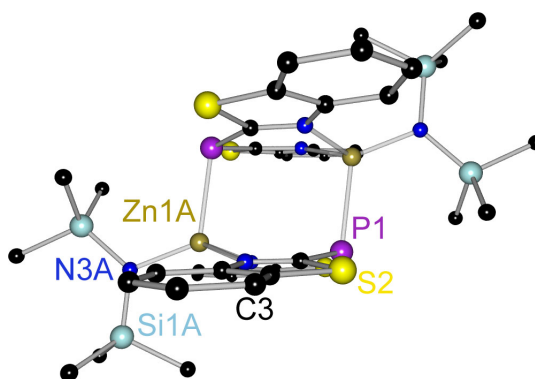


Figure 3-8: Displacement of zinc and phosphorus atoms in $[(\text{Me}_3\text{Si})_2\text{NZn}(\text{bth})_2\text{P}]_2 \cdot 2(\text{THF})$ (**4**) (THF molecules omitted for clarity)

The angle between the centre of gravity of the two ring nitrogen atoms N1 and N2, the phosphorus atom P1, and the zinc atom Zn1 is 103° . The C–P–C angle is $103.8(2)^\circ$. The Zn–P–C angles are 101.2° on average. Limitations regarding the geometrical parameters for the di(benzothiazol-2-yl)phosphanide are indicated by the fact that the standard angle for an sp^3 hybridised phosphorus atom is not reached. Therefore, the room available for the non-coordinating lone pair at the phosphorus atom is increased.

The environment around the fourfold coordinated zinc atom is best described as a distorted tetrahedron. The angles at the zinc atom range from $96.4(1)^\circ$ for $\text{N}_{\text{bth}}\text{--Zn--N}_{\text{bth}'}$ to av. $119.7(5)^\circ$ for $\text{N}_{\text{bth}}\text{--Zn--N}_3$. The plane defined by the atoms Si1A, N3A, and Si2A is almost perpendicular to the best plane defined by the two ring nitrogen atoms and the two *ipso* carbon atoms (89.4°).

The methyl groups of the trimethylsilyl groups are staggered in order to reduce steric interactions. Additionally, the trimethylsilyl groups are arranged in a way that the nearby phosphorus atom points into the bisection between two methyl groups. The sum of the angles around the nitrogen atoms N3 and N6 is av. 360.0° . The environment around these atoms is planar, suggesting an sp^2 hybridisation for the $(\text{Me}_3\text{Si})_2\text{N}$ nitrogen atoms. The lone pair has p-character. The Si–N–Si angles are $125.9(2)^\circ$ on average. The Si–N–Zn angles are $117.0(9)^\circ$ on average. This demonstrates the high steric demand of the trimethylsilyl groups.

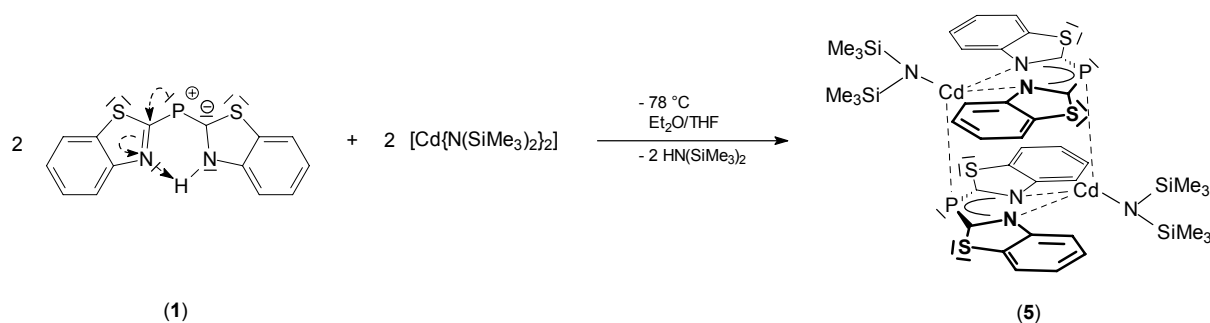
The tetrahydrofuran molecules do not interact with the complexes directly as they are lattice solvent and located at vacant crystal sites.

3.4 Synthesis and Structure of $[(\text{Me}_3\text{Si})_2\text{NCd}(\text{bth})_2\text{P}]_2 \cdot (\text{THF})$ (5)

As shown for $[(\text{Me}_3\text{Si})_2\text{NZn}(\text{bth})_2\text{P}]_2 \cdot 2(\text{THF})$ (4) the di(benzothiazol-2-yl)phosphanide moiety is able to donate electron density not only via the nitrogen atoms but also via the phosphorus atom. It was of interest to investigate whether an increase in the cation size would cause a more pronounced change in ligand geometry and coordination behaviour. It seems challenging to see whether a coordination by the soft phosphorus atom exclusively without any further metal–nitrogen contacts can be achieved. For this purpose it was tried to react di(benzothiazol-2-yl)phosphane (1) with a metal bis(trimethylsilyl)amide that transfers a metal that is considerably bigger than the zinc cation. Cadmium bis(bis(trimethylsilyl)amide) was the obvious choice. This results in an increase of the ionic radius from 60 pm for the four-fold coordinated Zn^{2+} ion to 78 pm for the fourfold coordinated Cd^{2+} cation.^[75] Additionally, the cations should not differ too much in terms of absolute hardness. The absolute hardness (η) is defined to be half the difference between ionisation energy (I) and electron affinity (A) of the referred ion (*Equation 3-1*).^[23] For the Zn^{2+} ion and the Cd^{2+} ion this equation gives 10.8 and 10.3, respectively,^[76] although the radii differ by 18 pm.

$$\eta = \frac{I - A}{2} \quad \text{Equation 3-1}$$

Di(benzothiazol-2-yl)phosphane (1) was suspended in diethylether and cooled to -78°C . Over a period of 0.5 h cadmium bis(bis(trimethylsilyl)amide)^[71] was added in a 1:1 ratio. After stirring the reaction mixture for 3 h at -78°C the temperature was raised slowly to room temperature. The solvent was removed under reduced pressure and the solid residue was dissolved in tetrahydrofuran (*Scheme 3.4*). Storage of the solution at -38°C for two weeks yielded crystals suitable for a single crystal X-ray diffraction experiment.



Scheme 3.4: Synthesis of $[(\text{Me}_3\text{Si})_2\text{NCd}(\text{bth})_2\text{P}]_2 \cdot (\text{THF})$ (5)

Di(benzothiazol-2-yl)phosphane (**1**) is deprotonated by the amide to yield di(benzothiazol-2-yl)phosphanide and bis(trimethylsilyl)amine. The second amide group of the employed metal diamide remains coordinated to the cadmium atom. The reaction yielding **5** is analogue to the one described in the previous section.

$[(\text{Me}_3\text{Si})_2\text{NCd}(\text{bth})_2\text{P}]_2 \cdot (\text{THF})$ (**5**) crystallises in the triclinic space group $P\bar{1}$ and is isomorphous to $[(\text{Me}_3\text{Si})_2\text{NZn}(\text{bth})_2\text{P}]_2 \cdot 2(\text{THF})$ (**4**). The asymmetric unit consists of half the dimer and one non coordinating molecule of tetrahydrofuran. The dimer is completed by inversion at 0, 1, 0.

The phosphanide ligand adopts a *trans-trans* conformation with both ring nitrogen atoms at the same side coordinated to the metal. The metal is additionally coordinated by the nitrogen atom of the remaining bis(trimethylsilyl)amide residue. The coordination sphere of the cadmium centre is completed by a contact to the phosphorus atom of the second ligand molecule of the dimer.

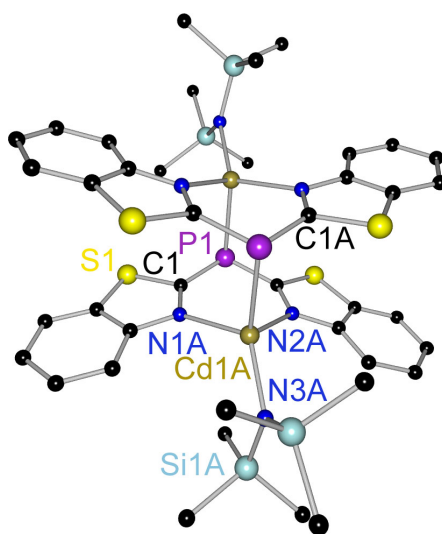


Figure 3-9: Crystal structure of $[(\text{Me}_3\text{Si})_2\text{NCd}(\text{bth})_2\text{P}]_2 \cdot (\text{THF})$ (**5**) (THF molecule omitted for clarity)

The P–C bonds are 181.0(2) pm (P1–C1) and 180.6(2) pm (P1–C8) (**Table 3-4**). They are slightly shorter than those in tri(benzothiazol-2-yl)phosphane but match the values of **4**. Again, the P–[M] interaction is responsible for geometric changes and relatively long P–C bond distances. The $C_{\text{ipso}}\text{--N}$ bonds (av. 131.7(3) pm) do not differ in lengths compared to those in **4** (av. 131.4(6) pm). The $C_{\text{ipso}}\text{--N}$ bond distances differ from those of a standard double bond due to the fact that electron density is transferred from the phosphorus centre to the heteroaromatic rings.

Table 3-4: Selected bond lengths [pm] and bond angles [°] of **5**

	bond length [pm]		bond angle [°]	
P1–C1	181.0(2)	C1–P1–C8	105.0(1)	
P1–C8	180.6(2)	N _{bth} –Cd–N _{bth'}	87.9(1)	
P1–Cd1	260.9(1)			
C1–N1A	131.6(2)		angle between planes [°]	
C8–N2A	131.7(2)	(bth)⋯(bth')	19.9	
N1A–Cd1A	228.9(2)			
N2A–Cd1A	229.3(2)			
N3A–Cd1A	212.6(2)			
N1⋯N2	318.1(2)			

The N1A–Cd1A bond distance is 228.9(2) pm and the N2A–Cd1A bond distance is 229.3(2) pm. Amidic N–Cd bond distances range from approx. 218 to 235 pm.^[77] N–Cd distances for dative bonds range from approx. 220 to 265 pm.^[78] Although bond distances are not the decisive argument for judging on bond characters, the N–Cd bonds in **5** are best described having a bond character between amidic and dative bonds analogous to the N–[M] bonds in the compounds discussed so far.

The N1⋯N2 distance is 318.1(2) pm. The angle between the heteroaromatic rings is 19.9°. This arrangement is a consequence of both, the by 18 pm larger radius of a fourfold coordinated Cd²⁺ ion (78 pm) compared to a fourfold coordinated Zn²⁺ ion (60 pm)^[75] and the participation of the phosphorus atoms in metal coordination.

P–Cd bond distances listed in the CSD range from 243 pm to 280 pm.^[72] In [(Me₃Si)₂NCd(bth)₂P]₂•(THF) (**5**) the P1–Cd1 bond distance is 260.9(1) pm. The phosphorus centre is involved in metal complexation like in [(Me₃Si)₂NZn(bth)₂P]₂•(THF) (**4**). Again, the cation is not positioned as anticipated for an sp³ hybridised phosphorus atom.

The bigger cation forces the bite distance to increase significantly. This causes the heteroaromatic rings to rotate about the P–C bonds even more than in [(Me₃Si)₂NZn(bth)₂P]₂•2(THF) (**4**). Like in the latter, they are rotated in the same direction.

Therefore, the dislocation of the phosphorus as well as of the metal atom from the $N_{\text{bth}}-C_{\text{ipso}}\cdots C_{\text{ipso}}-N_{\text{bth}}$ plane was expected to be more pronounced. However, the phosphorus atom is displaced by 22.9 pm from the best plane spanned by the atoms $N_{\text{bth}}-C_{\text{ipso}}\cdots C_{\text{ipso}}-N_{\text{bth}}$. In **4** the corresponding value is 20.0 pm on average. Taking the differences in angles included by the heteroaromatic rings (11.3° in **4** and 19.9° in **5**) into account, the phosphorus centre in **4** is significantly more out of plane than in $[(\text{Me}_3\text{Si})_2\text{NCd}(\text{bth})_2\text{P}]_2\cdot(\text{THF})$ (**5**). The cadmium cation is located 60.2 pm out of the $N_{\text{bth}}-C_{\text{ipso}}\cdots C_{\text{ipso}}-N_{\text{bth}}$ plane. This value is still not remarkably higher than the 53.8 pm in **4** (**Figure 3-10**). The displacement is an additional factor, that has to be considered for judging on the N–Cd bond characters.

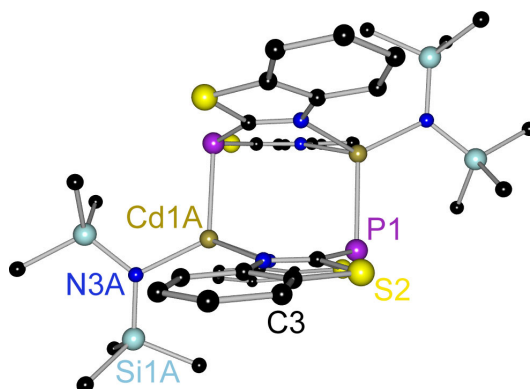


Figure 3-10: Displacement of cadmium and phosphorus atoms in $[(\text{Me}_3\text{Si})_2\text{NCd}(\text{bth})_2\text{P}]_2\cdot 2(\text{THF})$ (**5**) (THF molecule omitted for clarity)

The $\text{Me}_3\text{SiN}-\text{Cd}$ bond distance in **5** is 212.6(2) pm. The CSD lists bond distances for similar bonds from 207 to 214 pm.^[72] Hence, the value found in **5** is at the upper end of this range. This indicates that a lot of electron density is donated to the metal by the two ring nitrogen atoms and the phosphorus centre already, so that the bis(trimethylsilyl)amide group does not have to transfer much electron density to the metal. The N3–Cd1 distance in **5** is more affected by P–[M] interactions than the corresponding bond in **4**, which stresses the relevance of P–[M] interactions in $[(\text{Me}_3\text{Si})_2\text{NCd}(\text{bth})_2\text{P}]_2\cdot(\text{THF})$ (**5**).

In **5** the C–P–C angle of $105.0(1)^\circ$, is almost identical to the value found in $[(\text{Me}_3\text{Si})_2\text{NZn}(\text{bth})_2\text{P}]_2\cdot 2(\text{THF})$ (**4**) ($103.8(2)^\circ$). The angle included by the centre of gravity of N1A and N2A, P1 and Cd1 is 98.3° . In comparison to $[(\text{Me}_3\text{Si})_2\text{NZn}(\text{bth})_2\text{P}]_2\cdot 2(\text{THF})$ (**4**) (103° on average), the metal cations are closer to the centre of gravity of the whole molecule.

The Cd1–P1–C angles are 97.1(1)° for C1 and 100.8(1)° for C8. The cadmium cation is shifted towards the carbon atom C1.

The geometry at the cadmium atom is best described as a distorted tetrahedron. The N_{bth}–Cd–N_{bth} angle is 87.9(1)°. The corresponding angle in **4** is 96.4(1)°. A consequence of the larger radius of the Cd²⁺ ion compared to the Zn²⁺ ion is the wider N1...N2 bite distance (from 307.0(5) pm in **4** to 318.1(2) pm in **5**), although it is not fully reflecting the 18 pm increase in radius. The difference in the abovementioned angle is based on the fact that the rotation of the heteroaromatic rings about the P–C_{ipso} bond in **5** is more distinct than in **4**. The (Me₃Si)₂N–Cd–N_{bth} angles differ by 6.7° as the N3–Cd1–N1 angle is 122.8(1)° and the N3–Cd1–N2 angle is 116.2(1)°. The plane spanned by the atoms Si1A, N3A, and Si2A includes an angle of 81.8° with the best plane defined by the atoms N1A, C1, C8, and N2A.

The sum of the angles around N3A is 359.4°, indicating a planar environment at the sp² hybridised (Me₃Si)₂N nitrogen atom. The lone pair at N3A has p-character. The Si1–N3–Si2 angle is 125.8(1)°, the Si1–N3–Cd1 angle is 118.1(1)°, and the Si2–N3–Cd1 angle is 115.5(1)°. The higher steric demand of the three methyl groups at the silicon centres relative to the steric demand of the metal centre is responsible for differences of the actual angles from the theoretical value of 120°.

The trimethyl groups of the bis(trimethylsilyl)amide groups are staggered to minimise steric interactions. Moreover, they are positioned so that the nearby phosphorus atom is pointing at the bisection between two methyl groups.

Although the Cd²⁺ ion is remarkably bigger than the Zn²⁺ ion, both complexes **4** and **5** do not differ significantly. These facts suggest that the effects leading to a better interaction between the metal centre and the soft P-donating site of the ligand are levelled out by the increase in size, which makes changes in ligand geometry unnecessary (*Figure 3-11*).

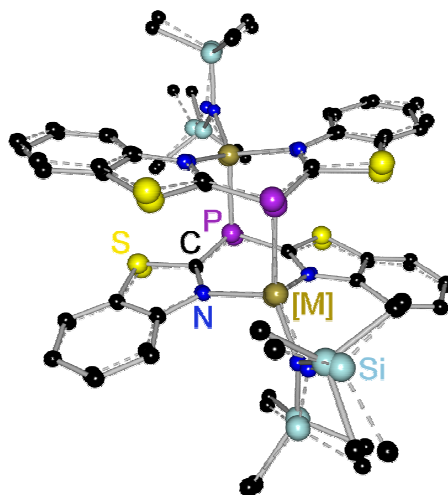


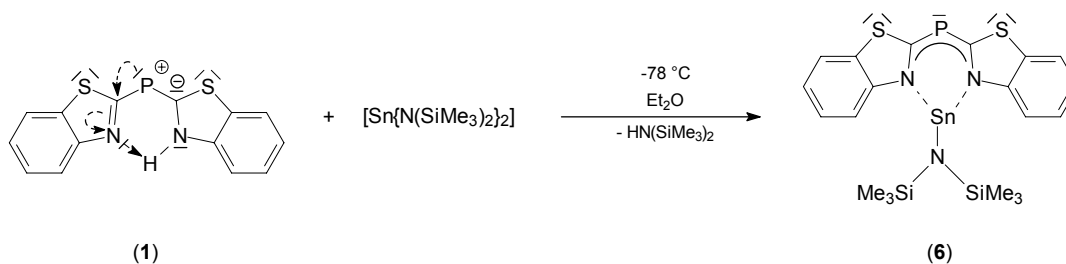
Figure 3-11: Superposition of $[(\text{Me}_3\text{Si})_2\text{NZn}(\text{bth})_2\text{P}]_2 \cdot 2(\text{THF})$ (4) (solid lines) and $[(\text{Me}_3\text{Si})_2\text{NCd}(\text{bth})_2\text{P}]_2 \cdot (\text{THF})$ (5) (dashed lines) (solvent molecules omitted for clarity)

3.5 Synthesis and Structure of $[(\text{Me}_3\text{Si})_2\text{NSn}(\text{bth})_2\text{P}] \cdot 0.49(\text{Et}_2\text{O})$ (6)

The most interesting question arising from the results of the single crystal X-ray diffraction experiments discussed in the previous sections is the one about the influence of P–[M] interactions.

Sn^{2+} has an ion radius between the ones of Zn^{2+} and Cd^{2+} .^[79] Since tin is a main group element it should show differences concerning the coordination chemistry of d-block metals. It was expected that tin is coordinated exclusively by the ring nitrogen atoms of a di(benzothiazol-2-yl)phosphanide moiety similar to the situation in $[(\text{Me}_3\text{Si})_2\text{NZn}(\text{bth})_2\text{P}]_2 \cdot 2(\text{THF})$ (4) and $[(\text{Me}_3\text{Si})_2\text{NCd}(\text{bth})_2\text{P}]_2 \cdot (\text{THF})$ (5). No additional P–Sn contacts are required as tin(II) already has a lone pair and is not as *Lewis* acidic as zinc or cadmium. In order to get more insight into the effects of additional P–[M] interactions di(benzothiazol-2-yl)phosphane (1) was reacted with tin bis(bis(trimethylsilyl)amide).

Di(benzothiazol-2-yl)phosphane (1) was suspended in diethylether, cooled down to $-78\text{ }^\circ\text{C}$, and reacted with tin bis(bis(trimethylsilyl)amide)^[80] in a 1:1 ratio (**Scheme 3.5**). The reaction mixture was kept at $-78\text{ }^\circ\text{C}$ for four hours. The colour changed from bright yellow to an intense orange. Afterwards the temperature was slowly raised to room temperature. Deep red crystals suitable for a single crystal X-ray diffraction experiment formed at the phase boundary of the solution.



Scheme 3.5: Preparation of $[(\text{Me}_3\text{Si})_2\text{NSn}(\text{bth})_2\text{P}] \cdot 0.49(\text{Et}_2\text{O})$ (**6**)

$[(\text{Me}_3\text{Si})_2\text{NSn}(\text{bth})_2\text{P}] \cdot 0.49(\text{Et}_2\text{O})$ (**6**) crystallises in the monoclinic space group $C2/c$. The asymmetric unit contains one formula unit. Both trimethylsilyl groups are disordered over two positions, the site occupation factors refined to 0.53/0.47 and 0.50/0.50. Additionally a non coordinating diethylether molecule is present. Its site occupation factor refined to 0.49.

In solid state the cationic tin centre is coordinated by the two ring nitrogen atoms of the di(benzothiazol-2-yl)phosphanide unit and the nitrogen atom of the bis(trimethylsilyl)amide residue (**Figure 3-12**). The phosphorus centre is not directly involved in coordination.

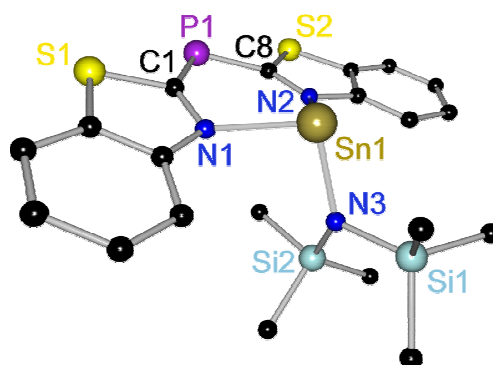


Figure 3-12: Crystal structure of $[(\text{Me}_3\text{Si})_2\text{NSn}(\text{bth})_2\text{P}] \cdot 0.49(\text{Et}_2\text{O})$ (**6**) (disorder and Et_2O molecule omitted for clarity)

The P–C bond distances are 176.3(4) pm (P1–C1) and 176.9(4) pm (P1–C8) (**Table 3-5**). These distances are significantly shorter than the related ones in $[(\text{Me}_3\text{Si})_2\text{NZn}(\text{bth})_2\text{P}]_2 \cdot 2(\text{THF})$ (**4**) (180.6(4) pm) and $[(\text{Me}_3\text{Si})_2\text{NCd}(\text{bth})_2\text{P}]_2 \cdot (\text{THF})$ (**5**) (180.8(4) pm). Nevertheless, these bond distances are between those expected for a P–C single and double bond (185 pm vs. 167 pm).^[50] The participation of the phosphorus atom in metal coordination in **4** and **5** affected the ligand geometry and precluded complete charge delocalisation over the entire ligand system leading to longer P–C bond distances. In **6**, no direct P–[M] interaction is observed. As a consequence, the P–C bond distances are shorter.

Table 3-5: Selected bond lengths [pm] and angles [°] of [(Me₃Si)₂NSn(bth)₂P]•0.49(Et₂O) (**6**)

	bond length [pm]		bond angle [°]
P1–C1	176.3(4)	C1–P1–C8	103.6(2)
P1–C8	176.9(4)	N _(bth) –Sn–N _(bth)	84.3(1)
C1–N1	133.5(5)		
C8–N2	133.1(4)		angle between planes [°]
N1–Sn1	225.7(3)	(bth)⋯(bth')	12.7
N2–Sn1	224.7(3)		
N3–Sn1	209.5(3)		
N1⋯N2	302.1(4)		

The C_{ipso}–N bond distances of 133.5(5) pm and 133.1(4) pm in **6** are rather long in this series of compounds. In [(Me₃Si)₂NZn(bth)₂P]₂•2(THF) (**4**) the C_{ipso}–N bond distance is 131.4(6) pm on average. In [(Me₃Si)₂NCd(bth)₂P]₂•(THF) (**5**) the C_{ipso}–N bond distance is 131.7(3) pm on average. Apparently, the C_{ipso}–N bond distances are not as sensitive to the P–[M] coordination as the P–C bond distances.

The C–P–C angle is 103.6(2)°, a value very close to those found in the other structures discussed so far. Once again, the formally negatively charged phosphorus centre can be rationalised to be sp³ hybridised with the two lone pairs coupling in the heteroaromatic ring systems. The benzothiazol-2-yl rings are rotated about the P–C bonds in opposite directions. The best planes defined by the atoms of each ring intersect at an angle of 12.7°. The phosphorus atom is only 0.3 pm out of the N_{bth}–C_{ipso}⋯C_{ipso}–N_{bth'} plane. The direct comparison of the crystal structures of [(Me₃Si)₂NZn(bth)₂P]₂•2(THF) (**4**), [(Me₃Si)₂NCd(bth)₂P]₂•(THF) (**5**), and [(Me₃Si)₂NSn(bth)₂P]•0.49(Et₂O) (**6**) is difficult because of the rotation in opposite directions.

The N_{bth}–Sn bond distance is 225.7(3) pm for N1–Sn1 and 224.7(3) pm for N2–Sn1. Lengths of comparable bonds range from approx. 214 pm to 240 pm.^[81] The distances between the ring nitrogen atoms and the metal centre are mainly a consequence of the displacement of the metal centre from the best plane defined by the ligand atoms. As the lone pairs at the ring nitrogen atoms are not in line with metal centred unoccupied π-orbitals, the distance between the nitrogen atoms and the metal centre has to decrease in order to increase the overlap integral between

both types of orbitals. The $(\text{Me}_3\text{Si})_2\text{N-Sn}$ bond distance of 209.5(3) pm is quite short, because $(\text{Me}_3\text{Si})_2\text{N-Sn}$ bond distances for threefold coordinated tin compounds range from approx. 205 to 240 pm.^[82] The short $(\text{Me}_3\text{Si})_2\text{N-Sn}$ bond distance indicates the electron depletion at the metal centre is not entirely compensated by the weakly bonded phosphanide ligand.

The angles around the Sn^{2+} centre are $84.3(1)^\circ$ for the $\text{N}_{\text{bth}}-\text{Sn}-\text{N}_{\text{bth}'}$ angle, $97.4(1)^\circ$ for the N1-Sn1-N3 angle, and $97.7(1)^\circ$ for the N2-Sn1-N3 angle. The sum of the angles at the tin centre is approx. 279° . The tin atom is not hybridised. Thus, the tin and the nitrogen atoms form a pyramid (**Figure 3-13**).

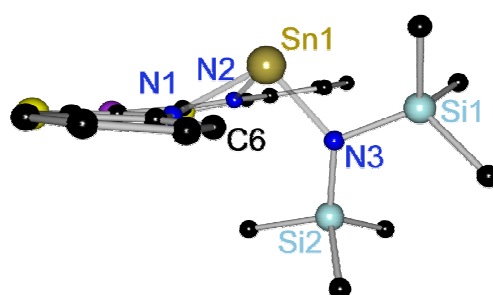


Figure 3-13: Coordination of Sn^{2+} in $[(\text{Me}_3\text{Si})_2\text{NSn}(\text{bth})_2\text{P}] \cdot 0.49(\text{Et}_2\text{O})$ (**6**) (disorder and Et_2O molecule omitted for clarity)

The Sn^{2+} centre is 78.7 pm out of the best plane defined by the ring nitrogen atoms and the C_{ipso} atoms. The displacement can be explained by the steric demand of the trimethylsilyl groups and the non-hybridised state of the metal atom. A position in-plane with the heteroaromatic rings would be advantageous. But this arrangement is precluded because at least one trimethylsilyl group would be too close to the di(benzothiazol-2-yl)phosphanide residue. Moreover, an in-line arrangement of the tin centred p orbitals with the sp^2 orbitals of the ring nitrogen atoms would cause an immense bending of the P-C bonds. To minimise steric interactions, the metal is forced out of the ligand plane. This unfavourable arrangement is partly compensated by the relatively short $\text{N}_{\text{bth}}-\text{Sn}$ bond distances.

The $\text{N}_{\text{bth}}-\text{C}_{\text{ipso}} \cdots \text{C}_{\text{ipso}}-\text{N}_{\text{bth}'}$ plane includes an angle of approx. 86° with the best plane defined by N3 and the silicon atoms. The methyl groups are staggered. The sum of the angles at the nitrogen atom N3 is approx. 358° . This indicates an almost planar environment at the sp^2 hybridised nitrogen atom N3.

The structure of $[(\text{Me}_3\text{Si})_2\text{NSn}(\text{bth})_2\text{P}] \cdot 0.49(\text{Et}_2\text{O})$ (**6**) is a compromise of numerous factors, such as the preference of metal centres to be in plane with the heteroaromatic ring systems,

the tendency of the di(benzothiazol-2-yl)phosphanide system to keep planarity, the necessity to reduce steric interactions and the need to maximise the overlap between unoccupied metal centred p-orbitals and occupied sp^2 -orbitals of the ring nitrogen atoms. Of course the size of the cation has a distinct influence on the complex geometry concerning bond distances and the distance of the metal centre from the best plane spanned by the atoms N1, C1, C8, and N2.

In solid state $[(Me_3Si)_2NSn(bth)_2P] \cdot 0.49(Et_2O)$ (**6**) forms rods along the b-axis (**Figure 3-14a**). The molecules are stacked with an intermolecular distance of approx. 310 pm and shifted by approx. 851 pm. The molecules are coplanar (**Figure 3-14b**). The rods are arranged with the soft S-P-S sides of the di(benzothiazol-2-yl)phosphanides facing each other and the trimethylsilyl sides separated from each other by non-coordinating diethylether molecules (**Figure 3-14c**).

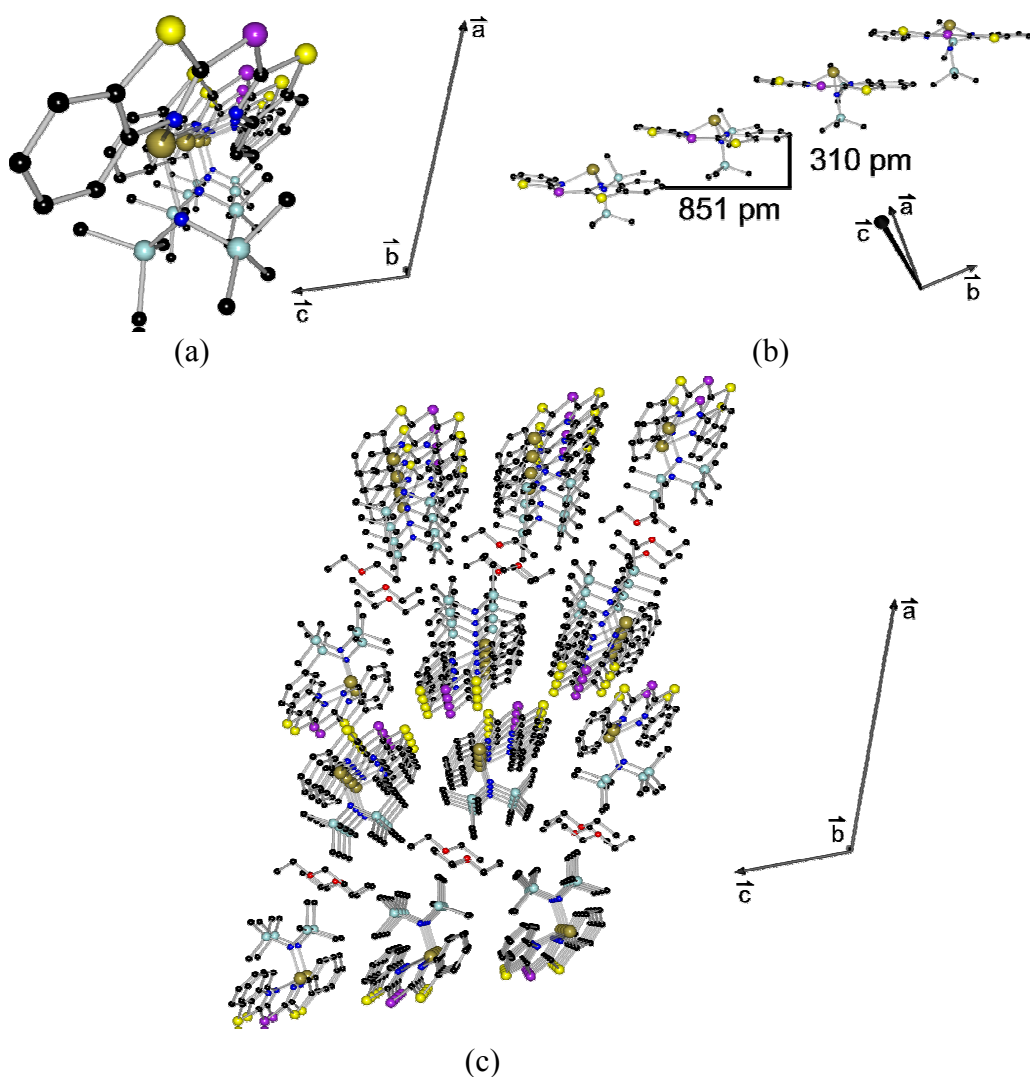


Figure 3-14: Solid state arrangement of $[(Me_3Si)_2NSn(bth)_2P] \cdot 0.49(Et_2O)$ (**6**) (Et_2O molecules omitted for clarity in (a) and (b))

3.6 Synthesis and Structure of $[\text{Fe}\{(\text{bth})_2\text{P}\}_2]\cdot 0.5(\text{Tol})$ (7)

Iron is a very important element, not only because of its economical impact but also because of its relevance in life science. Iron plays a vital role in biological systems. The function of iron in the erythrocytes is commonly known. It is essential for the oxygen supply of any cell to keep up oxidative processes. In the erythrocytes the iron atom is embedded in a heme porphyrin system. The porphyrin system is a four dentate nitrogen ligand derived from porphin (**Figure 3-15**). The central metal atom is coordinated by the four nitrogen atoms. In the iron complex, additional donors are usually placed above and below the porphyrin plane, increasing the coordination number to six.^[83] In other structures, the iron centre is fivefold^[84] or fourfold^[85] coordinated. In rare cases, both additional donor centres are placed at the same side of the porphyrin plane.^[86] For oxy-haemoglobin the additional donors are dioxygen and a sulfur atom from a histidine residue.

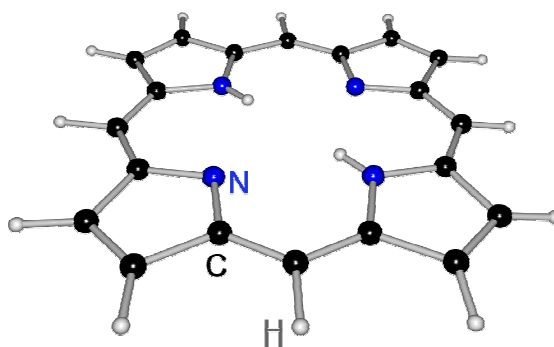


Figure 3-15: Crystal structure of porphin^[87]

Another very prominent heme-enzyme is cytochrome P450. This enzyme catalyses a broad variety of reactions. For example, hydrocarbon hydroxylation, alkene epoxidation, various dealkylations, diverse oxidations, isomerisations and even reductions are catalysed.^[88]

Other iron containing heme-proteins are the secondary amine monooxygenase, the heme oxygenase, the prostaglandin H synthase, the indoleamine 2,3-dioxygenase, or the tryptophan 2,3-dioxygenase.^[88]

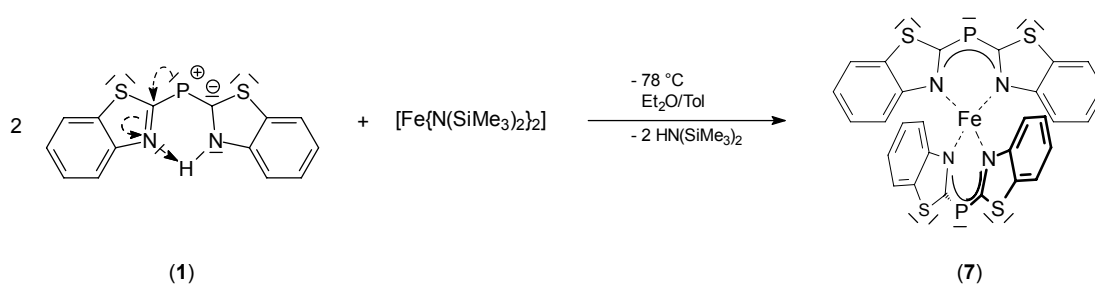
Besides heme systems, there are other iron containing enzymes playing important roles in biochemistry. For example phenylalanine hydroxylase is an enzyme that catalyses the oxidation of phenylalanine to tyrosine.^[89] The disease caused by the malfunction of this enzyme is called phenylketonuria. It leads to mental underdevelopment if not medicated. Other non-heme iron enzymes are for example monooxygenases^[90], lipoxygenases,

clavaminate synthase, isopenicilin N-synthase, ribonucleotide diphosphate reductase, rubreythrin, or ferritin.^[91]

But iron is not only important in biochemistry. The importance of α -iron in the *Haber-Bosch* process to generate ammonia from atmospheric nitrogen and hydrogen is also commonly known. In *Friedel-Crafts* reactions, namely alkylations and acylations, the lewis acidic iron(III) chloride works as an activator. Moreover, iron catalysts are used for the endothermic dehydrogenation of ethylbenzene to styrene^[92], the hydroformylation and hydrogenation of styrene,^[93] the oxidative coupling of 2-naphthols,^[94] the asymmetric *Mannich*-type reactions,^[95] chlorinations,^[96] ammoxidations,^[97] the water gas shift reaction,^[98] and the catalytic oxidation of H₂S.^[99]

Thus, it was of interest to investigate the coordination behaviour of di(benzothiazol-2-yl)-phosphanide towards iron centres. Iron(II) bis(bis(trimethylsilyl)amide) was employed as iron source.

Di(benzothiazol-2-yl)phosphane (**1**) was suspended in diethylether, cooled to -78 °C, and reacted with iron bis(bis(trimethylsilyl)amide)^[100] in a 2:1 ratio (**Scheme 3.6**). The reaction mixture turned from bright yellow to dark red. After stirring for two hours, the temperature was allowed to rise to room temperature. The solvent was removed under reduced pressure, and afterwards the solid residue was dissolved in toluene. Storage of the solution at room temperature for several weeks yielded crystals suitable for a single crystal X-ray diffraction experiment.



Scheme 3.6: Preparation of [Fe{(bth)₂P₂}]•0.5(Tol) (**7**)

Compound **7** crystallises in the triclinic space group $P\bar{1}$ with two complete formula units and a non coordinating toluene molecule in the asymmetric unit. There are only minor differences in the structural parameters between both moieties. Therefore, the values given below are average values.

Similar to porphyrin systems the iron centre is fourfold coordinated by the ring nitrogen atoms. The phosphorus atom is not directly involved in metal coordination. In contrast to iron porphyrin systems, the four nitrogen atoms in **7** are not located in the same plane. The spherical molecule contains two ligands, which are arranged like the two units of a tennis ball separated by the rubber imprint. The best plane defined by the atoms N–C_{ipso}...C_{ipso}–N' of one di(benzothiazol-2-yl)phosphanide unit intersects the corresponding one of the second phosphanide unit at an angle of 82.0° on average (**Figure 3-16**). This is not unprecedented as similar environments around iron centres are reported.^[101] The P1...Fe1...P2 angle of 170.4° indicates, that the benzothiazol-2-yl rings are tilted against each other.

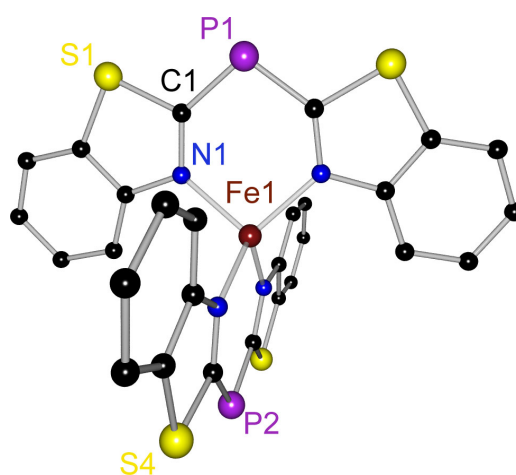


Figure 3-16: Crystal structure of $[Fe\{(bth)_2P\}_2] \cdot 0.5(Tol)$ (**7**) (only one formula unit depicted, toluene molecules omitted for clarity)

The P–C bond distances are 177.5(7) pm on average. This value is very close to the ones found in compounds **1** to **3**. It is between the values for standard P–C single and double bonds. The P–C bond distances are rather short because of the missing P–[M] interaction.

The C_{ipso}–N bond distances are 133.7(8) pm on average. The bond distance is between the values found for standard C_{sp2}–N_{sp2} single and double bonds (140 pm vs. 129 pm).^[50] The elongation compared to a standard double bond results from the electron density transfer from the phosphorus centre to the heteroaromatic rings.

The N...N bite distance is 303.8(16) pm. The corresponding values in $[(Et_2O)_2Li(bth)_2P]$ (**2**) and $[Me_2Al(bth)_2P]$ (**3**) are 308.7(2) pm and 292.4(5) pm, respectively. In **7** the angles included by the heteroaromatic rings of each phosphanide unit range from 4.3° to 12.3° (**Table 3-6**).

Table 3-6: Selected bond lengths [pm] and angles [°] of 7 (average values)

	bond length [pm]		bond angle [°]
P1–Cipso	177.5(7)	C1–P1–C8	104.0(2)
Cipso–N	133.7(8)	Nbth–Fe–Nbth'	98.2(2)
N–Fe	201.0(8)		
N...N	303.8(16)		
			angle between planes [°]
		(bth)...(bth')	4.3 to 12.3

The N–Fe distances are 201.0(8) pm on average. The CSD lists distances for similar N–Fe bonds from approx. 190 pm to 213 pm.^[72;101b,c;102] The bond is best described as having a character between amidic and a dative bond.

The C–P–C angle is 104.0(2)° on average. This value is in accordance with an sp³ hybridised phosphorus atom. The phosphorus atom is dislocated 8.4 pm on average out of the N_{bth}–C_{ipso}...C_{ipso}–N_{bth'} plane.

The environment at the metal centre is best described as a distorted tetrahedron. The N–Fe–N angles vary from 97.9(1)° to 124.6(1)°. The acuter angles are found with both nitrogen atoms of the same chelating di(benzothiazol-2-yl)phosphanide ligand (av. 98.2(4)°). The other N–Fe–N angles range from 106.4(1)° to 124.6(1)°.

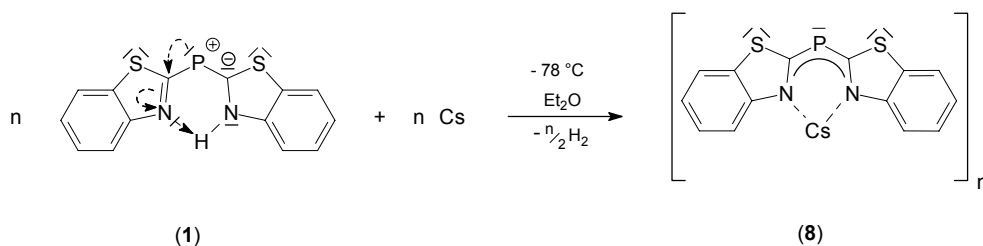
A hypothetical coplanar arrangement like in porphyrin systems is precluded as the steric demand of annulated six-membered rings would enlarge the distances between the nitrogen atoms of the two ligands, making them unattractive for iron coordination. This leaves the iron(II) centre with the coordination number of four and a sum of 14 valence electrons.

3.7 Synthesis and Structure of [Cs(bth)₂P]_∞ (8)

As seen in the previous complexes, the phosphorus centre does not necessarily participate in metal coordination. One approach to involve the bridging phosphorus atom in metal coordination seems to introduce a very soft metal. Caesium seems the obvious choice as the caesium cation has the largest cationic radius.

Consequently, the phosphane **1** was reacted with elemental caesium in a 1:1 ratio in diethyl-ether at $-78\text{ }^{\circ}\text{C}$ (**Scheme 3.7**). The reaction mixture turned deep red while gas evolved. After four hours of stirring at this temperature, the solution was allowed to warm to ambient temperature.

After reducing the amount of solvent, the reaction mixture was stored at $+4\text{ }^{\circ}\text{C}$, yielding red crystals suitable for a single crystal X-ray diffraction experiment.



Scheme 3.7: Preparation of $[\text{Cs}(\text{bth})_2\text{P}]_{\infty}$ (**8**)

Compound **8** crystallises in the orthorhombic space group $\text{Cmc}2_1$ with the asymmetric unit consisting of half the monomer. The di(benzothiazol-2-yl)phosphanide is generated via an a-mirror plane and translation 2, 0, 0. The neighbouring molecule is composed by a 2_1 screw axis in z and translation 2, 2, 0.5.

In the coordination polymer the caesium cations are bonded to four ring nitrogen atoms and two phosphorus atoms of four different phosphanide units. Hence, each phosphanide ligand is coordinates four different caesium cations (**Figure 3-17**).

The P–C bond distance in the anionic ligand is 179.2(4) pm (**Table 3-7**). As there are P–[M] interactions and a charge delocalisation throughout the whole ligand system is limited, a distorted geometry is observed. This results in relatively long P–C bond distances and is also responsible for the fact that a coordination mode similar to the one observed for $[(\text{PMDETA})\text{Cs}(\text{py})_2\text{P}]_2$ is not realised.^[38] The pyridyl compound shows a phospho-aza-allylic coordination. Each phosphanide coordinates two metal atoms. For the benzothiazol-2-yl compound the addition of donor bases might have resulted in a similar coordination mode, probably with the sulfur atom as the second heteroatom of the allylic system instead of the hard nitrogen donor. Experimental evidence therefore is still missing.

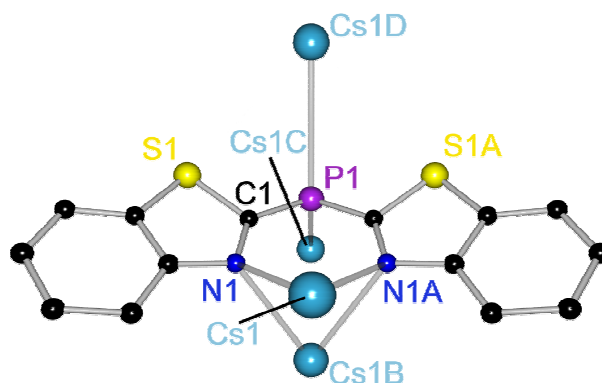


Figure 3-17: Crystal structure of $[Cs(bth)_2P]_\infty$ (**8**) (only part of the polymer depicted)

Table 3-7: Selected bond lengths [pm] and angles [$^\circ$] of $[Cs(bth)_2P]_\infty$ (**8**)

	bond length [pm]		bond angle [$^\circ$]	
P1–C	179.2(4)	C–P–C	103.3(3)	
C _{ipso} –N	131.3(5)	Nbth–Cs1–Nbth'	60.0(1)	
N1–Cs1	321.4(4)	Nbth–Cs1B–Nbth'	60.6(1)	
N1–Cs1B	318.6(3)	Cs1C–P–Cs1D	126.1(1)	
P1–Cs1C	367.2(2)			
P1–Cs1D	361.6(2)			angle between planes [$^\circ$]
N1...N1A	321.4(7)	(bth)...(bth')	32.5	

The C_{ipso} –N bond distances are 131.3(5) pm on average. A standard C–N single bond distance is approx. 140 pm for sp^2 hybridised atoms and a double bond distance is approx. 129 pm.^[50] As electron density is shifted directly from the phosphorus centre to the metal centres, the amount of electron density available for a transfer into the heteroaromatic rings is reduced. As a consequence, the C_{ipso} –N bond distances almost have the value of a standard double bond.

The N–Cs bond distances are 321.4(4) pm for the N1–Cs1 bond and 318.6(3) pm for the N1–Cs1B bond. The shortest N–CS bond listed is found in $[CsN(H)SiMe_3]_4$ (291.5(5) pm).^[103] In polymeric $[(THF)Cs_2\{Ph(Me_3SiN)P\}_2]_\infty$ the N–Cs bond distances range from 309.5(4) to 316.2(4) pm.^[104] The N–Cs bond distances in dimeric caesium bis(trimethylsilyl)amide are 307.4(2) pm and 314.9(2) pm.^[67a] In a polymer, with the caesium

atoms additionally coordinated by dioxane molecules the N–Cs bond distances are 306.7(1) and 338.8(2) pm.^[105] The latter is one of the longest listed in the CSD.

The P–Cs bond distances are 367.2(2) pm for the P1–Cs1C bond and 361.6(2) pm for the P1–Cs1D bond. Corresponding bond distances listed in the CSD range from 342 to 411 pm.^[72] In $[\mu_2(\text{THF})\{\text{CsP}(\text{H})^t\text{Bu}_3\text{C}_6\text{H}_2\}_2]$ the P–Cs bond distances range from 350.5(3) to 409.7(3) pm.^[106] In $[\mu_2(\text{py})\{\text{CsP}(\text{H})^t\text{Bu}_3\text{C}_6\text{H}_2\}_2]_\infty$ the P–Cs bond distances range from 362.6(3) pm to 398.6(3) pm.^[106] In $[(18\text{-crown-6})\text{CsP}(\text{H})^t\text{Bu}_3\text{C}_6\text{H}_2]$ two independent molecules are present in the asymmetric unit. The P–Cs bond distances are 384.7(2) and 406.9(3) pm stressing the extreme flexibility of caesium regarding bond distances.

The N1...N1A distance in **8** is 321.4(7) pm. This is the largest distance observed for the bite distance in di(benzothiazol-2-yl)phosphanides so far. The benzothiazol-2-yl rings are rotated about the P–C_{ipso} bonds in the same direction. The best planes defined by the atoms of the heteroaromatic rings include an angle of 32.5°. The maximum in bite distance in this compound is caused by the maximum rotation of the heteroaromatic rings about the P–C bonds (**Figure 3-18a**). The reason is the size of the cation (radius of 167 pm for the sixfold coordinated Cs⁺ cation).^[75] The cations are displaced from the plane defined by the atoms N1, C1, C1A, and N1A. Cs1 is approx. 178 pm, Cs1B approx. 263 pm out of plane. This arrangement is a compromise between the preference for planarity and the tendency to achieve greatest possible proximity of the cationic metal centres to electron density maxima.

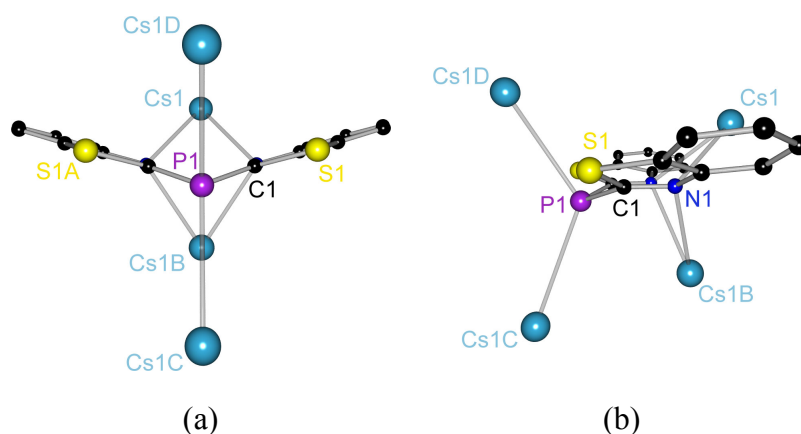


Figure 3-18: Lateral views on $[\text{Cs}(\text{bth})_2\text{P}]_\infty$ (**8**) (only part of the polymer depicted)

The rotation of the heteroaromatic rings about the P–C_{ipso} bonds causes a decrease of the S1...Cs1D distance (412.7(1) pm) (**Figure 3-18b**). In the literature, only a few S–Cs bond distances are listed. Thiolato complexes show the shortest distances from approx. 330 to

360 pm.^[107] Bond distances for dative bonds found in thioethers or thioketones range from approx. 370 to 390 pm.^[108] The caesium as well as the sulfur atoms are soft and polarisable enough to enable them to establish interactions. These support the folding of the ligand and enhance the formation of the butterfly arrangement.

The C–P–C angle is 103.3(3)°. The Cs1C–P1–Cs1D angle is 126.1(1)° and the C–P–Cs angles are 114.8(1)° for C1–P1–Cs1C and 97.0(1)° for C1–P1–Cs1D. This is in accordance with an sp^3 hybridisation of the phosphorus centre. Different to the situation in [(Me₃Si)₂NZn(bth)₂P]₂•2(THF) (**4**) and [(Me₃Si)₂NCd(bth)₂P]₂•(THF) (**5**), the metal atoms Cs1C and Cs1D in **8** are located in the direction of the sp^3 lone pairs. Thus, the electron density shift is facilitated.

The N_{bth}–Cs–N_{bth} angles are 60.0(1)° for N1–Cs1–N1A and 60.6(1)° for N1–Cs1B–N1A. These quite acute angles are due to the multiple coordination of each metal centre, the electron density demand of the metals, and geometrical restrictions.

All cations coordinated by a single di(benzothiazol-2-yl)phosphanide unit are arranged on a mirror plane through the bridging phosphorus atom (**Figure 3-18a**). The coordination number of each caesium centre is six. The coordination polyhedron of each cation is best described as a distorted trigonal prism (**Figure 3-19**).

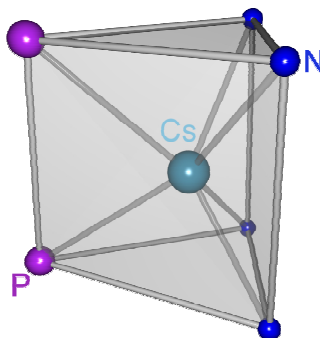


Figure 3-19: Distorted trigonal prismatic environment of caesium cations in [Cs(bth)₂P]_∞ (**8**)

Each caesium centre is coordinated by four nitrogen atoms of two different di(benzothiazol-2-yl)phosphanide ligands. The two additional phosphorus atoms are contributed from two further ligands (**Figure 3-20**). In solid state caesium di(benzothiazol-2-yl)phosphanide (**8**) forms layers parallel to the crystallographic b-c plane. These layers do not interact.

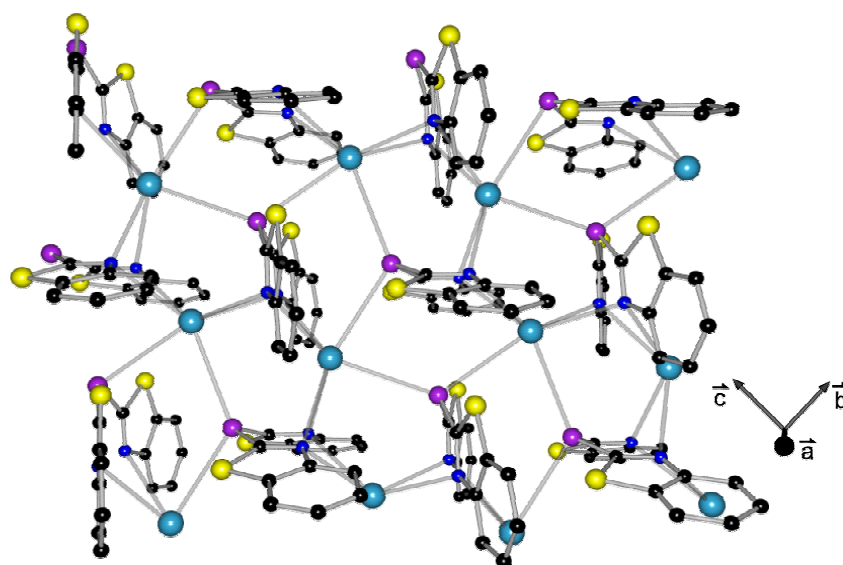


Figure 3-20: Packing of $[Cs(bth)_2P]_\infty$ (**8**) in solid state (only part of the polymer depicted)

Despite the huge caesium cation the hard nitrogen donor centres of the ligand system seem to be dominant in metal coordination. Nevertheless, the phosphorus centre is involved in charge density transfer to some extent. It is not only the size of the cation that forces the caesium centres out of the plane spanned by the atoms N1–C1...C1A–N1A, but also the electron density transfer of neighbouring phosphanide units via their nitrogen atoms to the metal centres. Additionally, electron density located at the phosphorus centres of adjacent di(benzothiazol-2-yl)phosphanide units attracts the metal centres and therefore enhances the displacement of the caesium centres.

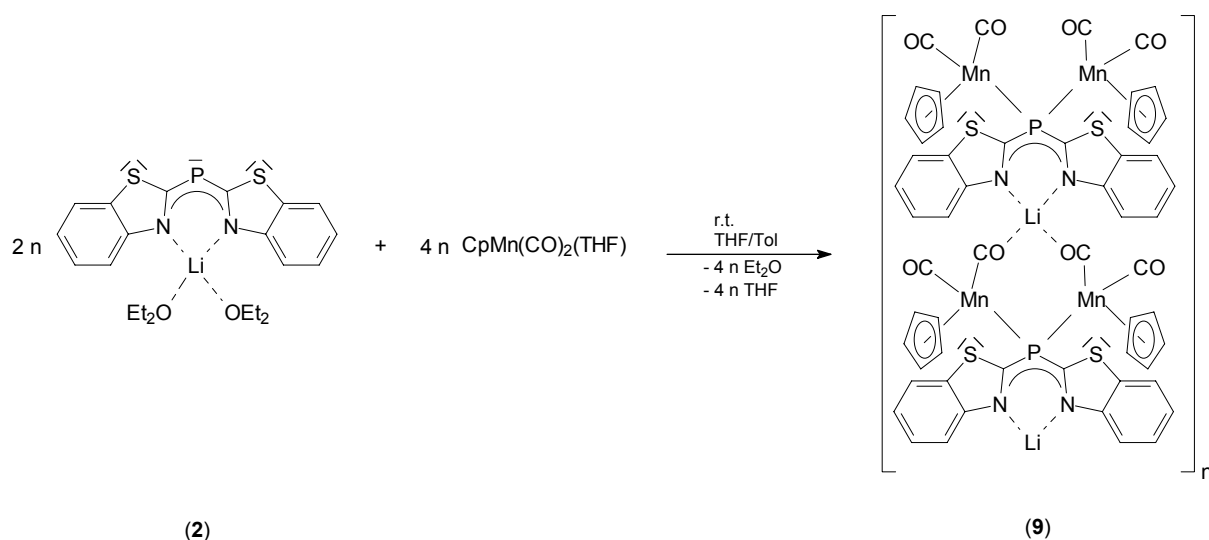
3.8 Synthesis and Structure of $[Li(bth)_2P\{Mn(CO)_2Cp\}_2]_\infty \cdot 2.5(Tol)$ (**9**)

The results, discussed so far, showed, that the di(benzothiazol-2-yl)phosphanide coordinates metal centres predominantly by the ring nitrogen atoms regardless of size and hardness of the metal cation offered. Despite the very big caesium cation the major amount of electron density seems to be transferred from the hard nitrogen atoms. But as shown for $[(Me_3Si)_2NZn(bth)_2P]_2 \cdot 2(THF)$ (**4**), $[(Me_3Si)_2NCd(bth)_2P]_2 \cdot (THF)$ (**5**), and $[Cs(bth)_2P]_\infty$ (**8**), the phosphorus centre can be utilised in metal coordination. To further substantiate this fact, it was necessary to synthesise complexes with phosphorus–metal contacts definitely separated from N–[M] contacts

Changing size, charge, and hardness of the employed basic metal fragments did not furnish dominantly phosphorus coordinated metal species yet. Therefore, more sophisticated d-block organometallic moieties needed to be utilized to be coordinated to the phosphorus face of the *Janus head* ligand. Those transition metal organometallics should be accessible for the metal phosphanide via a vacant coordination site, possibly *in situ* generated by the release of a weakly coordinated labile donor ligand.

Transition metal carbonyls are known to form complexes with almost every electron density donor available. Group six pentacarbonyls for example even interact with noble gases.^[109] In the course of this thesis the cyclopentadienyl manganese dicarbonyl fragment was selected as a promising starting material. Although cyclopentadienyl manganese tricarbonyl does not react with triphenylphosphane even if heated up to 200 °C, one carbon monoxide ligand is readily removed under photolytic conditions.^[110] If the photolysis is carried out in tetrahydrofuran, the cyclopentadienyl manganese dicarbonyl is trapped by an ether molecule yielding the tetrahydrofuran substituted species. The Mn–O_{THF} bond dissociation energy was found to be about 100 kJ/mol.^[111] Therefore, it is not astonishing that cyclopentadienyl dicarbonyl manganese is a ubiquitous metal fragment in organometallic chemistry.^[112]

Tetrahydrofuran coordinated cyclopentadienyl dicarbonyl manganese was reacted with [(Et₂O)₂Li(bth)₂P] (**2**) in a 2:1 ratio in tetrahydrofuran at room temperature. The solvent was removed under reduced pressure. Toluene was added to the grey precipitate and the deep red suspension was filtered over celite. The solution was stored at -35 °C for several days to gain red crystals suitable for a single crystal X-ray diffraction experiment (**Scheme 3.8**).



Scheme 3.8: Synthesis of [Li(bth)₂P{Mn(CO)₂Cp}₂]_∞•2.5(Tol) (**9**)

$[\text{Li}(\text{bth})_2\text{P}\{\text{Mn}(\text{CO})_2\text{Cp}\}_2]_\infty \cdot 2.5(\text{Tol})$ (**9**) crystallises in the monoclinic space group $C2/c$ with one complete formula unit in the asymmetric unit and two and a half non coordinating toluene molecules one of which is disordered over two positions.

As anticipated, the lithium di(benzothiazol-2-yl)phosphanide (**2**) coordinates the manganese metal, replacing the THF molecule in the transition metal complex. Each phosphorus atom in the product is bridging two $\text{CpMn}(\text{CO})_2$ moieties, akin the cationic metal fragment $[\{\text{Cp}(\text{CO})_2\text{Fe}\}_2\{\mu\text{-P}\text{py}_2\}]^+$.^[38] The nitrogen face of the ligand coordinates the lithium atom like in the starting material **2** (**Figure 3-21**). The diethylether molecules of the employed phosphanide are replaced by two bridging carbon monoxide molecules. This leads to infinite strands.

The P–C bond distances in this structure are the longest ever observed in related species as they are 185.2(4) pm for the P1–C1 bond and 185.5(4) pm for the P1–C8 bond (**Table 3-8**). In $(\text{bth})_3\text{P}$ the P–C bond distances are 182.0(2) pm on average.^[51] These values match those of standard P–C single bonds.^[50] Employing the phosphorus centre in metal coordination leads to long P–C bond distances.

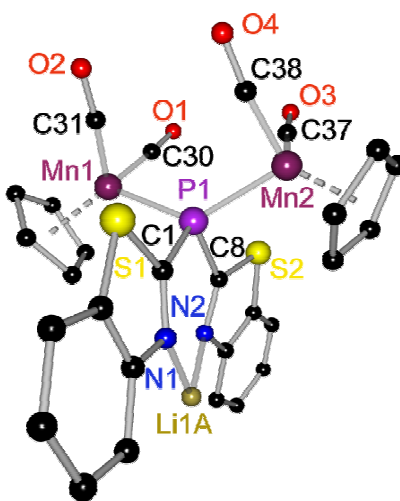


Figure 3-21: Crystal structure of $[\text{Li}(\text{bth})_2\text{P}\{\text{Mn}(\text{CO})_2\text{Cp}\}_2]_\infty \cdot 2.5(\text{Tol})$ (**9**) (only part of the polymer depicted; toluene molecules omitted for clarity)

The C1–N1 bond distance is 129.6(4) pm and the C8–N2 bond distance is 129.7(4) pm. These bond distances indicate double bonds between the related atoms. The P–C bond distances in **9** are maximum values in the series of compounds **1** to **9** while the $C_{\text{ipso}}\text{-N}$ bond distances are minimum values. The simultaneous coordination of the manganese and the lithium centres therefore causes distinct changes in the bond distances of the ligand. The electron density transfer into the heteroaromatic systems via the P– C_{ipso} bonds is only marginal, which can be

seen by the more pronounced twist of both heteroaromatic rings compared to the starting material. In **9** the best planes defined by the atoms of the benzothiazol-2-yl rings intersect at an angle of 24.7°. The corresponding angle in **2** is 9.9°.

Table 3-8: Selected bond lengths [pm] and angles [°] of $[Li(bth)_2P\{Mn(CO)_2Cp\}_2]_{\infty} \cdot 2.5(Tol)$ (**9**)

	bond length [pm]		bond angle [°]	
P1–C1	185.2(4)	C1–P1–C8	102.7(2)	
P1–C8	185.5(4)	Mn1–P1–Mn2	130.7(1)	
C1–N1	129.6(4)	Mn1–P1–C1	104.6(1)	
C8–N2	129.7(4)	Mn1–P1–C8	103.8(1)	
N1–Li1A	199.0(7)	Mn2–P1–C1	105.3(1)	
N2–Li1A	199.5(7)	Mn2–P1–C8	106.6(1)	
P–Mn1C	229.2(1)	N1–Li1A–N2	100.7(3)	
P–Mn2	229.6(1)			
O2–Li1	194.8(7)			angle between planes [°]
O4–Li1	192.6(7)	(bth)···(bth')	24.7	
Cp–Mn1	178.1			
Cp–Mn2	178.3			
C30–Mn1	178.5(4)			
C31–Mn1	173.7(4)			
C37–Mn2	176.5(4)			
C38–Mn2	174.1(4)			
C30–O1	116.0(5)			
C31–O2	118.0(5)			
C37–O3	116.8(5)			
C38–O4	117.3(5)			
N1···N2	306.9(4)			

The rotation is limited by the coordination to the lithium cation, which forces the heteroaromatic rings closer to coplanarity. Nevertheless, the nitrogen lone pairs do not point at one position. Similar to the situation in $[(\text{Et}_2\text{O})_2\text{Li}(\text{bth})_2\text{P}]$ (**2**), the lithium atom is forced out of the benzothiazol-2-yl ring planes. As in **2**, the displacement is asymmetric. The lithium cation is located 25.2 pm above the plane defined by one heteroaromatic ring, while it is located 90.4 pm below the plane defined by the other heteroaromatic ring. This asymmetry is more distinct in **9** than in **2**, where the lithium cation is almost in plane with one ring system and 45.1 pm out of plane for the other heteroaromatic system. As the geometric mismatch increases, the lithium cation has to get closer to the nitrogen atoms to compensate reduced overlap with the sp^2 nitrogen orbitals. The N–Li bond distances are 199.0(7) pm for the N1–Li1A bond and 199.5(7) pm for the N2–Li1A bond. The N–Li bond distances in $[(\text{Et}_2\text{O})_2\text{Li}(\text{bth})_2\text{P}]$ (**2**) are 202.9(8) pm on average. The changes in bond distances discussed above (P–C and C–N bonds) lead to longer N···N distances. This is partly compensated by the C–P–C angle getting more acute. It decreases from $104.2(1)^\circ$ in **2** to $102.7(2)^\circ$ in $[\text{Li}(\text{bth})_2\text{P}\{\text{Mn}(\text{CO})_2\text{Cp}\}_2]_\infty \cdot 2.5(\text{Tol})$ (**9**). In fact this causes the bite distance N1···N2 to decrease from 308.7(2) pm in **2** to 306.9(4) pm in **9**.

There is enough electron density left at the phosphorus centre to replace a tetrahydrofuran ligand in the manganese organometallic starting material. With the manganese centres getting coordinated, the electron density at the phosphorus centre that usually couples into the heteroaromatic ring systems is needed for the coordination of the manganese atoms. This leads to P– C_{ipso} bond distances in the range of single bonds. Consequently, a C_{ipso} –N bond elongation is not observed. The C_{ipso} –N bond distances are in good agreement with double bonds. The phosphorus centre in **9** is a four electron donor as it formally transfers two electrons to each of the two manganese centres. The manganese atoms are located almost in the direction of the lone pairs at the sp^3 hybridised phosphorus centre. The deduced hybridisation is in accordance with the results of the theoretical calculations for the parent di(benzothiazol-2-yl)-phosphane (**1**) (see *chapter 2.3*).

Each manganese centre is additionally coordinated to a cyclopentadienide ligand. The distances between the centres of gravity of the cyclopentadienide rings and the coordinated manganese atoms are 178 pm on average. In the parent cyclopentadienyl manganese tricarbonyl the distance between the manganese atom and the centre of gravity of the C_5 perimeter is 177.2 pm.^[113] Furthermore, each manganese atom is coordinated by two carbon monoxide donor molecules. One of which is bridging the manganese and lithium atoms. (*Figure 3-22*). Thus, the electron density in the bridging carbonyls has to be shared

between two metals and is reduced in comparison to the non-bridging carbonyl ligands. This electronic depletion is partly compensated by an emphasised back bonding from metal centred occupied d-orbitals into π^* -orbitals of the bridging carbonyl moieties. This leads to shorter Mn–CO_{bridging} bond distances (173.7(4) pm for Mn1–C31 and 174.1(4) pm for Mn2–C38). The Mn1–C30 bond distance is 178.5(4) pm and the Mn2–C37 bond distance is 176.5(4) pm. OC–Mn bond distances range from 147 to 218 pm.^[114] If the carbonyl bridges two metals the OC–[M] bond distances range from 172 pm to 182 pm.^[115]

A consequence of the population of the π^* -orbitals is the elongation of the corresponding C–O bond distances to 118.0(5) pm for the C31–O2 bond and 117.3(5) pm for the C38–O4 bond. The C30–O1 bond distance is 116.0(5) pm and the C37–O3 bond distance is 116.8(5) pm. In carbonyl complexes the C–O bond distances span a wide range from 60 pm up to 191 pm.^[116] The bond distance depends on the electron density shifts as there are OC→[M] σ -bonding and the [M]→CO $d\pi$ – $p\pi$ -back bonding interactions. For bridging carbonyls the C–O bond distances range from 113 to 138 pm.^[117] When lithium is coordinated by oxygen the bond distances only range from 114 to 118 pm.^[118] Long C–O bond distances go along with short CO–Li distances. The O2–Li1 bond distance is 194.8(7) pm and the O4–Li1 bond distance is 192.6(7) pm. These bond distances are rather short, as one can expect from the long C–O bond distances.

The angles around the phosphorus centre range from 102.7(2)° for the C–P–C angle to 130.7(1)° for the Mn1–P1–Mn2 angle. The environment around P1 is best described as a distorted tetrahedron as is for the lithium atom.

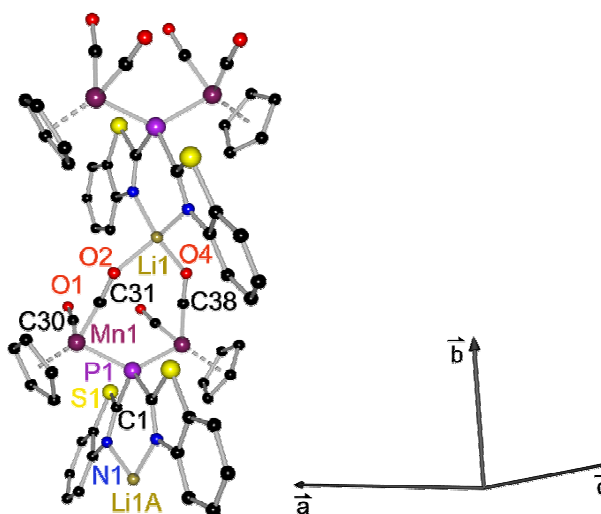


Figure 3-22: Polymeric chain of $[Li(bth)_2P\{Mn(CO)_2Cp\}_2]_\infty \cdot 2.5 (Tol)$ (**9**) (only part of the polymer depicted, toluene molecules omitted for clarity)

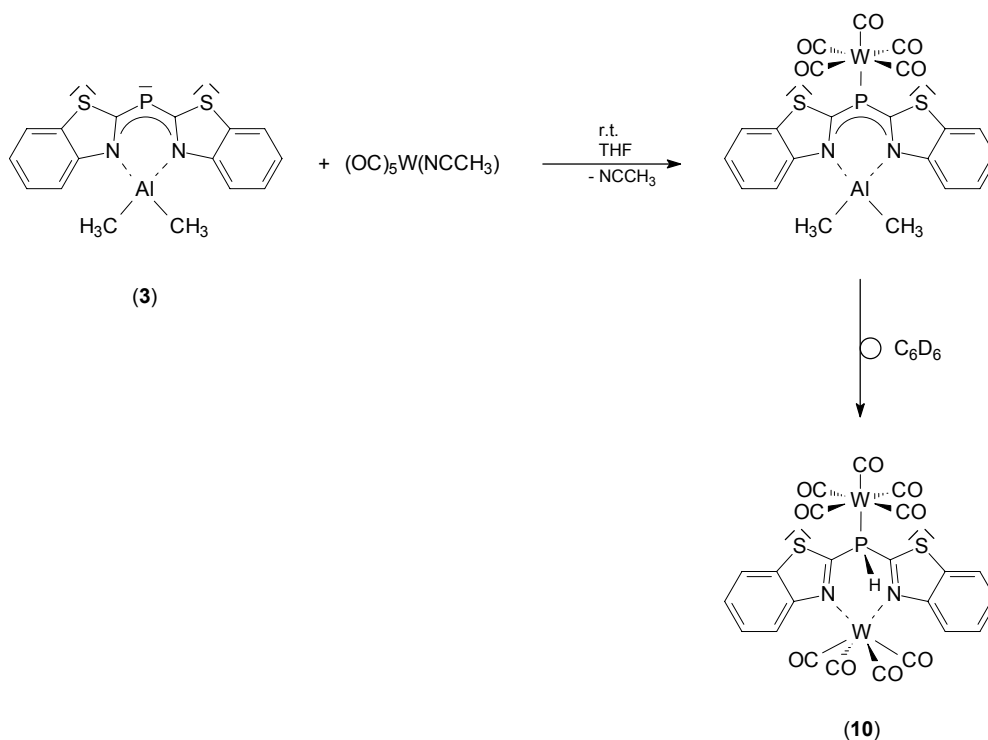
The bridging carbonyl units are responsible for the coordination polymer of **9** (*Figure 3-22*). CO–Li distances for bridging carbon monoxide units range from 191 pm to 217 pm.^[118] The coordination leads to polymeric chains in solid state. Single chains do not interlock. They are arranged in a way that neighbouring chains are oriented in opposite directions.

In summary, the di(benzothiazol-2-yl)phosphanide ligand in $[\text{Li}(\text{bth})_2\text{P}\{\text{Mn}(\text{CO})_2\text{Cp}\}_2]_\infty \cdot 2.5(\text{Tol})$ (**9**) has proven to be an advanced *Janus head* ligand. It was shown that the ligand is able to coordinate different metals at the same time, as long as a suitable metal fragment is present. It was shown that both qualitative different donating sides of the ligand coordinate as expected. Moreover, an sp^3 hybridisation state of the central phosphorus atom in accordance with theoretical findings (see *chapter 2.3*) can be verified in experiment.

3.9 Syntheses and Structure of $[(\text{OC})_4\text{W}(\text{bth})_2\text{P}(\text{H})\text{W}(\text{CO})_5] \cdot \text{C}_6\text{D}_6$ (**10**)

We succeeded in coordinating two different metal centres at the same time in $[\text{Li}(\text{bth})_2\text{P}\{\text{Mn}(\text{CO})_2\text{Cp}\}_2]_\infty \cdot 2.5(\text{Tol})$ (**9**), so the next aim was to replace the lithium atom by metals more relevant in catalysis. As discussed earlier, aluminium is one of the most important co-catalysts. Thus, $[\text{Me}_2\text{Al}(\text{bth})_2\text{P}]$ (**3**) was reacted with acetonitrile-coordinated tungsten pentacarbonyl.^[119]

Acetonitrile-coordinated tungsten pentacarbonyl was added to $[\text{Me}_2\text{Al}(\text{bth})_2\text{P}]$ (**3**), dissolved in tetrahydrofuran, at room temperature. After stirring the solution for five hours the solvent was removed and deuterio-benzene was added. Insoluble parts were removed and the red solution was stored at room temperature. The storage yielded red crystals suitable for a single crystal X-ray diffraction experiment after 3 weeks (*Scheme 3.9*).



Scheme 3.9: Synthesis of $[(OC)_4W(bth)_2P(H)W(CO)_3] \cdot C_6D_6$ (10)

^{31}P NMR spectra showed, that the reaction was completed after 22 hours. After additional 24 hours a second signal in the ^{31}P NMR spectrum was growing in on the expense of the first. The X-ray diffraction experiment revealed, that the phosphorus centre coordinates a tungsten fragment in the axial position. This tungsten atom is coordinated by one additional axial and four equatorial carbonyl donors. Unfortunately, the dimethyl aluminium fragment from the starting material is replaced by a second tungsten moiety in the product. In the latter a tungsten tetracarbonyl moiety is coordinated by both nitrogen atoms of the ligand. Furthermore, the phosphorus centre of the product is protonated, as proven by IR spectroscopy (**Figure 3-23**).

In order to trace the origin of the P–H hydrogen atom an analogue reaction was carried out with tetrahydrofuran-coordinated tungsten pentacarbonyl instead of the acetonitrile compound. The work-up of the latter involves the treatment with water during its synthesis and it was suspected that the starting product might not have been water-free. Tetrahydrofuran-coordinated tungsten pentacarbonyl was prepared from tungsten hexacarbonyl by photolysis in tetrahydrofuran without any aqueous preparation step.^[110a]

The reaction yielded in $[(OC)_4W(bth)_2P(H)W(CO)_5] \cdot C_6D_6$ (**10**) as well. Therefore, residual water can be excluded as source of the hydrogen atom bonded to the phosphorus centre. As there are some insoluble by-products, which could not be identified so far, the reaction path could not be revealed. Traces of water might be responsible for the protonation in the first synthesis while acidic hydrogen atoms in THF might generate the secondary phosphane in the second. However, the hydrogen atom might also originate from the Me_2Al^+ -fragment, lost in the ligand fragmentation reaction.

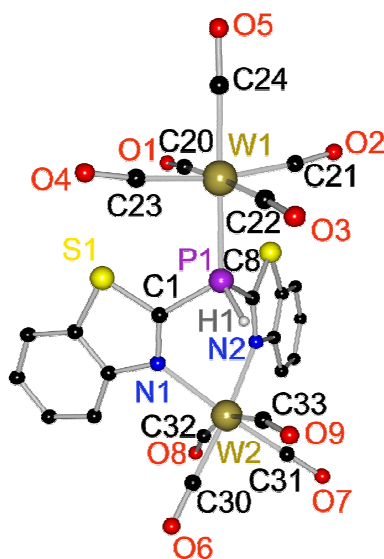


Figure 3-23: Crystal structure of $[(OC)_4W(bth)_2P(H)W(CO)_5] \cdot C_6D_6$ (**10**) (C_6D_6 molecules omitted for clarity)

With the hydrogen atom at the phosphorus centre, the ligand adopts the geometry expected for secondary phosphanes. In contrast to the parent tri(benzothiazol-2-yl)phosphane,^[51] the heteroaromatic rings are *trans-trans* arranged. This is caused by the tungsten moiety that is coordinated by the two ring nitrogen atoms.

The P1–C1 bond distance is 182.6(3) pm and the P1–C8 bond distance is 182.5(4) pm (**Table 3-9**). These bond distances match those of tri(benzothiazol-2-yl)phosphane (182.0(2) pm).^[51] The bonds can be regarded as single bonds.

The position of the hydrogen atom was taken from the Fourier difference map and refined freely. The P1–H1 bond distance is 134.1(44) pm. In phenyl substituted secondary phosphanes with a metal fragment coordinated to the phosphorus centre, the P–H bond distances range from approx. 98 to 180 pm.^[120] In $(OC)_5W-P(H)Ph_2$ the P–H bond distance is 112.3 pm.^[121]

The P1–W1 bond distance is 246.9(1) pm. P–W bond distances of secondary phosphanes range from approx. 240 to 250 pm.^[120a;122] The longest listed is found in (OC)₅W–P(H)Ph₂ (252.5 pm).^[121]

Table 3-9: Selected bond lengths [pm] and angles of [(OC)₄W(bth)₂P(H)W(CO)₅]•C₆D₆ (**10**)

	bond length [pm]		bond angle [°]
P1–C1	182.6(3)	C1–P1–C8	95.0(2)
P1–C8	182.5(4)	C _{ipso} –P1–H1 (av.)	98.0(20)
P1–H1	134.1(44)	C _{ipso} –P1–W1 (av.)	120.4(2)
C1–N1	131.3(4)	H1–P1–W1	119.7(18)
C8–N2	131.4(4)		
P1–W1	246.9(1)		angle between planes [°]
N1–W2	227.6(3)	(bth)···(bth')	101.4
N2–W2	227.7(3)		
C24–W1	201.4(4)		
C _{eq} –W1 (av.)	204.7(22)		
C–W2 (av.)	199.8		
N1···N2	293.3(4)		

The C1–P1–C8 angle is 95.0(2)° and the heteroaromatic rings include an angle of 101.4°. The analogue optimised structure ‘*trans-trans*’ (see **chapter 2.3**) shows a C–P–C angle of 102.4°. The C_{ipso}–P1–H1 angles are 98.0(20)° on average. These angles are in accordance with a non-hybridised phosphorus centre. Therefore, the lone pair at the phosphorus centre has mainly s-character. The electron density of the lone pair does not interact with the electron density of the heteroaromatic rings. The hybridisation explains the angles included by P1, W1, and the atoms attached to P1 as well. The W1–P1–C angles are 120.4(2)° on average and the W1–P1–H1 angle is 119.7(18)°.

The angles included by adjacent equatorial carbon atoms and the tungsten centre are $90.2(5)^\circ$ on average. The sum of these angles is 360.7° . The equatorial carbonyl groups are arranged in a way that one of them is orientated along the bisector between both heteroaromatic rings. The opposite one is orientated along the P1–H1 bonding vector (**Figure 3-24**).

The angle C24–W1–P1 is $179.0(1)^\circ$, resembling an almost linear arrangement of the atoms. The angle C24–W1–C21 is $85.0(2)^\circ$, the angle C24–W1–C23 is $85.3(2)^\circ$, and the angle C21–W1–C23 is $170.2(1)^\circ$. The carbonyl groups, arranged eclipsed to the phosphane, are considerably bent towards the apical CO ligand. The angle C20–W1–C22 is $176.2(2)^\circ$. The angle C24–W1–C20 is $90.1(2)^\circ$, while the angle C24–W1–C22 is $93.6(2)^\circ$. The tungsten pentacarbonyl moiety is tilted towards the hydrogen atom H1. Nevertheless, the environment around the tungsten atom W1 is best described as a distorted octahedron. The carbonyl groups are arranged almost linear, with W1–C–O angles from $174.6(3)^\circ$ to $178.9(5)^\circ$.

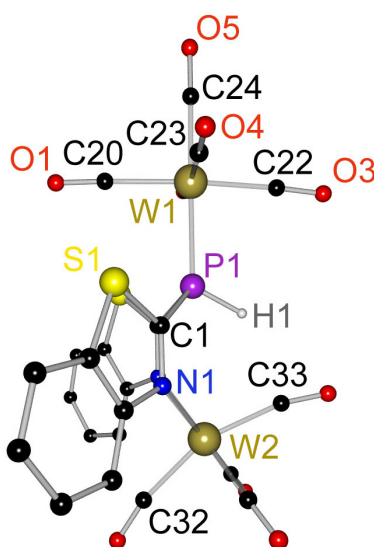


Figure 3-24: Lateral view on of $[(OC)_4W(bth)_2P(H)W(CO)_5] \cdot C_6D_6$ (**10**) (C_6D_6 molecules omitted for clarity)

The C1–N1 bond distance is 131.3(4) pm and the C8–N2 bond distance is 131.4(4) pm. These bond distances are between those of the corresponding single and double bonds.^[50] The N_{bth} –W bond distances are 227.6(3) pm (N1–W2) and 227.7(3) pm (N2–W2). The N–W bond distances of similar complexes range from approx. 220 to 230 pm.^[123]

The tungsten atom W2 is av. 24.1 pm out of the planes defined by the heteroaromatic rings. The C_{ipso} – N_{bth} –W2 angles are $123.7(3)^\circ$ on average. The C1–N1–C7 angle is $109.7(3)^\circ$ and

the C8–N2–C14 angle is 109.9(3)°. The angle C7–N1–W2 is 126.2(2) and the angle C14–N2–W2 is 126.2(2)°. Therefore, the tungsten atom W2 is positioned almost in line with the lone pairs at the nitrogen atoms N1 and N2.

The environment of W2 is best described as a distorted octahedron. The carbonyl groups around W2 are arranged eclipsed relative to those at W1. The carbonyl groups orientated along the bisector between the heteroaromatic rings and in line with the P–H bond, are bent away from the phosphane moiety. The angle C32–W2–C33 is 159.8(1)°. As the crystal structure shows, the dimethyl aluminium fragment is replaced by a tungsten tetracarbonyl moiety during the reaction. The NMR spectra suggest, that in the first step [Me₂Al(bth)₂P] (**3**) reacts as expected to form the heterobimetallic [Me₂Al(bth)₂PW(CO)₅] complex which is subject to a ligand rearrangement process, not yet fully understood.

The reaction of lithium di(benzothiazol-2-yl)phosphanide (**2**) with di(^tbutyl) aluminium chloride proved, that the P–C bond in the ligand system can be cleaved. One product of this reaction, which was isolated and characterised, is di(2-benzothiazol). Therefore, it should be possible to cleave the P–C bonds in [Me₂Al(bth)₂PW(CO)₅] as well. This suggests, that another by-product of the reaction is aluminium phosphide, which is obtained as solid. From a thermodynamic point of view the formation of aluminium phosphide is reasonable. The enthalpy of formation Δ_fH° of aluminium phosphide is -116.5 kJ/mol and -318.0 kJ/mol for aluminium nitride.^[76]

The electronic situation within the *Janus head* ligand is changed significantly by coordination of the first tungsten moiety, leading to alterations in the aluminium fragment. Another possibility for the second step of the reaction is therefore, that the C–H bonds in the AlMe₂ moiety are activated. The phosphorus centre is protonated to give a classical phosphane arrangement. This arrangement is metal stabilised, as the electron density at the nitrogen atoms is occupied by another tungsten centre. Although the reaction path is not fully understood yet, this result seems very promising in respect to catalytic chemistry.

3.10 Comparison of Compounds 1 to 10

As the previous chapters showed, the di(benzothiazol-2-yl)phosphanide is a very flexible ligand. It is possible to employ the ligand in the coordination of metals as different as lithium and tungsten. Altering the metals leaves the ligand geometry almost unchanged.

Predominantly the hard nitrogen atoms donate electron density to the metal centres, regardless of their size and hardness. The phosphorus centre is only involved in coordination of huge soft ions and transition metal fragments in which weakly bonded ligands can be replaced by the phosphorus atom. The amount of electron density shifted into the heteroaromatic rings correlates with the strength of P–[M] contacts.

The P–C bond distances in the phosphanide complexes **2** to **8** range from 177 to 181 pm (**Table 3-10**). In [Li(bth)₂P{Mn(CO)₂Cp₂}]_∞·2.5(Tol) (**9**) the ligand shows its *Janus head* nature. The P–C_{ipso} bond distance is at its maximum of 185.4(6) pm in **9**. Taking the by approx. 4 pm reduced radius of a sp² carbon atom compared to a sp³ carbon atom into account, this is a quite long P–C bond distance, even for a single bond. The coordination of the manganese centres inhibits the electron density shift to the heteroaromatic systems. As a consequence, the C_{ipso}–N bond distances reach their minimum in **9**. In the other compounds the C_{ipso}–N bond distances are between those for a standard single and a double bond.^[50] To some extent the C_{ipso}–N bond distances correlate with the P–C bond distances. Shorter P–C bond distances, indicating stronger interactions, cause longer C_{ipso}–N bond distances. The other bond distances in the ligand system are hardly affected by these changes.

The (bth)⋯(bth') angles vary from 2.1° to 32.5° in compounds **1** to **9**. The heteroaromatic rings can be rotated about the P–C_{ipso} bonds. The rotation is in the same direction (compounds **3**, **4**, **5**, **7**, **8**, and **10**) or in opposite direction for the heteroaromatic rings (compounds **2**, **6**, and **9**). For compounds in which the heteroaromatic rings are rotated in the same direction, an almost linear progression in N_{bth}⋯N_{bth'} distances with increasing angles is observed. The more the rings are rotated, the less electron density is shifted from the phosphorus centre to the heteroaromatic rings. Therefore, increasing angles result in longer P–C bond distances. An exception of this is compound **8**, in which the P–C bond distance is almost the same as the ones in compound **6**.

The rotation is counterbalanced by the ligand's preference to stay planar to facilitate full conjugation. This principle is broken if the phosphorus centre is employed in metal coordination.

In compounds **2** to **8** it was shown that the di(benzothiazol-2-yl)phosphanide moiety is a very useful ligand system, which coordinates almost any metal in a pincer ligand like way. In $[\text{Li}(\text{bth})_2\text{P}\{\text{Mn}(\text{CO})_2\text{Cp}\}_2]_\infty \cdot 2.5(\text{Tol})$ (**9**) the ligand acts as real *Janus head* system. The qualitatively different metals are coordinated by the appropriate donor centres in terms of hard and soft acids and bases (HSAB).^[23]

Although the reaction pathway is not completely understood, the reaction to $[(\text{CO})_4\text{W}(\text{bth})_2\text{P}(\text{H})\text{W}(\text{CO})_5] \cdot \text{C}_6\text{D}_6$ (**10**) is very promising. The system is able to activate bonds, for example in aluminium alkyl fragments.

Table 3-10: Comparison of compounds 1 to 10

	P-C _{ipso}	C _{ipso} -N	N-[M]	N...N	C-P-C	bth...bth'
(bth)P(bthH) (1)	178.1(8)	133.3(8)	-	262.3(5)	98.7(2)	10.6
[(Et ₂ O) ₂ Li(bth) ₂ P] (2)	177.9(2)	131.2(4)	203.1(10)	308.7(2)	104.2(1)	9.9
[Me ₂ Al(bth) ₂ P] (3)	176.5(16)	133.8(15)	192.7(8)	292.4(5)	102.3(2)	2.1
[(Me ₃ Si) ₂ NZn(bth) ₂ P] ₂ •2(THF) (4)	180.6(4)	131.4(6)	205.9(5)	307.0(5)	103.8(2)	11.3
[(Me ₃ Si) ₂ NCd(bth) ₂ P] ₂ •(THF) (5)	180.8(4)	131.7(3)	229.1(4)	318.1(2)	105.0(1)	19.9
[(Me ₃ Si) ₂ NSn(bth) ₂ P] ₂ •0.49(Et ₂ O) (6)	176.6(7)	133.3(7)	225.2(8)	302.2(4)	103.6(2)	12.7
[Fe{(bth) ₂ P} ₂] ₂ •0.5(Tol) (7)	177.5(7)	133.7(8)	201.0(8)	303.8(16)	104.0(2)	4.3 to 12.3
[Cs(bth) ₂ P] _∞ (8)	179.2(4)	131.3(5)	320(17)	321.4(7)	103.3(3)	32.5
[Li(bth) ₂ P{Mn(CO) ₂ Cp} ₂] _∞ •2.5(Tol) (9)	185.4(6)	129.7(5)	199.3(10)	306.9(4)	102.7(2)	24.7
[(OC) ₄ W(bth) ₂ P(H)W(CO) ₅] _∞ •C ₆ D ₆ (10)	182.6(5)	131.4(5)	227.7(4)	293.3(4)	95.0(2)	101.4

3.11 Prospects

For future work, it is interesting to react metal fragments similar to $(OC)_5W(THF)$ with metal di(benzothiazol-2-yl)phosphanides. By altering the N-coordinated metal fragments it should be possible to protect them from ligand rearrangements as observed in the reaction to $[(OC)_4W(bth)_2P(H)W(CO)_5] \cdot C_6D_6$ (**10**), although this reaction is interesting in its own right.

$[Me_2Al(bth)_2P]$ (**3**) should for example be reacted with $[(Cp)_2Zr(THF)N^tBu]^{[124]}$ to investigate possible catalytic properties of resulting products.

Crystals of high quality should not only be grown from these complexes but as well from the compounds discussed above. With these crystals at hand it ought to be possible to get high resolution X-ray diffraction data. This data could be used to investigate the bonding situations in the structures and clarify the electronic situation especially in $(bth)P(bthH)$ (**1**), $[(Me_3Si)_2NZn(bth)_2P]_2 \cdot 2(THF)$ (**4**), $[(Me_3Si)_2NCd(bth)_2P]_2 \cdot (THF)$ (**5**), and $[Li(bth)_2P\{Mn(CO)_2Cp\}_2]_{\infty} \cdot 2.5(Tol)$ (**9**). This would be helpful in order to understand how the metal fragments at each face of the *Janus head* have to be altered to obtain complexes with tailor-made properties.

4 The (Benzothiazol-2-yl)phenylphosphanide System

From a synthetic point of view the topic of bond stabilities is of crucial importance for the design of new ligand systems. As shown for tri(benzothiazol-2-yl)phosphane and (benzothiazol-2-yl)phosphanides the P–C bonds can be cleaved. For example, one P–C bond in tri(benzothiazol-2-yl)phosphane is cleaved when reacted with elemental lithium.

Hemilabile coordination is one feature not yet observed for the ligand system discussed above. This was inhibited by the two hard nitrogen donor centres in the ligand system. Any metal from lithium to caesium preferred a double coordination by both nitrogen atoms. In no case the ligand adopted a *cis-trans* arrangement, bringing together the hard and soft potential donating sites. The *cis-trans* arrangement is realised for example in [(PMDETA)Cs{(μ -Ppy)py}]₂.^[38] In this complex the caesium atom is coordinated by both, a hard nitrogen and a soft phosphorus centre of the di(pyrid-2-yl)phosphanide unit.

Therefore, the ligand system was to be modified. It was planned to synthesise (benzothiazol-2-yl)phenylphosphane. In this ligand system the second nitrogen atom is missing and the *cis-trans* conformer should be realised easier.

As possible starting materials (benzothiazol-2-yl)diphenylphosphane (**11**) and di(benzothiazol-2-yl)phenylphosphane^[42] were reacted with elemental lithium in tetrahydrofuran.

4.1 Crystal Structure and Reaction of (bth)PPh₂ (**11**) with Elemental Lithium

Besides the reaction of (benzothiazol-2-yl)diphenylphosphane (**11**) with elemental lithium, the solid state structure was investigated. The results of a single crystal X-ray diffraction experiment are shown in *Figure 4-1*.

(Benzothiazol-2-yl)diphenylphosphane (**11**) crystallises in the orthorhombic space group Pbc_a with one complete formula unit in the asymmetric unit. The P1–C1 bond distance is 183.8(2) pm (*Table 4-1*). Taking the by about 4 pm reduced radius of an sp² carbon atom compared to an sp³ carbon atom into account, this value indicates a single bond.^[50] The P–C_{ipso}(phenyl) bonds are av. 183.6(5) pm. In the benzothiazol-2-yl moiety the

C1–N1 bond distance is 129.9(3) pm. This value is very close to the one found in tri(benzothiazol-2-yl)phosphane (129.3(2) pm).^[51]

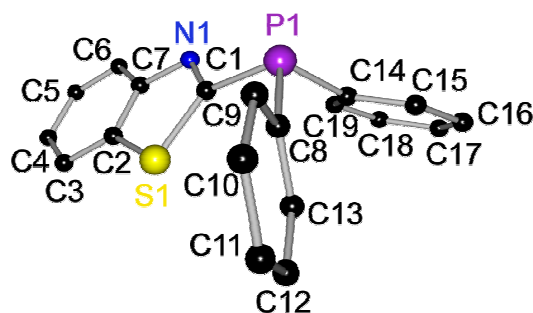


Figure 4-1: Crystal structure of (bth)Ph₂P (**11**)

Table 4-1: Selected bond lengths [pm] and angles [°] of (bth)Ph₂P (**11**)

bond length [pm]		bond angle [°]	
P1–C1	183.8(2)	C1–P1–C8	100.0(1)
P1–C8	183.3(2)	C1–P1–C14	102.1(1)
P1–C14	183.8(2)	C8–P1–C14	102.8(1)
C1–N1	129.9(3)		
		angle between planes [°]	
		(bth)⋯Ph1	104.9
		(bth)⋯Ph2	112.2
		Ph1⋯Ph2	108.0

The sum of the angles around the phosphorus centre is approx. 305°. The angles range from 100.0(1)° (C1–P1–C8) to 102.8(1)° (C8–P1–C14). The phosphorus centre is sp³ hybridised. The differences between the actual angle and the standard angle for a tetrahedron are caused by steric demands. To avoid steric interactions the substituents at the central atom are rotated about the P–C bonds. The best plane defined by the atoms of the heteroaromatic ring includes

an angle of 104.9° with the plane defined by the atoms C8 to C13 and an angle of 112.2° with the plane defined by the atoms C14 to C19. The latter two planes include an angle of 108.0° .

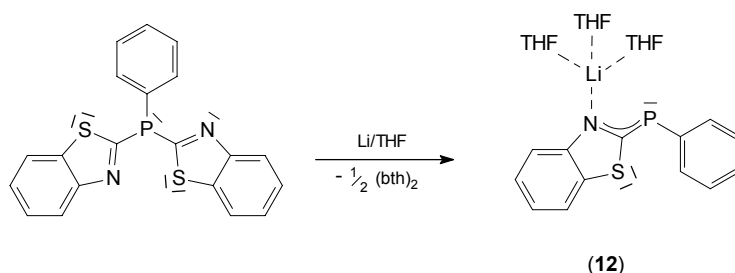
In contrast to the compounds discussed so far, the benzothiazol-2-yl ring is *cis* arranged. So the conformer, necessary for a hemilabile coordination mode, is already adopted.

The reaction of **11** with elemental lithium yielded lithium diphenylphosphanide. The P1–C1 bond is cleaved. The benzothiazol-2-yl substituents of two units couple and form di(2-benzothiazol). Compound **11** did not turn out to be the right starting material for the synthesis of (benzothiazol-2-yl)phenylphosphane, because the P–C_{bth} bond is not as stable as the P–C_{phenyl} bonds.

4.2 Synthesis and Structure of [(THF)₃Li(bth)PPh] (**12**)

As the reaction of (benzothiazol-2-yl)diphenylphosphane (**11**) with elemental lithium resulted in the formation of lithium diphenylphosphanide, di(benzothiazol-2-yl)phenylphosphane was used instead.

An excess of elemental lithium was added to a solution of di(benzothiazol-2-yl)phenylphosphane in tetrahydrofuran at room temperature. The reaction mixture was stirred for 72 h. During this time the solution turned deep red. The reaction mixture was filtered and the solution stored at -38°C . Storage for two months resulted in red crystals suitable for a single crystal X-ray diffraction experiment (*Scheme 4.1*).



Scheme 4.1: Synthesis of [(THF)₃Li(bth)PPh] (**12**)

[(THF)₃Li(bth)PPh] (**12**) crystallises in the monoclinic space group P2₁/c with two complete formula units in the asymmetric unit. As the bond distances and angles differ only marginally for both moieties, the values given below are average values. Exceptions hereof are the values concerning best planes. In these cases, single values are given.

The ligand is *cis* arranged with the nitrogen and phosphorus centres at the same side of the ligand (**Figure 4-2**). The lithium atom is coordinated by the nitrogen atom. The N–Li bond distance is 206.7(5) pm (**Table 4-2**). In [(Et₂O)₂Li(bth)₂P] (**2**) the N–Li bond distances are 203.1(10) pm on average. The lithium atom in **12** is donated less electron density by the ligand than the lithium centre in **2** as it is only coordinated by a single nitrogen atom. This is compensated by three tetrahydrofuran molecules in the coordination sphere of the lithium atom in **12** compared to only two diethylether molecules in **2**. The P⋯Li distance is 337.0(12) pm on average. P–Li bond distances in phosphanides range from approx. 238 to 268 pm.^[125] Bond distances in dative bonds of tertiary phosphorus centres to lithium cations range from approx. 250 to 273 pm.^[126] Hence, the distance in **12** is too long to be regarded a bond. The O–Li bond distances are 194.8(27) pm on average. The environment around each lithium atom is best described as a distorted tetrahedron. The N–Li–O angles range from 104.4(1)° to 127.3(2)°. The O–Li–O angles range from 99.3(1)° to 109.5(2)°.

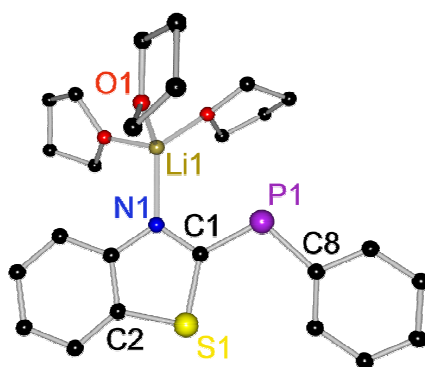


Figure 4-2: Crystal structure of [(THF)₃Li(bth)PPh] (**12**) (only one formula unit shown)

Table 4-2: Selected bond lengths [pm] and angles [°] of [(THF)₃Li(bth)PPh] (**12**) (average values)

	bond length [pm]		bond angle [°]
P1–C _{ipso} (bth)	175.8(5)	C–P–C	108.6(9)
P1–C _{ipso} (Ph)	181.7(4)		
C _{ipso} (bth)–N	134.3(2)		angle between planes [°]
N–Li	206.7(5)	(bth)⋯Ph	16.7
O–Li	194.8(27)	(bth')⋯Ph'	27.3

The P–C_{ipso}(bth) bond distance is 175.8(5) pm on average. In comparison to compounds **1** to **11**, these are the shortest bond distances observed. The average value is in between the values for standard P–C single and double bonds.^[50] The P–C_{ipso}(phenyl) bond distances are av. 181.7(4) pm. The negative charge, formally generated at the phosphorus centre, couples into the heteroaromatic ring. In fact, the negative charge is predominantly located at the nitrogen atom. As in the compounds discussed so far, the P–C_{ipso}(bth) bond distances are shorter, the less the phosphorus centre is involved in metal coordination. With just one heteroaromatic ring in the ligand system, the conjugation is predominant in one direction. This leads to the shortest P–C_{ipso}(bth) bond distance found so far. The P–C_{ipso}(Ph) bond distance of 181.7(4) pm is significantly longer. Nevertheless, they are shorter than the corresponding bonds in (bth)PPh₂ (**11**). Hence, the charge is partly transferred to the phenyl substituent as well. The bond distances within the phenyl rings show no bond length alternation.

The conjugation of the phosphorus atom with the heteroaromatic ring results in elongated C_{ipso}(bth)–N bonds. The C_{ipso}(bth)–N bond distance is 134.3 pm on average. In tri(benzothiazol-2-yl)phosphane the C_{ipso}–N bond distance is 129.3(2) pm.^[51]

The C–P–C angles are av. 108.6(9)°. This value is in accordance with a sp³ hybridisation at the phosphorus centre.

The two molecules in the asymmetric unit differ remarkably in the angle included by the two ring systems. In one moiety this angle is 16.7°, whilst in the other the angle is 27.3°. Other features are almost not affected by this difference.

The crystal structure of **12** shows, that even if the ligand has the right conformation with the nitrogen atom and the phosphorus centre close-by lithium atom is not coordinated by the ligand in a hemilabile manner.

4.3 Prospects

By varying the metal fragment and the solvent it should be possible to alter the ligand's coordination behaviour. Therefore, the lithium compound should be reacted with different metal sources. Depending on the metal fragment, the ligand can adopt different conformations. Generally, it should be possible to employ the system as a P,N- or P,S-hemilabile ligand.

(Benzothiazol-2-yl)phenylphosphane should be accessible from the hydrolysis of $[(\text{THF})_3\text{Li}(\text{bth})\text{PPh}]$ (**12**). The presumably P–H functionalised secondary phosphane could be reacted with various bases analogously to di(benzothiazol-2-yl)phosphane (**1**).

With (benzothiazol-2-yl)phenylphosphane a whole new field of research might be opened up. Moreover, the phenyl ring could be replaced by other substituents, introducing steric shielding as well as stereo information in *Janus head* phosphane ligands.

5 Coupling of Di(benzothiazol-2-yl)methane

As for example shown for picolyphosphanes, it is interesting to incorporate methyl bridges between the phosphorus centre and the heteroaromatic rings.^[39;127] Di(benzothiazol-2-yl)methane (**13**) was used as starting material to introduce methylene bridges into (benzothiazol-2-yl)phosphanes. As the crystal structure of **13** was not known, crystals of Di(benzothiazol-2-yl)methane (**13**), purchased from Sigma-Aldrich, were grown from a tetrahydrofuran solution.

Di(benzothiazol-2-yl) methane (**13**) crystallises in the monoclinic space group $C2/c$ with half a formula unit in the asymmetric unit. The whole molecule is generated via a twofold screw axis along a .

The crystal structure of **13** shows no remarkable alterations from the expected features. The C50–C1 bond distance is 150.8(2) pm. Taking the by 4 pm smaller radius of an sp^2 carbon atom in comparison to an sp^3 carbon atom into account, this value matches the one for a standard P–C single bond.^[50] The C_{ipso} –N bond distance of 129.3(2) pm indicates a double bond. The angle C1–C50–C1A is 109.8(2)°. This is in good agreement with an sp^3 hybridisation of the carbon atom C50. The heteroaromatic rings are arranged in a way that the sulfur atom S1 is closer to N1A than to S1A. The two heteroaromatic rings include an angle of 80.0°.

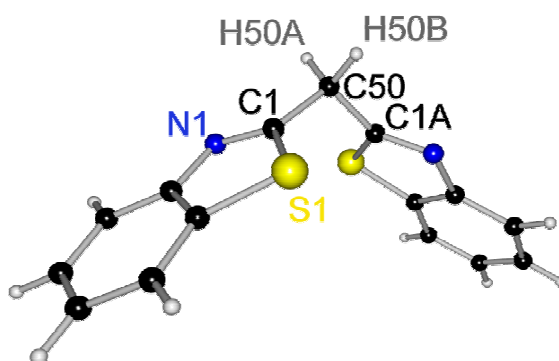


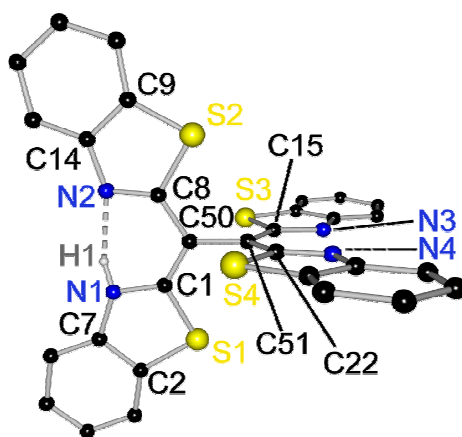
Figure 5-1: Crystal structure of $(bth)_2CH_2$ (**13**)

Table 5-1: Selected bond lengths [pm] and angles [°] of (bth)₂CH₂ (**13**)

bond length [pm]		bond angle [°]	
C50–C1	150.8(2)	C1–C50–C1A	109.8(2)
C1–N1	129.3(2)		
			angle between planes [°]
(bth)...(bth')			80.0

To synthesise (di(benzothiazol-2-yl)methyl)diphenylphosphane, di(benzothiazol-2-yl)methane (**13**) was deprotonated with an equimolar amount of *n*-butyl lithium at -78 °C in diethylether. The reaction mixture was allowed to warm up to room temperature after stirring for two hours. Chlorodiphenylphosphane was added at room temperature. The solvent was removed in vacuo and the solid residue dissolved in THF. Storage in a temperature gradient (room temperature to 37 °C) yielded crystals suitable for a single crystal X-ray diffraction experiment.

The results of the X-ray diffraction experiment revealed that the reaction sequence did not yield (di(benzothiazol-2-yl)methyl)diphenylphosphane, but 1,1,2,2 tetra-(benzothiazol-2-yl)ethane. The structural parameters are consistent with those derived from room temperature data earlier.^[128] Different to the already published structure, asymmetry is more prominent in the structure presented here (*Figure 5-2*).

**Figure 5-2:** Crystal structure of $[(bth)(bthH)C]_2\{(THF)_2LiCl\}_2$ (**14**) ($[LiCl \cdot 2(THF)]_2$ moiety omitted for clarity)

1,1,2,2-tetra(benzothiazol-2-yl)ethane crystallises in the monoclinic space group *Cc* with a complete formula unit and dimeric twofold tetrahydrofuran-coordinated lithium chloride in the asymmetric unit. The attempt to solve and refine the structure in the centrosymmetric space group *C2/c* resulted in by far worse R-values.

The central C–C bond distance is 148.5(7) pm (**Table 5-2**). For a standard single bond between two sp^2 hybridised carbon atoms a value of 146.65 pm is reported.^[50] The hetero-aromatic rings are *trans-trans* arranged on each side. The position of only one hydrogen atom located at a ring nitrogen atom was taken from the Fourier difference map and refined freely. The N1–H1 bond distance is 85(8) pm. The N2...H1 distance is 196 (8) pm. The bond distances are similar to the ones found in di(benzothiazol-2-yl)phosphane (**1**) (see **chapter 2.2**).

Table 5-2: Selected bond lengths [pm] and angles [°] of [$\{(bth)(bthH)C\}_2\{(THF)_2LiCl\}_2$] (**14**)

	bond length [pm]		bond angle [°]
C50–C51	148.5(7)	C1–C50–C8	118.4(5)
C50–C1	136.1(9)	C15–C51–C22	121.0(5)
C50–C8	145.6(7)		
C51–C15	139.0(9)		angle between planes [°]
C51–C22	142.0(10)	(bth) _I ... (bth) _{II}	5.5
C1–N1	136.7(8)	(bth) _{III} ... (bth) _{IV}	6.1
C8–N2	131.2(8)	(bth) ₂ C...C(bth) ₂	87.7
C15–N3	135.5(8)		
C22–N4	130.8(8)		
N1–H1	85(8)		
N2...H1	196(8)		

From the $C_{50/51}-C_{ipso}$ and $C_{ipso}-N$ bond lengths it can be deduced that the second hydrogen atom is located at the nitrogen atom N3. But as the differences in bond distances in this half of the molecule are not so distinct, it is reasonable to assume, that the second tautomeric

hydrogen atom is disordered over two positions, of which the one near N3 is clearly favoured. This double-minimum for the second hydrogen bond explains why only the first hydrogen atom position could be found in the Fourier map. The angles at the carbon atoms C50 and C51 are in good agreement with an sp^2 hybridisation. The best planes defined by the heteroaromatic rings bonded to C50 include an angle of 5.5° . The best planes defined by the heteroaromatic rings bonded to C51 include an angle of 6.1° . Hydrogen bonds are responsible for the *trans-trans* arrangement of the heteroaromatic rings and their almost planar alignment at each side.

The best planes defined by C50 and the heteroaromatic rings bonded to it include an angle of 87.7° with the best plane defined by C51 and the heteroaromatic rings bonded to C51 (**Figure 5-3**). The π -electron system is not extended over the whole system as the sulfur atoms would get in too close proximity.

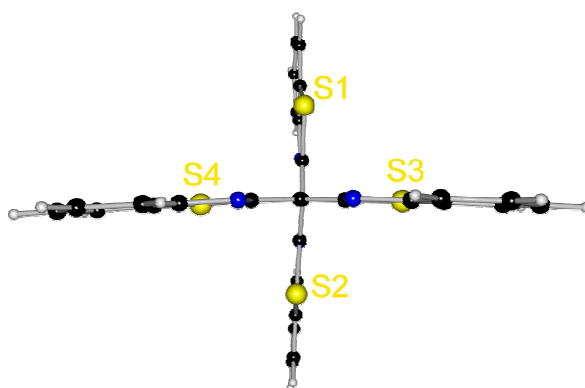


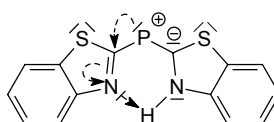
Figure 5-3: Lateral view on $[(bth)(bthH)C]_2\{(THF)_2LiCl\}_2$ (**14**); $([LiCl \cdot 2(THF)]_2)$ moiety omitted for clarity)

(Di(benzothiazol-2-yl)methyl)diphenylphosphane is still to be synthesised. This system or compounds in which one or both phenyl rings are substituted by heteroaromatic ring systems are promising targets for coordination chemistry.

6 Conclusion and Prospects

6.1 Conclusion

The main scope of this thesis was to synthesise an advanced *Janus head* ligand and to investigate its reactivity and coordination behaviour. Di(benzothiazol-2-yl)phosphane (**1**) was chosen as target molecule (**Scheme 6.1**). The heteroaromatic substituents of this ligand do not only contain hard donor sites but also soft ones which make the system even more flexible in comparison to e.g. di(pyrid-2-yl)phosphanide.



Scheme 6.1: Di(benzothiazol-2-yl)phosphane (**1**)

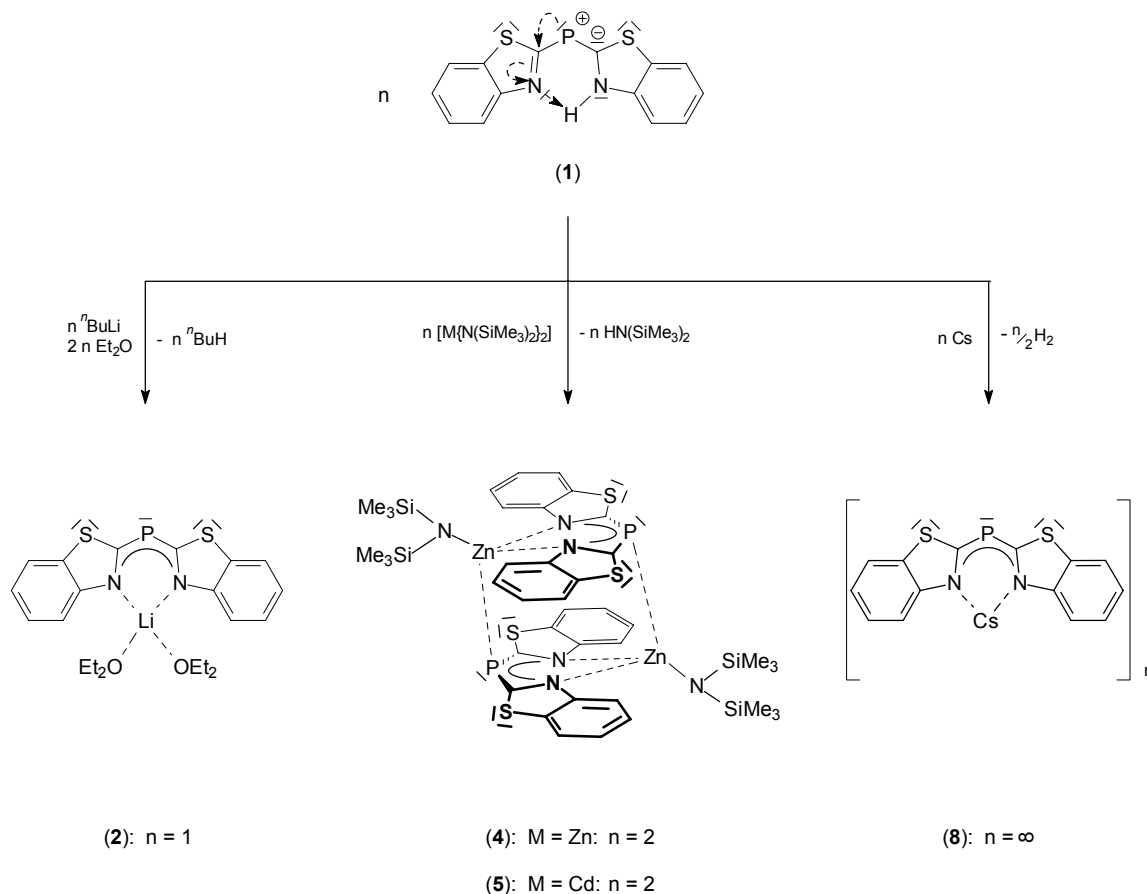
In solid state the phosphorus centre in di(benzothiazol-2-yl)phosphane (**1**) is divalent. The hydrogen atom is bonded to one ring nitrogen atom and tied to the second nitrogen atom via a strong hydrogen bond. The sp^3 hybridisation of the phosphorus centre is proven by theoretical calculations as well as by the findings of single crystal X-ray diffraction experiments.

The phosphane **1** is readily deprotonated by *n*-butyl lithium, elemental caesium, and metal amides yielding the corresponding phosphanides (**Scheme 6.2**). Metal complexes of the phosphane can also be synthesised by metathesis reactions, as shown for the preparation of $[\text{Me}_2\text{Al}(\text{bth})_2\text{P}]$ (**3**).

Similar to the situation in **1**, the phosphanide coordinates metals predominantly via the ring nitrogen atoms. This is valid for metals as different in size and hardness as aluminium and caesium. Hence, the electron density at the nitrogen centres is reduced by these metal contacts. The electron density depletion is partly compensated by an electron density shift from the formally negatively charged phosphorus centre to the heteroaromatic ring systems. In consequence, the P–C bonds get shorter and the $C_{\text{ipso}}\text{--N}$ bond distances increase. Furthermore, a distinct preference for planarity in the ligand geometry is observed.

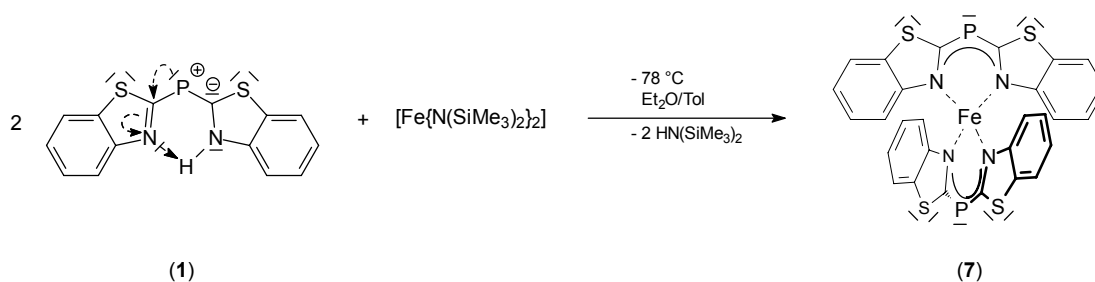
The phosphorus centre participates in metal coordination only if soft metals are employed, as shown by the zinc, cadmium, and caesium compounds. When the phosphorus centre is

directly involved in metal coordination, the coupling of the lone pairs at the phosphorus centre into the heteroaromatic rings is precluded. Consequently, the P–C bond distances are relatively long and the C_{ipso} –N bond distances are relatively short.



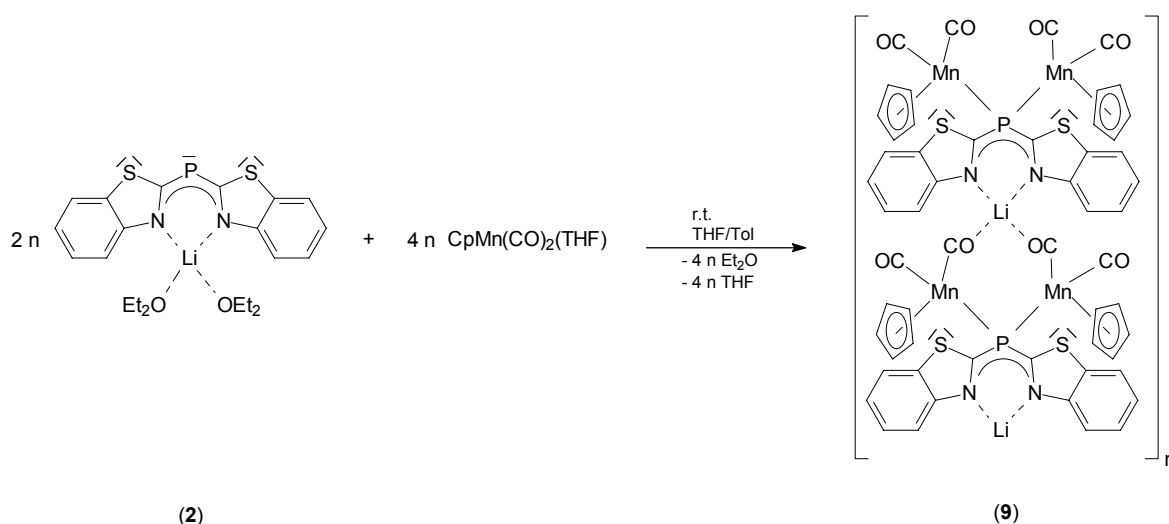
Scheme 6.2: Reactions of dibenzothiazol-2-ylphosphane (1)

The reaction of di(benzothiazol-2-yl)phosphane (1) with $[\text{Fe}\{\text{N}(\text{SiMe}_3)_2\}_2]$ yielded $[\text{Fe}\{(\text{bth})_2\text{P}\}_2] \cdot 0.5(\text{Tol})$ (7) (Scheme 6.3). In 7 both amide groups of the employed metal fragment are replaced by phosphanide units. The metal is coordinated by ring nitrogen atoms exclusively. The ligand molecules are arranged almost perpendicular to each other which leaves the metal atom fourfold coordinated with a total number of 14 valence electrons.



Scheme 6.3: Preparation of $[\text{Fe}\{\text{bth}\}_2\text{P}\}_2] \cdot 0.5(\text{Tol})$ (7)

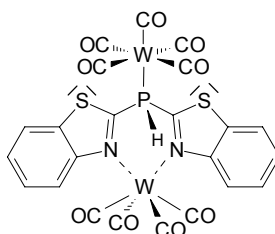
To introduce P–[M] contacts, without participation of the ring nitrogen atoms, the already metal coordinated advanced *Janus head* ligand was reacted with organometallic compounds containing very labile ligands. The presence of the latter is necessary to ensure that enough electron density is left at the phosphorus donor in the phosphanides for the replacement of that ligand. $[\text{CpMn}(\text{CO})_2(\text{THF})]$ was reacted with $[(\text{Et}_2\text{O})_2\text{Li}(\text{bth})_2\text{P}]$ (2) to form $[\text{Li}(\text{bth})_2\text{P}\{\text{Mn}(\text{CO})_2\text{Cp}\}_2]_\infty \cdot 2.5(\text{Tol})$ (9) (**Scheme 6.4**). The coordination of additional metal centres by the phosphorus centre changes the electronic situation in the ligand. The lone pairs at the phosphorous atom coordinate additional metal fragments, therefore, conjugation of the electron density throughout the ligand system is precluded. The P–C bond distances reach their maximum and the $\text{C}_{\text{ipso}}\text{–N}$ bond distances their minimum. An almost planar arrangement of the heteroaromatic rings is caused by the hard metal fragments so that the lone pairs of the ring nitrogen atoms stay almost directed to the same point.



Scheme 6.4: Preparation of $[\text{Li}(\text{bth})_2\text{P}\{\text{Mn}(\text{CO})_2\text{Cp}\}_2]_\infty \cdot 2.5(\text{Tol})$ (9)

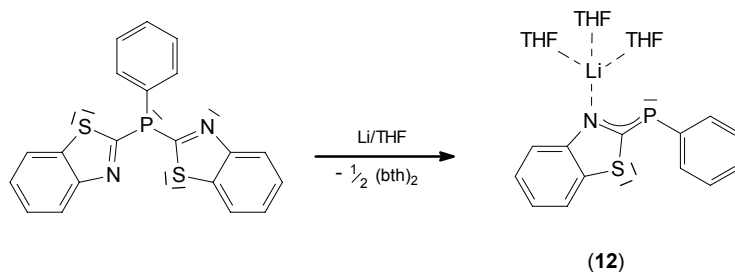
The reactions of $[\text{Me}_2\text{Al}(\text{bth})_2\text{P}]$ (**3**) with $[(\text{OC})_5\text{W}(\text{NCCH}_3)]$ or $[(\text{OC})_5\text{W}(\text{THF})]$ lead to the protonation of the phosphorus centre. The secondary phosphane coordinates one tungsten moiety via the phosphorus centre and a second one via the two ring nitrogen atoms (*Scheme 6.5*). The dimethyl aluminium fragment leaves the molecule in the course of the reaction. Although the reaction mechanism is not completely understood, the result is very promising in respect to catalytic chemistry.

Di(benzothiazol-2-yl)phosphane (**1**) has proven to be an advanced *Janus head* ligand. It is able to coordinate different metal centres simultaneously in a heterobimetallic complex. The ligand tolerates metals different in size and hardness.



Scheme 6.5: Lewis diagram of $[(\text{OC})_4\text{W}(\text{bth})_2\text{P}(\text{H})\text{W}(\text{CO})_5]$ (**10**)

A coordination mode anticipated for hemilabile ligands was not observed for the di(benzothiazol-2-yl)phosphanide ligand so far. Therefore, di(benzothiazol-2-yl)phenylphosphane was synthesised and reacted with elemental lithium to form lithium (benzothiazol-2-yl)phenylphosphanide (**12**). In solid state a *cis* arrangement of the heteroaromatic ring in respect to the P–C bond is observed. Although this ligand contains all prerequisites for a hemilabile ligand, the lithium atom is only coordinated by the ring nitrogen atom of the ligand and three oxygen atoms of tetrahydrofuran molecules (*Scheme 6.6*).



Scheme 6.6: Preparation of $[(\text{THF})_3\text{Li}(\text{bth})\text{PPh}]$ (**12**)

6.2 Prospects

High resolution X-ray diffraction data and subsequent multipole refinement, as the key to a better understanding of the electronic situation in di(benzothiazol-2-yl)phosphane and its metal complexes, are still missing.

Di(benzothiazol-2-yl)phosphane should be reacted with e.g. tri(^tbutyl) aluminium followed by the reaction with various transition metal compounds that contain at least one labile ligand. The resulting complexes have to be examined regarding their catalytic applicability.

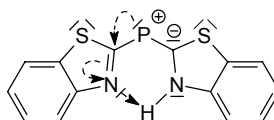
In non-donating solvents the phosphorus centre should be able to take over one coordination site, that is occupied by a tetrahydrofuran molecule in lithium (benzothiazol-2-yl)phenylphosphanide (**12**).

The chemistry of (benzothiazol-2-yl)phenylphosphane, readily accessible by the hydrolysis of lithium (benzothiazol-2-yl)phenylphosphanide (**12**), is a new field of research. The (benzothiazol-2-yl)phenylphosphanide is to be tested as a hemilabile ligand.

7 Zusammenfassung und Ausblick

7.1 Zusammenfassung

Ziel der vorliegenden Arbeit war die Synthese eines *Januskopfliganden* der zweiten Generation und die Untersuchung seiner Reaktivität und seines Koordinationsverhalten. Als Zielverbindung wurde Di(benzothiazol-2-yl)phosphan (**1**) gewählt (*Schema 7.1*). Neben harten Koordinationsstellen enthalten die heteroaromatischen Substituenten dieses Liganden zusätzlich weiche, die das System im Vergleich zu z. B. Di(pyrid-2-yl)phosphan im Bezug auf mögliche koordinierte Metallfragmente flexibler machen sollten.



Schema 7.1: Lewis-Diagramm von Di(benzothiazol-2-yl)phosphan (**1**)

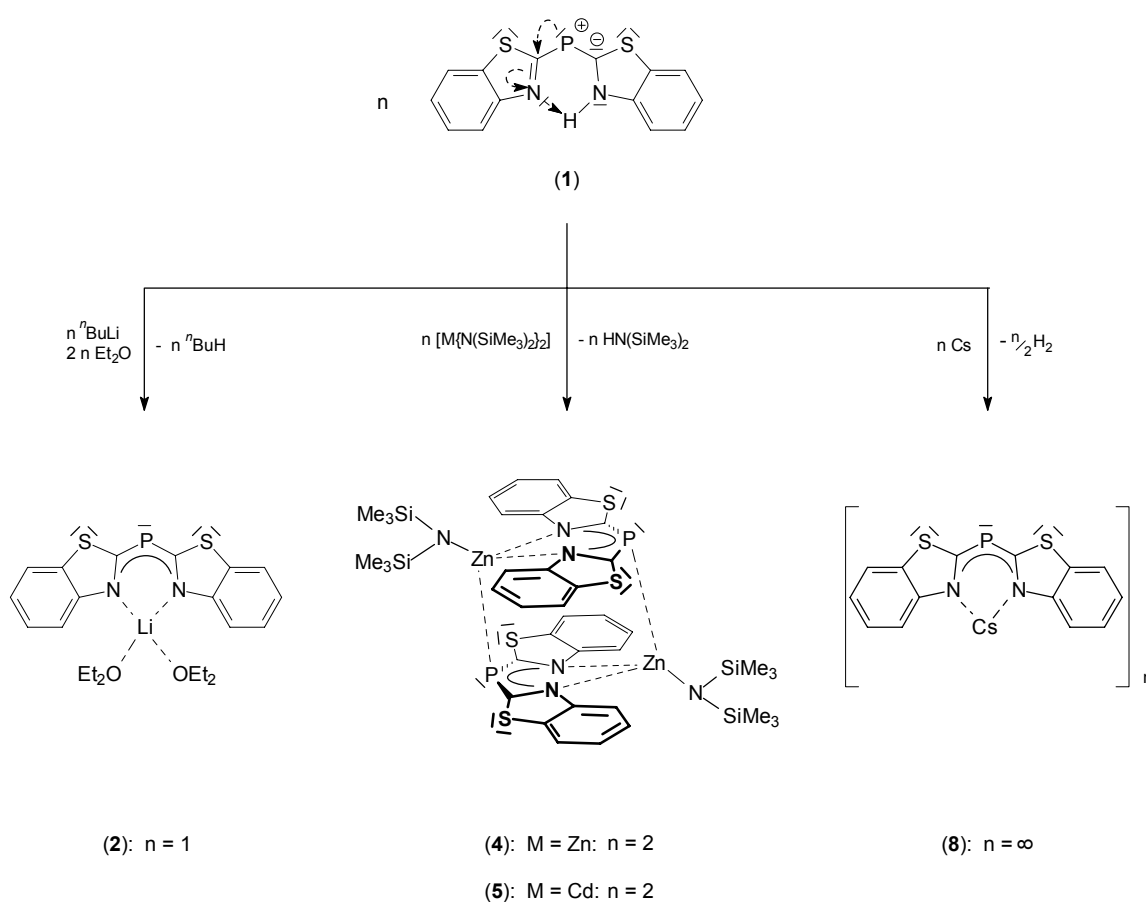
Im Festkörper ist das zentrale Phosphoratom des Di(benzothiazol-2-yl)phosphans divalent. Das Phosphan-Wasserstoffatom ist an ein Ringstickstoffatom gebunden und über eine starke Wasserstoffbrücke an dem zweiten Stickstoffatom fixiert. Sowohl theoretische Berechnungen als auch die Ergebnisse von Röntgenbeugungsexperimenten zeigen, dass das Phosphoratom sp^3 -hybridisiert ist.

Das Phosphan **1** wird von ⁿButyllithium, elementarem Cäsium und Metallamiden leicht deprotoniert, was zu den entsprechenden Phosphaniden führt (*Schema 7.2*). Einige Metallkomplexe des Phosphans sind über Metathesereaktionen zugänglich, wie für die Darstellung von $[Me_2Al(bth)_2P]$ (**3**) gezeigt wurde.

Ähnlich wie in **1** koordiniert die Phosphanideinheit Metalle überwiegend über die Ringstickstoffatome. Dies gilt auch für Metalle, die in ihrer Größe und Härte so unterschiedlich sind wie Aluminium und Cäsium. Durch diese Metallkontakte wird die Elektronendichte an den Stickstoffatomen erniedrigt. Der Elektronendichtemangel wird zum Teil durch eine Elektronendichterverschiebung vom formal negativ geladenen Phosphoratom in die heteroaromatischen Ringe ausgeglichen. Als Folge sind die P–C-Bindungen verkürzt und die

C_{ipso} -N-Bindungen verlängert. Darüber hinaus beobachtet man, dass eine planare Konformation des Liganden deutlich bevorzugt wird.

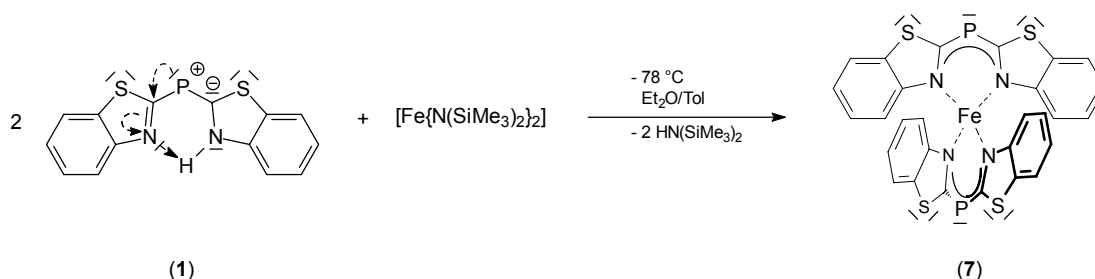
Das Phosphorzentrum beteiligt sich an der Metallkoordination nur, wenn sehr weiche Metalle komplexiert werden, wie anhand der Zink-, Cadmium- und Cäsiumverbindungen gezeigt werden konnte. Sobald sich das Phosphoratom direkt an der Metallkoordination beteiligt, ist das Einkoppeln der freien Elektronenpaare des Phosphoratoms in die heteroaromatischen Ringe erschwert. Deshalb sind die P-C-Bindungen relativ lang und die C_{ipso} -N-Bindungen relativ kurz.



Schema 7.2: Reaktionen des Di(benzothiazol-2-yl)phosphans (1)

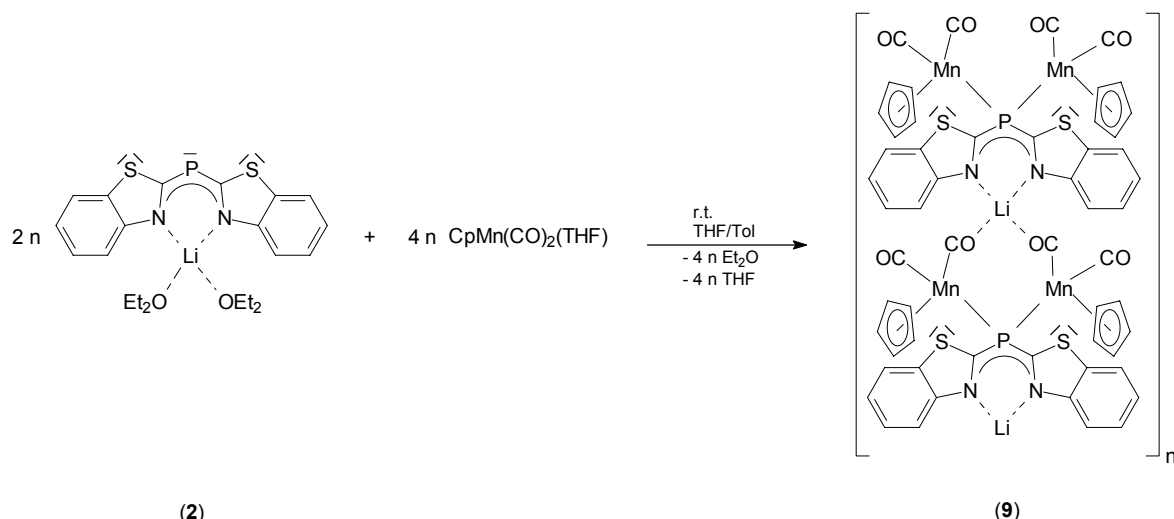
Die Reaktion von Di(benzothiazol-2-yl)phosphan (1) mit $[\text{Fe}\{\text{N}(\text{SiMe}_3)_2\}_2]$ führte zur Bildung von $[\text{Fe}\{(\text{bth})_2\text{P}\}_2] \cdot 0.5(\text{Tol})$ (7) (**Schema 7.3**). In Verbindung 7 sind beide Amidgruppen der eingesetzten Metallverbindung durch Phosphanideinheiten ersetzt worden. Das Metall wird ausschließlich von den Ringstickstoffatomen koordiniert. Die Liganden stehen

nahezu senkrecht aufeinander. Das Metallzentrum ist vierfach koordiniert und hat 14 Valenzelektronen.



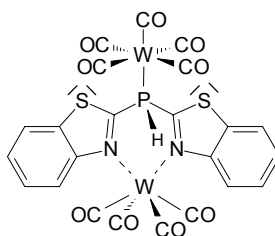
Schema 7.3: Darstellung von $[Fe\{(\text{bth})_2\text{P}\}_2] \cdot 0.5(\text{Tol})$ (7)

Um P–[M]-Kontakte zu knüpfen, an denen die Ringstickstoffatome des Liganden nicht direkt beteiligt sind, wurde der bereits metallkoordinierende *Januskopfligand* mit Übergangsmetallfragmenten, in denen wenigstens ein Ligand nur sehr schwach gebunden ist, zur Reaktion gebracht. Das Vorhandensein mindestens einer labilen Ligand–Metall-Bindung ist notwendig, um sicherzustellen, dass die Elektronendichte, die in den eingesetzten Phosphaniden am Phosphorzentrum lokalisiert ist, ausreicht, um eben einen solchen Liganden zu verdrängen. $[\text{CpMn}(\text{CO})_2\text{THF}]$ wurde mit $[(\text{Et}_2\text{O})_2\text{Li}(\text{bth})_2\text{P}]$ (2) zu $[\text{Li}(\text{bth})_2\text{P}\{\text{Mn}(\text{CO})_2\text{Cp}\}_2]_\infty \cdot 2.5(\text{Tol})$ (9) umgesetzt (**Schema 7.4**). Die Koordination zusätzlicher Metallfragmente durch das Phosphoratom ändert die elektronische Situation im Liganden. Weil die freien Elektronenpaare am Phosphoratom zusätzliche Metallfragmente koordinieren, ist eine Konjugation der Elektronendichte über das gesamte Ligandensystem erschwert. Die P–C-Bindungslängen erreichen ihr Maximum und die $\text{C}_{\text{ipso}}\text{–N}$ -Bindungslängen werden minimal. Die Koordination der harten Metallfragmente führt zu einer nahezu coplanaren Anordnung der heteroaromatischen Ringe, so dass die freien Elektronenpaare an den Ringstickstoffatomen nahezu auf einen Punkt hin ausgerichtet bleiben.



Schema 7.4: Darstellung von $[Li(bth)_2P\{Mn(CO)_2Cp\}_2]_\infty \cdot 2.5(Tol)$ (9)

Die Reaktionen von $[Me_2Al(bth)_2P]$ (3) mit $[(OC)_5W(NCCH_3)]$ oder $[(OC)_5W(THF)]$ führen zur Protonierung des Phosphoratoms. Das sekundäre Phosphan koordiniert eine Wolframcarbonyleinheit über das Phosphoratom und eine zweite Wolframcarbonyleinheit über die beiden Stickstoffatome (**Schema 7.5**). Das Dimethylaluminiumfragment wird im Verlauf der Reaktion freigesetzt. Obwohl der Reaktionsmechanismus noch nicht vollständig verstanden ist, ist dieses Ergebnis im Hinblick auf katalytische Chemie vielversprechend.

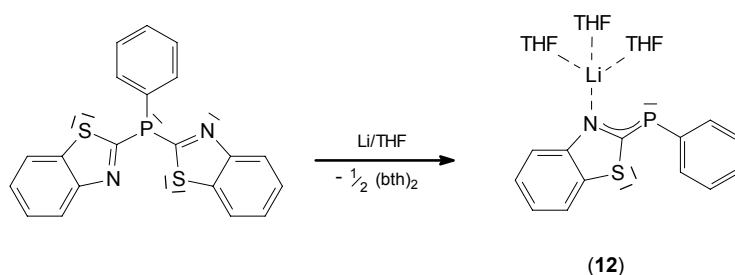


Schema 7.5: Lewis –Diagramm von $[(OC)_4W(bth)_2P(H)W(CO)_5]$ (10)

Di(benzothiazol-2-yl)phosphan (1) zeigt deutlich die Eigenschaften eines *Januskopfliganden* der zweiten Generation. Es ist in der Lage, unterschiedliche Metalle gleichzeitig in einem heterobimetallischen Komplex zu koordinieren. Der Ligand zeigt eine große Toleranz bezogen auf Größe und Härte der koordinierten Metalle.

Ein Koordinationsverhalten, wie es für hemilabile Liganden erwartet wird, wurde für den Di(benzothiazol-2-yl)phosphanid-Liganden bislang nicht beobachtet. Deshalb wurde Di(benzothiazol-2-yl)phenylphosphan synthetisiert und mit elementarem Lithium zum Lithium(benzothiazol-2-yl)phenylphosphanid (12) umgesetzt. Im Festkörper ist der hetero-

aromatische Ring bezüglich der P–C-Bindung *cis*-konfiguriert. Obwohl das Molekül alle Anforderungen an einen hemilabilen Liganden erfüllt, wird das Lithiumkation dennoch nur vom Ringstickstoffatom des Liganden und drei Sauerstoffatomen von Tetrahydrofuranmolekülen koordiniert (**Schema 7.6**).



Schema 7.6: Darstellung von $[(THF)_3Li(bth)PPh]$ (12)

7.2 Ausblick

Multipolverfeinerungen hochaufgelöster Röntgenbeugungsdaten als Schlüssel zu einem besseren Verständnis der elektronischen Situation in Di(benzothiazol-2-yl)phosphan und dessen Metallkomplexen stehen noch aus.

Di(benzothiazol-2-yl)phosphan sollte z. B. mit Tri(‘butyl)aluminium umgesetzt und anschließend mit verschiedenen Übergangsmetallen, die mindestens einen sehr schwach gebundenen Liganden tragen, zur Reaktion gebracht werden. Die erhaltenen Komplexe sollten dann auf mögliche Anwendungen in katalytischen Prozessen hin untersucht werden.

In nicht-donierenden Lösungsmitteln sollte das Phosphoratom in der Lage sein, eine der in Lithium(benziothiazol-2-yl)phenylphosphanid (12) von einem Tetrahydrofuranmolekül besetzten Koordinationsstellen zu übernehmen.

Die Chemie des (Benzothiazol-2-yl)phenylphosphans, das durch Hydrolyse von Lithium(benziothiazol-2-yl)phenylphosphanid leicht zugänglich sein sollte, ist ein neues Forschungsgebiet, das es zu bearbeiten gilt. Es sollte versucht werden, das (Benzothiazol-2-yl)phenylphosphanid als hemilabilen Liganden einzusetzen.

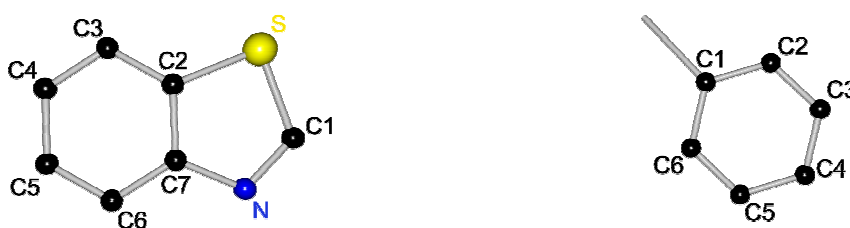
8 Experimental Section

8.1 General

All experiments were carried out either in an atmosphere of dry nitrogen by using modified Schlenk techniques or in an argon drybox. Solvents were freshly distilled from sodium-potassium alloy prior to use. The employed reactants used were commercially available or synthesised according to published procedures.

NMR spectra were recorded at room temperature on a Bruker DRX 300 spectrometer at 300.1 MHz (^1H), 75.5 MHz (^{13}C), or 121.5 MHz (^{31}P). Chemical shifts are δ values relative to the solvent used for ^1H and to H_3PO_4 (85%) for ^{31}P .

The obtained NMR shifts were assigned according to the following scheme:



Scheme 8.1: Numbering in NMR interpretation

Multiplicities are abbreviated as follows:

s = singlet, d = doublet, t = triplet, q = quartet, m = multiplet

Elemental analyses were performed by the Mikroanalytisches Labor des Instituts für Anorganische Chemie der Universität Würzburg.

The melting and decomposition points were determined *via* differential thermo analysis (DTA) with a Du Pont, Thermal Analyzer 9000 and a Differential Scanning Calorimetry (DSC) cell at the Institut für Anorganische Chemie, Würzburg.

IR spectra were recorded on a Bruker IFS 25 at the Institut für Anorganische Chemie, Würzburg.

For photolysis reactions the HERAEUS 411 F85 UV unit with a Q180 lamp was used.

8.2 Syntheses and Characterisation of Compounds 1 to 14

8.2.1 Synthesis and Characterisation of di(benzothiazol-2-yl)phosphane (1)

12.00 g (27.71 mmol) tri(benzothiazol-2-yl)phosphane were dissolved in 60 mL THF and reacted with an excess of elemental lithium. The colourless solution turned red. After two hours of stirring the resident metal was removed and THF was replaced by diethylether. The solution was diluted with diethylether and dried over magnesium sulfate. Storing the solution at $-40\text{ }^{\circ}\text{C}$ yielded pale yellow needles suitable for a single crystal X-ray diffraction experiment.

yield: 7.24 g (87%)

^1H NMR: 6.78 ppm (dd, $^3J_{\text{H3-H4}} = 7\text{ Hz}$, $^3J_{\text{H5-H4}} = 8\text{ Hz}$, 2 H, H4, H11), 6.92 ppm (dd, $^3J_{\text{H4-H5}} = 8\text{ Hz}$, $^3J_{\text{H6-H5}} = 8\text{ Hz}$, 2 H H5, H12), 7.22 ppm (d, $^3J_{\text{H5-H6}} = 8\text{ Hz}$, 2 H, H6, H13), 7.28 ppm (d, $^3J_{\text{H4-H3}} = 7\text{ Hz}$, 2 H H3, H10) 8.05 ppm (d, $^3J_{\text{P-H}} = 8\text{ Hz}$, 1 H, H2)

^{13}C NMR: 121.57 ppm (s, 2 C, C3, C10), 123.29 ppm (s, 2 C, C6, C13), 124.19 ppm (s, 2 C, C4, C11), 126.39 ppm (s, 2 C, C5, C12), 137.76 ppm (s, 2 C, C2, C9), 155.36 ppm (s, 2 C, C7, C14), 155.49 ppm (s, 2 C, C1, C8)

^{31}P NMR: 6.81 ppm (s, 1 P, P1)

elemental analysis: found (calc.)

C: 56.25% (55.99%), H: 3.31% (3.02%), N: 9.20% (9.33%), S: 20.77% (21.35%)

m.p.: $102\text{ }^{\circ}\text{C}$

8.2.2 Synthesis and Characterisation of $[(\text{Et}_2\text{O})_2\text{Li}(\text{bth})_2\text{P}]$ (2)

1.00g (3.33 mmol) **1** was suspended in 40 mL diethylether, cooled to $-78\text{ }^{\circ}\text{C}$, and 3.33 mL (3.33 mmol) of $n\text{BuLi}$ (1 molar in diethylether) added in a period of 25 min. The suspension turned from bright yellow to intense red. After stirring for 12 h and warming up to room temperature the solvent was removed in vacuo, the orange residue washed three times with 10 mL $n\text{hexane}$ and dissolved in 30 mL THF. Storage at $-35\text{ }^{\circ}\text{C}$ yielded orange crystals suitable for a single crystal X-ray diffraction experiment.

yield: 1.15 g (76%)

^1H NMR: 1.12 ppm (t, $^3J_{\text{H-H}} = 6.85$ Hz, 12 H, $\text{O}(\text{CH}_2\text{CH}_3)_2$), 3.39 ppm (q $^3J_{\text{H-H}} = 6.86$ Hz, 8 H, $\text{O}(\text{CH}_2\text{CH}_3)_2$), 6.93 – 8.08 ppm (m, 8 H, bth)

^{13}C NMR: 16.14 ppm (s, 4 C, $\text{O}(\text{CH}_2\text{CH}_3)_2$), 66.78 ppm (s, 4 C, $\text{O}(\text{CH}_2\text{CH}_3)_2$), 122.68 ppm (s, 2 C, C3, C10), 123.28 ppm (s, 2 C, C6, C13), 126.54 ppm (s, 2 C, C4, C11), 127.11 ppm (s, 2 C, C5, C12), 138.60 ppm (s, 2 C, C2, C9), 155.35 ppm (s, 2 C, C7, C14), 157.17 (s, 2 C, C1, C8)

^{31}P NMR: -4.55 ppm (s, 1 P, P1)

elemental analysis: found (calc.)

C: 58.14% (45.81%) H: 6.21% (4.61%), N: 6.16% (5.88%), S: 14.11% (13.56%)

m.p.: 42 °C (decomp.)

8.2.3 Synthesis and Characterisation of $[\text{Me}_2\text{Al}(\text{bth})_2\text{P}]$ (3)

0.73 mL (0.73 mmol) of dimethyl aluminium chloride in hexane was added to a solution of 0.3 g (0.66 mmol) **2** in 35 mL THF at -78 °C. After stirring the solution for 2 h it was allowed to warm up to room temperature.

The solvent was removed in vacuo and the precipitate washed with 10 mL ⁿhexane twice. The solid residue was dissolved in 20 mL THF and stored at -40 °C yielding orange crystals suitable for a single crystal X-ray diffraction experiment.

yield: 0.18 g (83%)

^1H NMR: -0.37 ppm (s, 6 H, Me), 7.23 ppm (dd $^3J_{\text{H}_3\text{-H}_4} = 7.32$ Hz, $^3J_{\text{H}_5\text{-H}_4} = 7.81$ Hz, 2 H, H4, H11), 7.39 ppm (ddd, $^3J_{\text{H}_4\text{-H}_5} = 7.81$ Hz, $^3J_{\text{H}_6\text{-H}_5} = 7.81$ Hz, $^4J_{\text{H}_3\text{-H}_5} = 1.21$ Hz, 2 H, H5, H12), 7.70 – 7.74 (m, 4 H H6, H13, H3, H10)

^{13}C NMR: 1.06 ppm (s, 2 C, Me), 116.54 ppm (s, 2 C, C3, C10), 122.34 ppm (s, 2 C, C6, C13), 125.11 ppm (s, 2 C, C4, C11), 127.26 ppm (s, 2 C, C5, C12), 131.99 ppm (s, 2 C, C2, C9), 150.12 ppm (s, 2 C, C7, C14), 150.14 ppm (s, 2 C, C1, C8)

^{31}P NMR: -1.14 ppm (s, 1 P, P1)

elemental analysis: found (calc.)

C: 44.65% (53.62%) H: 4.28% (4.50%), N: 7.71% (7.82%), S: 12.40% (17.89%)

m.p.: 222 °C

8.2.4 Synthesis and Characterisation of [(Me₃Si)₂NZn(bth)₂P]₂•2(THF) (4)

2.128 g (5.49 mmol) of zinc bis(bis(trimethylsilyl)amide) were added to a suspension of 1.50 g (4.99 mmol) **1** in 45 mL diethylether and cooled down to -78 °C, over a period of 0.5 h. After stirring the reaction mixture for four hours the temperature was allowed to raise to room temperature. The solvent was removed in vacuo and the solid residue dissolved in 25 mL THF. Storage of the red solution at -35 °C for two weeks yielded in yellow crystals suitable for a single crystal X-ray diffraction experiment.

yield: 1.55 g (63%)

¹H NMR: 0.05 ppm (s, 18 H, N(Si(CH₃)₃)₂), 7.07 ppm (ddd, ³J_{H3-H4} = 7.34 Hz, ³J_{H5-H4} = 8.15 Hz, ⁴J_{H6-H4} = 1.21 Hz, 2 H, H4, H11), 7.14 ppm (ddd, ³J_{H4-H5} = 8.15 Hz, ³J_{H6-H5} = 7.21 Hz, ⁴J_{H3-H5} = 1.27 Hz, 2 H, H5, H12) 7.22 ppm (dd, ³J_{H5-H6} = 7.21 Hz, ⁴J_{H4-H6} = 0.57 Hz, 2 H, H6, H13), 7.69 ppm (d, ³J_{H4-H3} = 7.34 Hz, 2 H, H3, H10)

¹³C NMR: 2.99 ppm (s, 6 C N(Si(CH₃)₃)₂), 116.65 ppm (s, 2 C, C3, C10), 122.54 (s, 2 C, C6, C13), 125.21 ppm (s, 2 C, C4, C11), 128.08 ppm (s, 2 C, C5, C12), 132.28 ppm (s, 2 C, C2, C9), 152.69 ppm (s, 2 C, C7, C14), 152.72 ppm (s, 2 C, C1, C8)

³¹P NMR: -6.11 ppm (s, 1 P, P1)

elemental analysis: found (calc.)

C: 58.14% (45.81%) H: 6.21% (4.61%), N: 6.16% (5.88%), S: 14.11% (13.56%)

m.p.: 108 °C

8.2.5 Synthesis and Characterisation of [(Me₃Si)₂NCd(bth)₂P]₂•(THF) (5)

2.38 g (5.49 mmol) of cadmium bis(bis(trimethylsilyl)amide), cooled down to -78 °C, were added to a suspension of 1.50 g (4.99 mmol) **1** in 45 mL diethylether over a period of 0.5 h. After stirring the reaction mixture for 3 h the temperature was allowed to raise to room

temperature. The solvent was removed in vacuo and the solid residue dissolved in 20 mL THF. Storage of the red solution at -35 °C for 2 weeks yielded in yellow crystals suitable for a single crystal X-ray diffraction experiment.

yield: 1.54 g (57%)

^1H NMR: 0.04 ppm (s, 18 H, $\text{NSi}(\underline{\text{C}}\text{H}_3)_3$), 7.18 ppm (dd, $^3J_{\text{H}_3\text{-H}_4} = 7.33$ Hz, $^3J_{\text{H}_5\text{-H}_4} = 7.69$ Hz, 2 H, H4, H11), 7.29 (d, $^3J_{\text{H}_5\text{-H}_6} = 7.87$ Hz, 2 H, H6, H13), 7.46 ppm (ddd, $^3J_{\text{H}_6\text{-H}_5} = 7.81$ Hz, $^3J_{\text{H}_4\text{-H}_5} = 6.97$ Hz, $^4J_{\text{H}_3\text{-H}_5} = 1.26$ Hz, 2 H, H5, H12), 8.32 ppm (d, $^3J_{\text{H}_4\text{-H}_3} = 7.27$ Hz, 2 H, H3, H10)

^{13}C NMR: 299 ppm (s, 6 C, $\text{NSi}(\underline{\text{C}}\text{H}_3)_2$), 121.18 ppm (s, 2 C, C3, C10), 123.39 ppm (s, 2 C, C6, C13), 125.06 ppm (s, 2 C, C4, C11), 126.39 ppm (s, 2 C, C5, C12), 133.35 ppm (s, 2 C, C2, C9) 153.32 ppm (s, 2 C, C7, C14), 155.21 ppm (s, 2 C, C1, C8)

^{31}P NMR: -49.87 ppm (s, 1 P, P1)

elemental analysis: found (calc.)

C: 44.03% (43.45%) H: 5.11% (4.97%), N: 6.46% (6.91%), S: 10.12% (10.54%)

m.p.: 71 °C (loss of THF), 93 °C (decomp.)

8.2.6 Synthesis and Characterisation of $[(\text{Me}_3\text{Si})_2\text{NSn}(\text{bth})_2\text{P}]\cdot 0.48(\text{Et}_2\text{O})$ (6)

2.40 g (5.46 mmol) tin bis(bis(trimethylsilyl)amide) were added to a suspension of 1.50 g (4.99 mmol) **1** in 45 mL diethylether cooled down to -78 °C. The reaction mixture was stirred for 4 h at this temperature and then allowed to warm up to room temperature. Red crystals suitable for a single crystal X-ray diffraction experiment grew at the phase interface.

yield: 0.33 g (12%)

^1H NMR: 0.10 ppm (s, 18 H $\text{NSi}(\underline{\text{C}}\text{H}_3)_3$), 7.29 ppm (dd, $^3J_{\text{H}_3\text{-H}_4} = 8.21$ Hz, $^3J_{\text{H}_5\text{-H}_4} = 7.15$ Hz, 2 H, H4, H11), 7.41 ppm (dd, $^3J_{\text{H}_4\text{-H}_5} = 8.41$ Hz, $^3J_{\text{H}_6\text{-H}_5} = 7.72$ Hz, 2 H, H5, H12), 7.67 ppm (d, $^3J_{\text{H}_5\text{-H}_6} = 7.72$ Hz, 2 H, H6, H13), 8.05 ppm (d, $^3J_{\text{H}_4\text{-H}_3} = 8.21$ Hz, 2 H, H3, H10)

The sample was not stable enough for a ^{13}C NMR experiment

^{31}P NMR: -6.20 ppm (s, 1 P, P1)

elemental analysis: found (calc.)

C: 34.30% (41.53%), H: 2.49% (4.53%), N: 5.16% (7.26%), S: 10.88% (11.09%)

m.p.: 58 °C (decomp.)

8.2.7 Synthesis and Characterisation of $[\text{Fe}\{\text{bth}\}_2\text{P}\}_2] \cdot 0.5(\text{Tol})$ (7)

1.50 g (4.99 mmol) of **1** were suspended in 45 mL diethylether and cooled down to -78 °C. 1.03 g (2.75 mmol) of iron bis(bis(trimethylsilyl)amide) were added to that mixture over a period of 0.5 h. The reaction mixture was stirred for 24 h and afterwards the solvent removed in vacuo. The solid residue was dissolved in 65 mL of toluene and the solution stored at room temperature for three months yielding red crystals suitable for a single crystal X-ray diffraction experiment at the phase interface.

yield: 0.77 g (43%)

NMR spectra could not be recorded due to paramagnetic parts of the sample.

elemental analysis: found (calc.)

C: 49.48% (51.38%), H: 2.62% (2.46%), N: 7.96% (8.56%), S: 18.56% (19.59%)

m.p.: 81 °C

8.2.8 Synthesis and Characterisation of $[\text{Cs}(\text{bth})_2\text{P}]_\infty$ (8)

1.00 g (7.52 mmol) elemental caesium in 60 mL diethylether was reacted with 2.00 g (6.66 mmol) **1** in 60 mL diethylether at -78 °C. The reaction mixture turned deep red evolving gas. After 4 h stirring at this temperature the solution was allowed to warm up to ambient temperature.

After reducing the amount of solvent the reaction mixture was stored at 4 °C yielding red crystals suitable for a single crystal X-ray diffraction experiment.

yield: 2.07 g (73%)

^1H NMR: 6.92 ppm (ddd $^3J_{\text{H3-H4}}$ 7.44 Hz, $^3J_{\text{H5-H4}}$ 7.44 Hz, $^4J_{\text{H6-H4}}$ 1.14 Hz, 2 H, H4, H11), 7.12 ppm (ddd $^3J_{\text{H4-H5}}$ 7.09 Hz, $^3J_{\text{H6-H5}}$ 8.14 Hz, $^4J_{\text{H3-H5}}$ 1.27 Hz, 2 H, H5, H12), 7.53 ppm (d, $^3J_{\text{H5-H6}} = 8.14$ Hz, 2 H, H6, H13), 7.60 ppm (d, $^3J_{\text{H4-H3}} = 7.44$ Hz, 2 H, H3, H10)

^{13}C NMR: 120.61 ppm (s, 2 C, C3, C10), 121.04 ppm (s, 2 C, C6, C13), 125.15 ppm (s, 2 C, C4, C11), 126.84 ppm (s, 2 C, C5, C12), 131.80 ppm (s, 2 C, C2, C9), 155.09 ppm (s, 2 C, C7, C14), 156.86 ppm (s, 2 C, C1, C8)

^{31}P NMR: 14.23 ppm (s, 1 P, P1)

elemental analysis : found (calc.)

C: 41.89% (38.90%), H: 3.97% (1.87%), 3.97% (6.48%), S: 9.06% (14.83%)

m.p.: 234 °C (decomp.)

8.2.9 Synthesis and Characterisation of $[\text{Li}(\text{bth})_2\text{P}\{\text{Mn}(\text{CO})_2\text{Cp}\}_2]_\infty \cdot 2.5(\text{Tol})$ (**9**)

1.20 g (2.64 mmol) of **2** dissolved in 20 mL THF were added to a solution of 0.90 g (2.90 mmol) $(\text{Cp})_2\text{Mn}(\text{CO})_2(\text{THF})$ in 200 mL THF at room temperature. The solvent was removed under reduced pressure. To the grey precipitate toluene was added and the deep red suspension filtered over celite. The solution was stored at -35°C for 3 weeks to get red crystals suitable for a single crystal X-ray diffraction experiment.

yield: 1.33 g (64%)

^1H NMR: 4.17 ppm (s, 20 H, Cp), 7.12 ppm (dd, $^3J_{\text{H3-H4}} = 6.11$ Hz, $^3J_{\text{H5-H4}} = 7.44$ Hz, 2 H, H4, H11), 7.19 ppm (dd, $^3J_{\text{H4-H5}} = 7.44$ Hz, $^3J_{\text{H6-H5}} = 7.18$ Hz, 2 H, H5, H12), 7.94 – 7.97 ppm (m, 4 H, H6, H13, H3, H10)

^{13}C NMR: 84.10 ppm (s, 10 C, Cp), 121.99 ppm (s, 2 C, C3, C10), 122.51 ppm (s, 2 C, C6, C13), 125.18 ppm (s, 2 C, C4, C11), 126.22 ppm (s, 2 C, C5, C12), 137.74 ppm (s, 2 C, C2, C9), 153.95 ppm (s, 2 C, C7, C14), 154.00 ppm (s, 2 C, C1, C8), 234.93 ppm (s, 4 C, CO)

^{31}P NMR: 103.3 ppm (s, 1 P, P1)

IR(THF): 1954 cm^{-1} , 1932 cm^{-1} , 1919 cm^{-1} , 1909 cm^{-1} , 1891 cm^{-1} , 1855 cm^{-1}

8.2.10 Synthesis and Characterisation of $[(OC)_4W(bth)_2P(H)W(CO)_5] \cdot C_6D_6$ (10)

a) 2.00 g (5.58 mmol) of **3** were dissolved in 20 mL tetrahydrofuran and reacted with acetonitrile-coordinated tungsten pentacarbonyl at room temperature. The mixture was stirred for 48 h. Afterwards the solvent was removed under reduced pressure. The brown residue was dissolved in deuterio benzene. Storage of the solution at room temperature yielded crystals suitable for a single crystal X-ray diffraction experiment.

b) 3.93 g (11.2 mmol) of tungsten hexacarbonyl were dissolved in 200 mL tetrahydrofuran and exposed to UV radiation for 45 min. The reaction mixture turned from colourless to red. To the solution were added 2.00 g (5.58 mmol) of **3** dissolved in 20 mL tetrahydrofuran at room temperature. The mixture was stirred for 4 h at room temperature and the solvent removed under reduced pressure. The brown residue was dissolved in deuterio benzene.

1H NMR: Due to various by-products the signals could not be assigned.

^{13}C NMR: 122.38 ppm (s, 2 C, C3, C10), 127.07 ppm (s, 2 C, C6, C13), 127.76 ppm (s, 2 C, C4, C11), 128.12 ppm (s, 2 C, C5, C12), 130.20 ppm (s, 2 C, C2, C9), 157.40 ppm (s, 2 C, C1, C8), 195.16 ppm (s, 4 C, CO), 195.22 ppm (s, 5 C, CO)

^{31}P NMR: -35.6 ppm (ddd, $^1J_{P-H}$ 104.12 Hz, $^1J_{P-W}$ 128 Hz, $^3J_{P-W}$ 24.59 Hz, 1 P, P1)

IR(THF): 2059 cm^{-1} , 1994 cm^{-1} , 1934 cm^{-1} , 1924 cm^{-1} , 1904 cm^{-1} , 1874 cm^{-1} , 1852 cm^{-1} , 1823 cm^{-1} , 2356 cm^{-1}

8.2.11 Synthesis and Characterisation of $[(THF)_3Li(bth)PPh]$ (12)

2.00 g (6.26 mmol) di(benzothiazol-2-yl)phenylphosphane were dissolved in 40 mL tetrahydrofuran and reacted with an excess of elemental lithium. The reaction mixture turned deep red. After 2 d the excessive elemental lithium was removed. The reaction mixture was filtered over celite. Storage of the solution at -38 °C yielded crystals suitable for a single crystal X-ray diffraction experiment.

yield: 2.21 g (76%)

1H NMR: 1.67 ppm (m, 12 H, *c*-O(CH₂CH₂)₂), 3.47 ppm (m, 12 H, *c*-O(CH₂CH₂)₂), 7.15 to 7.99 ppm (m, 9 H, Ph and bth)

^{13}C NMR: 24.83 ppm (s, 6 C, $c\text{-O}(\text{CH}_2\text{CH}_2)_2$), 66.94 ppm (s, 6 C, $c\text{-O}(\text{CH}_2\text{CH}_2)_2$), 118.40 ppm (s, 1 C, C3), 123.52 ppm (s, 1 C, C6), 126.23 ppm (s, 1 C, C4), 126.72 ppm (s, 1 C, C4 (Ph)), 126.86 ppm (s, 1 C, C1 (Ph)), 129.10 ppm (s, 1 C, C5), 134.81 ppm (s, 1 C, C2), 135.04 ppm (s, 2 C, C2/C6 (Ph)), 136.04 ppm (s, 2 C, C3/C5 (Ph)), 154.09 ppm (s, 1 C, C7)

^{31}P NMR: 34.44 ppm (s, 1 P, P1)

elemental analysis: found (calc.)

C: 58.61% (64.50%), H: 5.88% (7.15%), N: 4.46% (3.01%), S: 9.57% (6.98%)

m.p.: 84 °C (decomp.)

8.2.12 Synthesis and Characterisation of $\{(\text{bth})(\text{bthH})\text{C}\}_2 \{(\text{THF})_2\text{LiCl}\}_2$ (14)

4.00 g (14.2 mmol) of di(benzothiazol-2-yl)methane were dissolved in 50 mL diethylether and reacted with 9.74 mL (15.6 mmol (1.6 m in hexane)) $n\text{BuLi}$ at 0 °C and stirred for 2 h. To the reaction mixture were added 3.44 g (2.87 mL, 15.6 mmol) of diphenylchlorophosphine at room temperature. The solvent was removed in vacuo and the solid residue dissolved in 40 mL THF. Storage in a temperature gradient (room temperature to 37 °C) yielded crystals suitable for a single crystal X-ray diffraction experiment.

yield: 2.70 g (68%)

^1H NMR: 1.78 ppm (m, 16 H, $c\text{-O}(\text{CH}_2\text{CH}_2)_2$), 3.63 ppm (m, 16 H, $c\text{-O}(\text{CH}_2\text{CH}_2)_2$), 7.11 ppm (ddd, $^3J_{\text{H4-H5}} = 7.8$ Hz, $^3J_{\text{H6-H5}} = 7.5$ Hz, $^4J_{\text{H7-H5}} = 1.1$ Hz, 4 H, H5, H14, H23, H32), 7.35 ppm (ddd, $^3J_{\text{H5-H6}} = 7.5$ Hz, $^3J_{\text{H7-H6}} = 8.1$ Hz, $^4J_{\text{H4-H7}} = 1.1$ Hz, 4 H, H6, H15, H24, H33), 7.55 ppm (dd, $^4J_{\text{H5-H4}} = 7.8$ Hz, $^4J_{\text{H6-H4}} = 0.6$ Hz, 4 H, H4, H13, H22, H31), 7.71 ppm (d, $^3J_{\text{H6-H7}} = 8.1$ Hz, 4 H, H7, H16, H25, H34)

^{13}C NMR: 24.35 ppm (s, 8 C, $c\text{-O}(\text{CH}_2\text{CH}_2)_2$), 66.17 ppm (s, 8 C, $c\text{-O}(\text{CH}_2\text{CH}_2)_2$), 92.45 ppm (s, 2 C, $\text{C}_{\text{central}}$), 115.36 ppm (s, 4 C, C6, C13, C20, C27), 122.46 ppm (s, 4 C, C3, C10, C17, C24), 124.53 ppm (s, 4 C, C4, C11, C18, C25), 128.35 ppm (s, 4 C, C5, C12, C19, C26), 130.78 ppm (s, 4 C, C2, C9, C16, C23), 147.84 ppm (s, 4 C, C7, C14, C21, C28), 165.29 ppm (s, 4 C, C1, C8, C15, C22)

elemental analysis: found (calc.)

C: 56.90% (57.79%), H: 4.69% (4.08%), N: 6.77% (7.09%), S: 15.52% (16.24%)

m.p.: 108 °C

9 Crystallographic Section

9.1 Crystal application

A sample of the crystalline material was taken from the mother liquor using standard Schlenk techniques and put in inert oil.^[129] The crystals were separated from satellites and checked for twinning under a microscope fitted with a polarizer. A suitable crystal was mounted on top of a glass fibre in a drop of the inert oil and shock cooled on the diffractometer. Data of all compounds were collected at low temperatures.^[130]

9.2 Data collection

All data were measured using graphite monochromated MoK α radiation ($\lambda = 71.073$ pm) on a Bruker D8 goniometer platform, equipped with a Smart Apex CCD camera.

After mounting the crystal and centering with a optical camera a rotation frame was taken to align the beam centre relative to the CCD camera. A single run (usually 50 frames in the ω -scan mode with a step width of 0.3°) was performed to check the crystal's quality and the unit cell. The data collection was performed in the ω -scan mode with a step width usually between 0.1° - 0.3° . For every single run an exact orientation matrix was determined and refined using the tools of SMART V 5.6.^[131] The program SAINT-NT^[132] was employed to integrate the reflexes stored in the frames.

9.3 Absorption correction

The obtained data were absorption corrected with SADABS.^[133] The program uses an empirical model, in which a model function is refined by fitting reflexes of equal symmetry. With the obtained hkl-file structure solution and refinement were processed.

9.4 Structure solution and refinement

General: All structures were solved by direct methods with SHELXTL-NT V5.1.^[134] They were refined by full-matrix least-squares procedures on F^2 , using SHELXTL-NT V5.1. The values g_1 and g_2 of the weighting scheme are given in the crystallographic tables. The denoted R -values are defined as follows:

$$wR2 = \sqrt{\frac{\sum w(F_o^2 - F_c^2)^2}{\sum wF_o^4}} \quad w^{-1} = \sigma^2 \cdot F_o^2 + (g1 \cdot P)^2 + g2 \cdot P \quad R1 = \frac{\sum ||F_o| - |F_c||}{\sum |F_o|}$$

$$P = \frac{(F_o^2 + 2 \cdot F_c^2)}{3}$$

If not mentioned otherwise the hydrogen atoms of the molecules were usually refined using a riding model. The U_{iso} values for the hydrogen atoms of a CH_3 group were set to be 1.5, those of all other hydrogen atoms to be 1.2 of the U_{eq} values of the corresponding carbon atoms. The anisotropic replacement parameters (ADPs) were drawn at 50% probability level.

Disorder: Structures containing disordered fragments were refined using *constraints* and *restraints*. A *constraint* is a mathematical operation, fixing structural parameters on exact values. *Restraints* contain additional chemical or crystallographic information and have standard deviations. The *restraints* add to the data of the refinement.

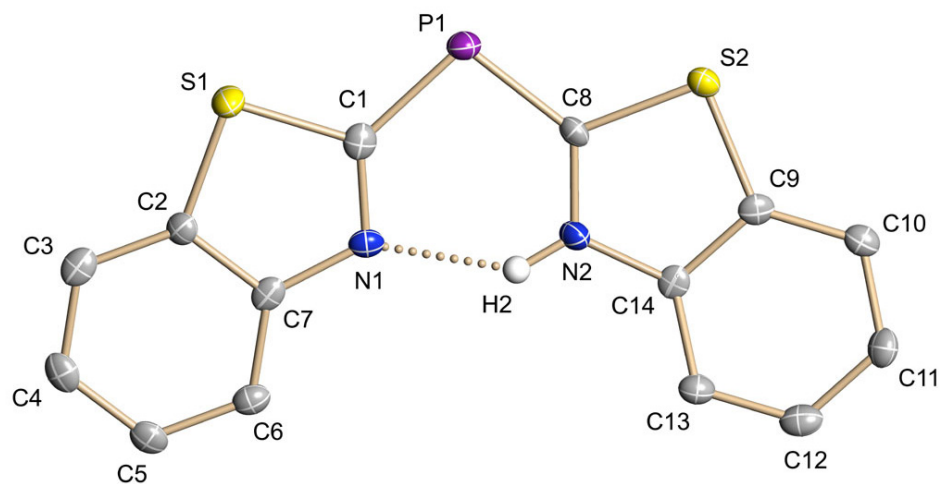
In structures featuring chemically identical, but crystallographic independent fragments, distance *restraints* are useful. The SAME instruction fits 1,2- and 1,3-distances of chemically equal groups with an effective standard deviation. The SADI instruction fits 1,2-distances with an effective standard deviation. The *rigid bond restraint* (DELU) fits components of the anisotropic displacement parameters in the direction of the bond to be equal within an effective standard deviation. *Similarity restraints* (SIMU) are weak *restraints* which adjust the ADPs of neighbouring atoms in a determined radius. *ISOR restraints* force the ADPs to be more spherical and isotropical, allowing anisotropic refinement of disordered atoms with minor occupation factors.

Non-coordinating solvent molecules on special positions can be refined using DFIX and DANG *restraints*. With DFIX, 1,2-distances are refined to a given value within a given standard deviation; the DANG instruction is applied in an analogous way to 1,3 distances.

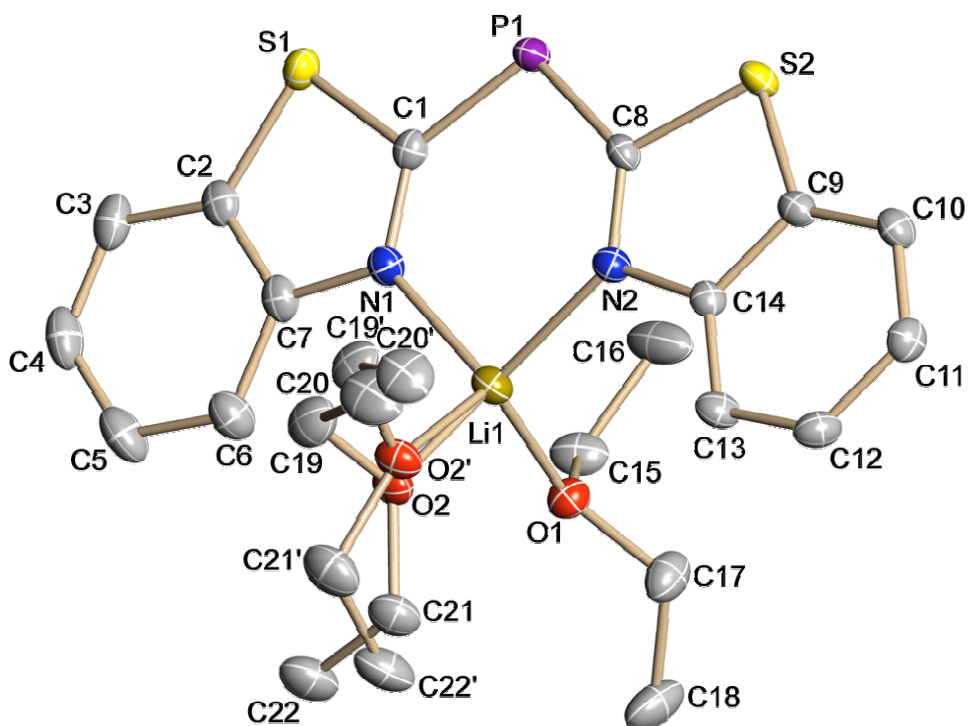
The symmetry operations for groups on special positions can be turned off using the PART-1/PART0 instruction.

9.5 Crystallographic Data for Compounds 1 to 14

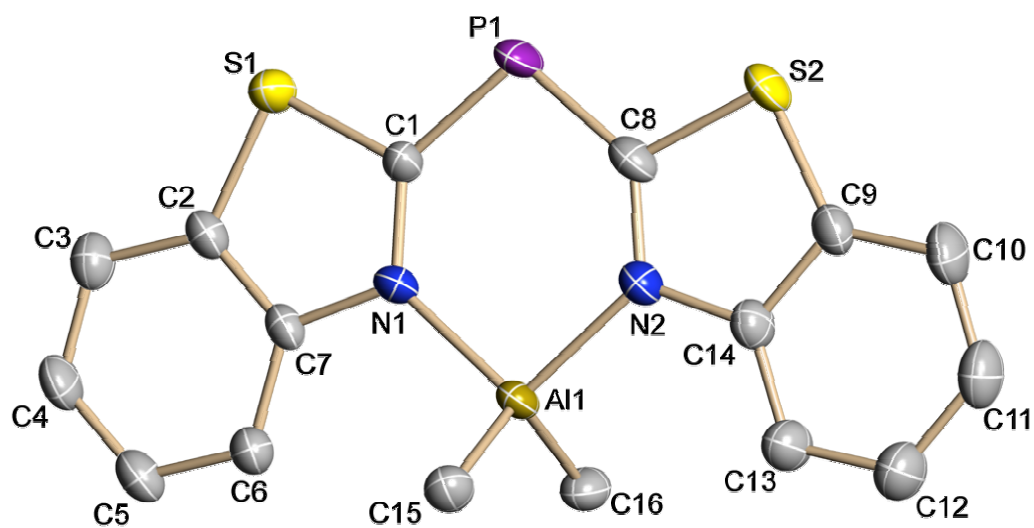
9.5.1 (bth)P(bthH) (1)



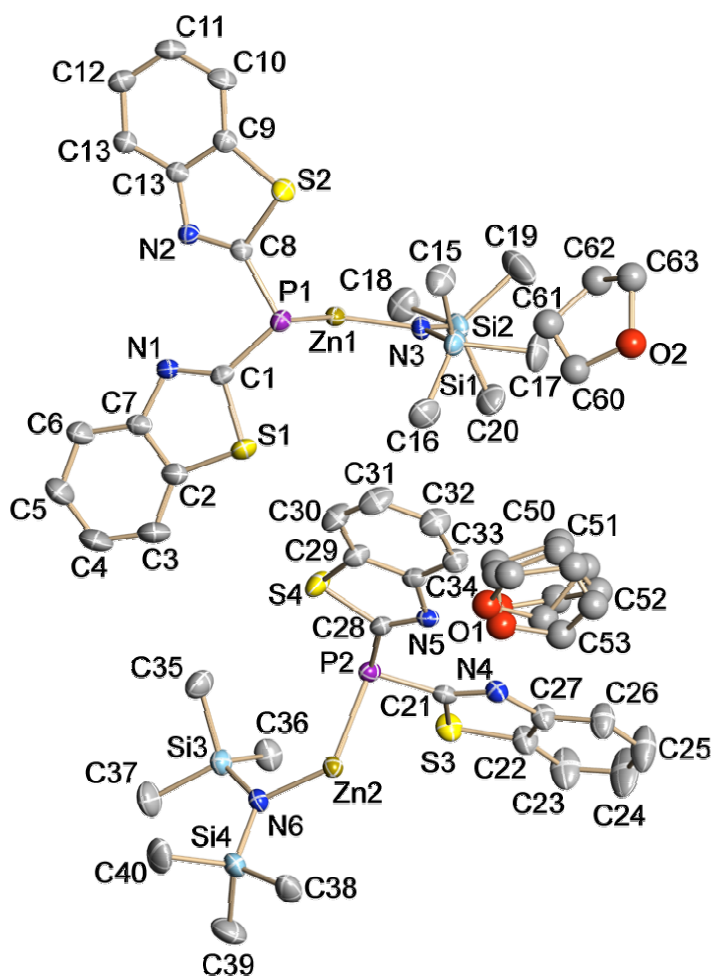
Compound **1** crystallises in yellow needles in the orthorhombic space group *Pbca*. The asymmetric unit contains a whole formula unit. The position of the hydrogen atom H2 was taken from the Fourier difference map and refined freely.

9.5.2 [(Et₂O)₂Li(bth)₂P] (2)

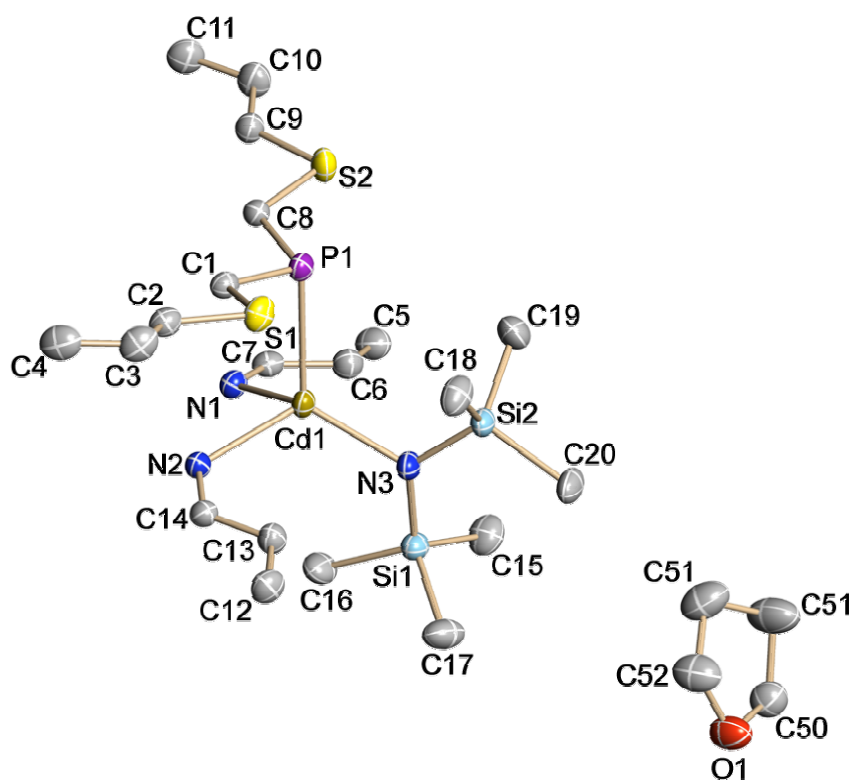
Compound **2** crystallises as red blocks in the orthorhombic space group $Pca2_1$. The asymmetric unit contains a whole molecule. The coordinated, disordered diethylether molecule was refined using distance and ADP *restraints* (SAME, SADI, SIMU, DELU). The site occupation factors refined to 51.7% and 48.3%.

9.5.3 [Me₂Al(bth)₂P] (3)

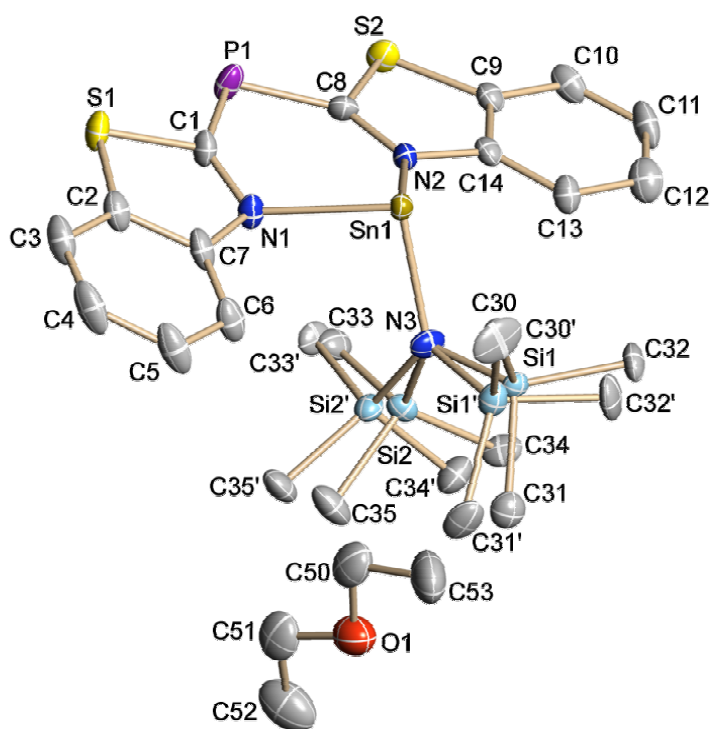
Compound **3** crystallises in orange blocks in the monoclinic space group $P2_1/c$. The asymmetric unit contains the complete formula unit.

9.5.4 [(Me₃Si)₂NZn(bth)₂P]₂•2(THF) (4)

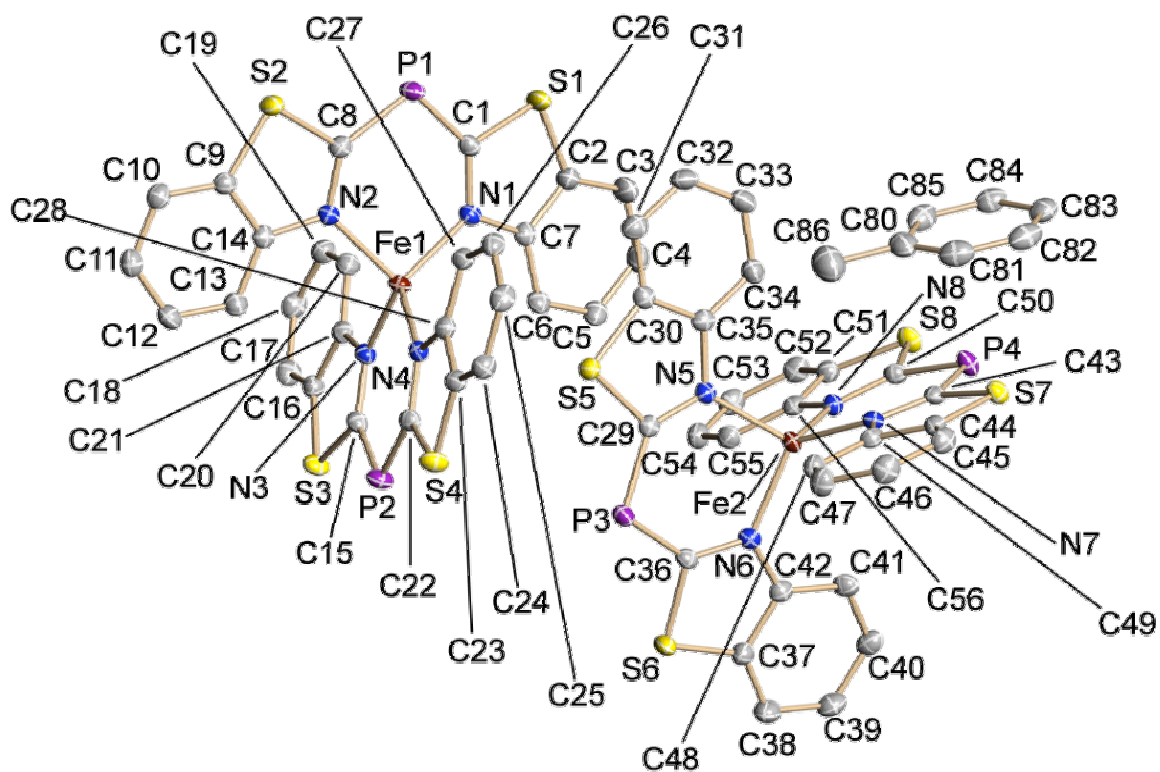
Compound **4** crystallises in yellow blocks in the triclinic space group $P\bar{1}$. The asymmetric unit consists of two independent molecules and two non-coordinating tetrahydrofuran molecules one of which is disordered over three positions. One molecule is completed via the centre of inversion at 0, 0, 0 and translation 0, 1, 0. The other molecule is completed via the centre of inversion at 0.5, 0.5, 0.5 and translation 1, 1, 1. The non-coordinating tetrahydrofuran molecules were refined isotropically. The non-coordinating, disordered tetrahydrofuran molecule was refined using distance restraints (SAME, SADI). The site occupation factors refined to 44.5%, 33.9%, and 21.6%.

9.5.5 [(Me₃Si)₂NCd(bth)₂P]₂•(THF) (5)

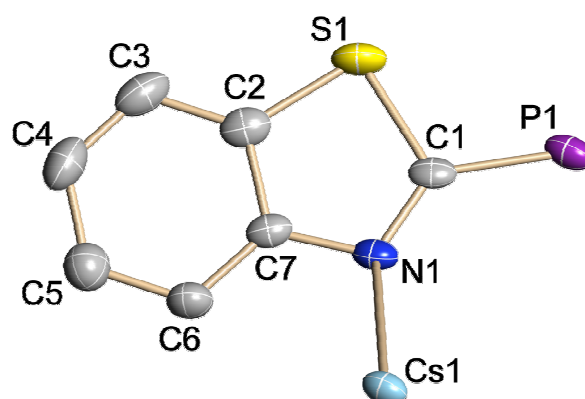
Compound **5** crystallises in yellow blocks in the triclinic space group $P\bar{1}$. The asymmetric unit consists of one non-coordinating molecule of tetrahydrofuran and half the dimer, which is completed via a centre of inversion located at 0, 1, 0.

9.5.6 [(Me₃Si)₂NSn(bth)₂P]•0.49(Et₂O) (6)

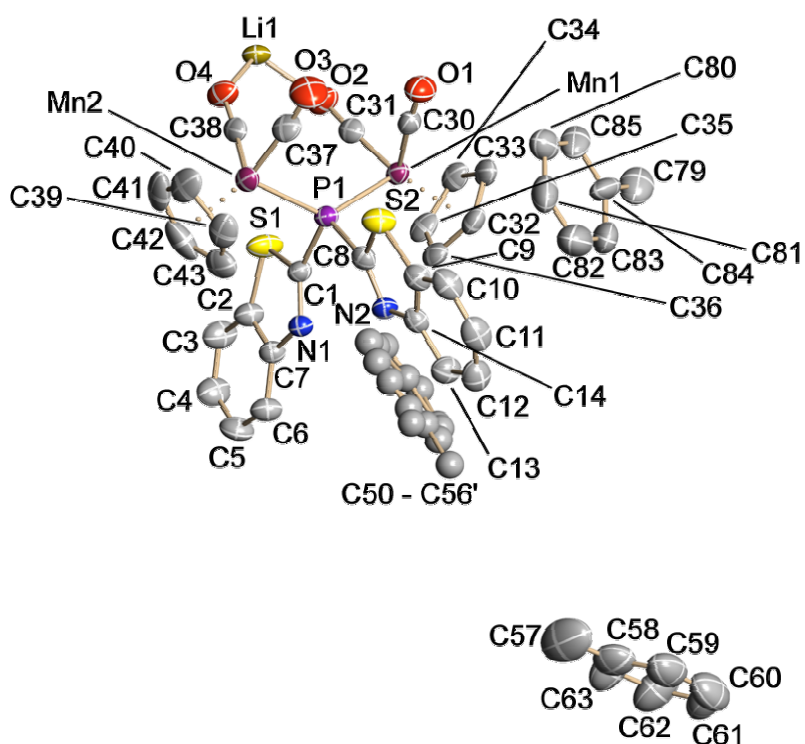
Compound **6** crystallises as red needles in the monoclinic space group $C2/c$. The asymmetric unit contains a whole formula unit and one non-coordinating diethylether molecule. The disordered trimethylsilyl group was refined by using distance and ADP *restraints* (SADI, SIMU, DELU). The site occupation factors (sof) for the disordered trimethylsilyl group containing Si1 refined to 53.2% and the sof of the trimethylsilyl group containing Si1' refined to 46.8%. The site occupation factors for the other disordered trimethylsilyl group refined to 49.7% (group including Si2) and 50.3% (group including Si2'). The non-coordinating diethylether molecule was removed from the special position using the PART-1/PART0 instruction. The site occupation factor of this molecule refined to 48.9%.

9.5.7 $[\text{Fe}\{(\text{bth})_2\text{P}\}_2] \cdot 0.5(\text{Tol})$ (7)

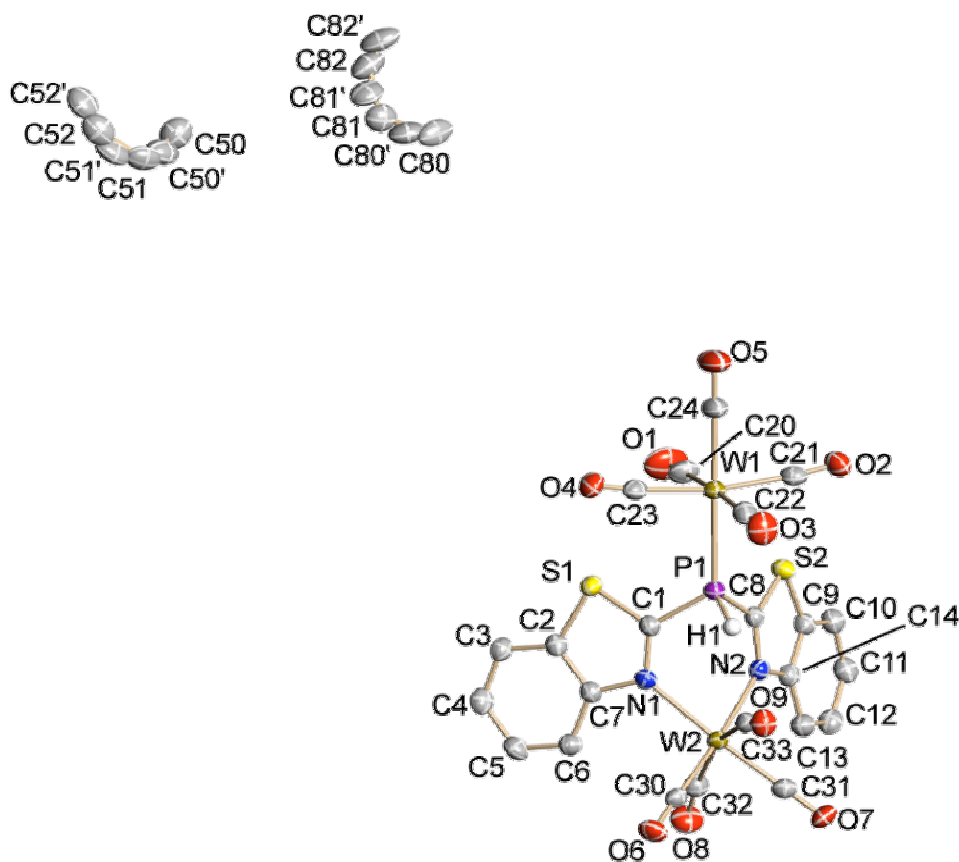
Compound 7 crystallises as deep red blocks in the triclinic space group $P\bar{1}$. The asymmetric unit contains two independent molecules and a non-coordinating toluene.

9.5.8 $[\text{Cs}(\text{bth})_2\text{P}]_\infty$ (**8**)

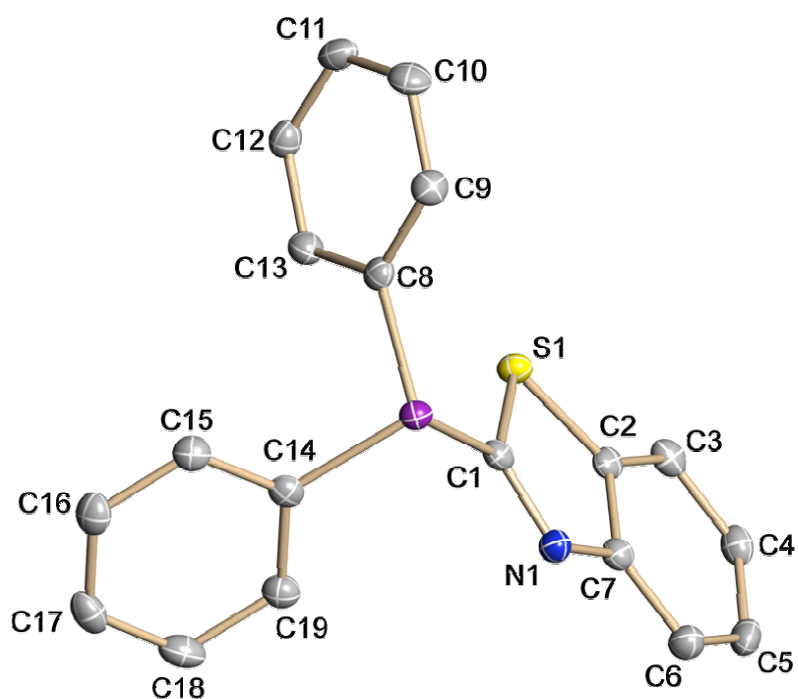
Compound **8** crystallises in deep red needles in the orthorhombic space group $\text{Cmc}2_1$. The asymmetric unit consists of half a monomeric unit. The di(benzothiazol-2-yl)phosphanide unit is completed via a reflection at a mirror in the y - z plane and translation $2, 0, 0$. The neighbouring molecule is generated by a 2_1 axis in z and translation $2, 2, 0.5$.

9.5.9 $[\text{Li}(\text{bth})_2\text{P}\{\text{Mn}(\text{CO})_2\text{Cp}\}_2]_\infty \cdot 2.5(\text{Tol})$ (9)

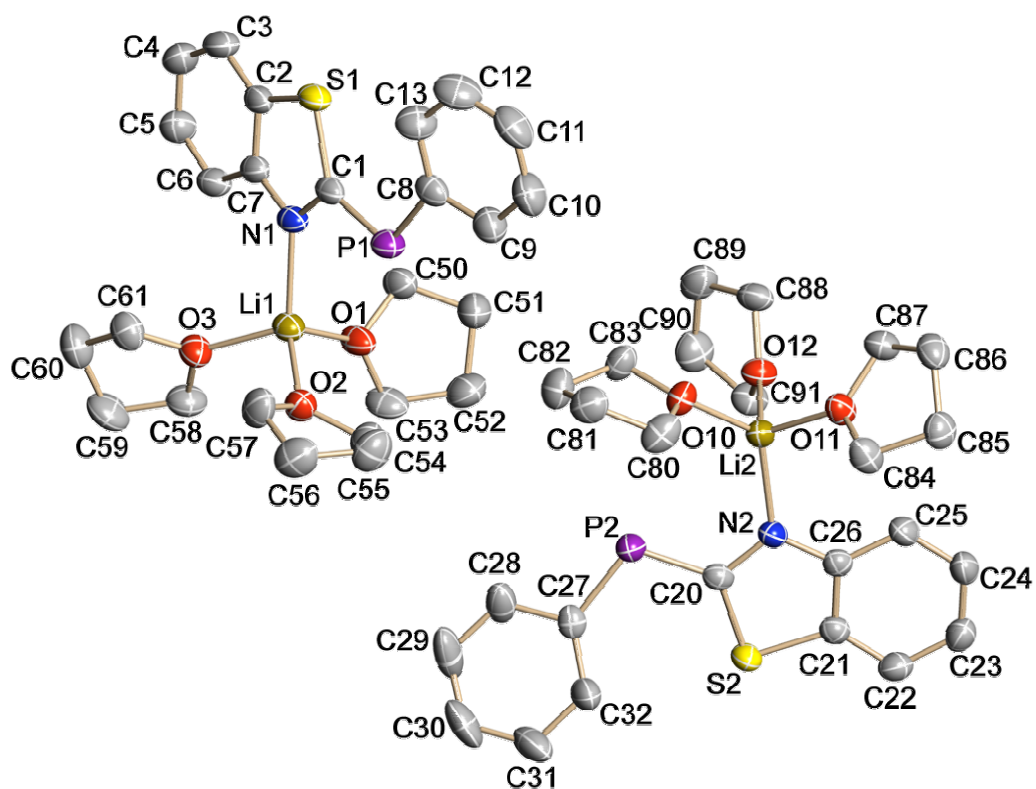
Compound **9** crystallises as red blocks in the monoclinic space group $C2/c$. The asymmetric unit consists of a whole molecule and two toluene molecules, one of which is disordered over two positions. The toluene molecules were refined using the restraints FLAT and DFIX. The disordered toluene molecule containing C50 was refined isotropically. The site occupation factors refined to 68.2% (toluene containing C50) and 31.8% (toluene containing C50'). The site occupation factor for the other toluene molecule refined to 49.4%.

9.5.10 $[(OC)_4W(bth)_2P(H)W(CO)_5] \cdot C_6D_6$ (10)

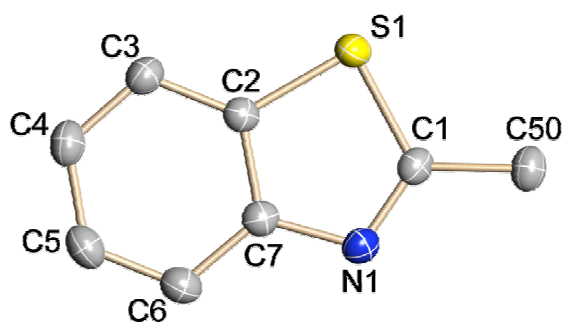
Compound **10** crystallises as dark red needles in the monoclinic space group $P2_1/n$. The asymmetric unit consists of a whole formula unit and two halves of non-coordinated deuterio benzene that are disordered over two positions. The position of the hydrogen atom H2 was taken from the Fourier difference map and refined freely. The non-coordinating, disordered deuterio benzene molecule halves were refined using distance and ADP *restraints* (SAME, SADI, SIMU, DELU). The site occupation factors refined to 47.8% (group containing C50) and 52.2% (group containing C50') for one half and to 50.8% (group containing C80) and 49.2% (group containing C80') for the other half. The first benzene molecule is completed via a centre of inversion at 0, 0, 0 and translation 2, 1, 2. The second benzene molecule is completed via a centre of inversion and translation 2, 1, 1.

9.5.11 (bth)Ph₂P (11)

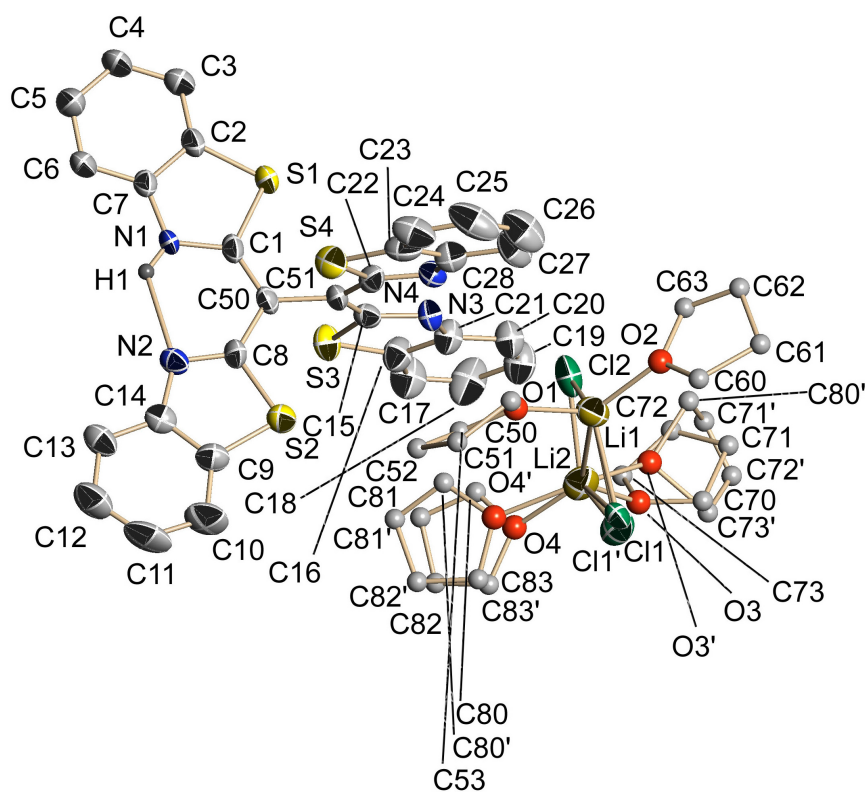
Compound **11** crystallises in colourless needles in the orthorhombic space group *Pbca*. The asymmetric unit consists of a whole formula unit.

9.5.12 [(THF)₃Li(bth)PPh] (12)

Compound **12** crystallises in deep red blocks in the monoclinic space group $P2_1/c$. The asymmetric unit consists of two independent molecules.

9.5.13 (bth)₂CH₂ (13)

Compound **13** crystallises in colourless needles in the monoclinic space group *C2/c*. The asymmetric unit consists of half a formula unit. The molecule is completed by a screw axis in *b* and a translation 0, 0, 0.5.

9.5.14 $[\{(bth)(bthH)C\}_2\{(THF)_2LiCl\}_2]$ (**14**)

Compound **14** crystallises in yellow needles in the chiral, monoclinic space group Cc . The Flack x parameter refined 0.16(11).^[135] The asymmetric unit consists of a $\{(bth)(bthH)C\}_2$ unit and dimeric lithium chloride which twofold tetrahydrofuran coordinated is. The tetrahydrofuran molecules were refined isotropically using distance *restraints* (SAME, SADI). The chloride anion Cl1 was refined using ADP *restraints* (SIMU, DELU).

The site occupation factors refined to 67.2% (molecule containing O3) and 32.8% (molecule containing O3') for one tetrahydrofuran molecule and to 42.8% (molecule containing O4) and to 57.2% (molecule containing O4') for the other tetrahydrofuran molecule.

9.5.15 Crystallographic Tables for Compounds 1 - 14

Table 9-1: Crystal data and structure refinement for compounds 1 and 2

Compound	1	2
Identification code	Stellberg	Bubenbader Steine
Formula	C ₁₄ H ₉ N ₂ PS ₂	C ₂₂ H ₂₈ LiN ₂ O ₂ PS ₂
M _r [g mol ⁻¹]	300.32	454.49
T [K]	100(2)	100(2)
Crystal system	orthorhombic	orthorhombic
Space group	Pbca	Pca2 ₁
a [pm]	1460.7(5)	1444.94(8)
b [pm]	727.2(3)	922.34(5)
c [pm]	2447.8(8)	177.95(10)
α [°]	90	90
β [°]	90	90
γ [°]	90	90
V [nm ³]	2.6001(16)	2.3695(2)
Z	8	4
ρ _{calc} [Mgm ⁻³]	1.534	1.274
μ [mm ⁻¹]	0.517	0.312
F(000)	1232	960
Crystal size [mm]	0.2 x 0.1 x 0.01	0.4 x 0.3 x 0.3
θ range [°]	2.17 to 25.04	2.21 to 28.19
Reflections collected	15966	17030
Unique reflections	2655	5925
R _{int}	0.1126	0.0272
Absorption correction	empirical	empirical
Max. and min. transmission	1.000 and 0.581	1.000 and 0.853
Data / restraints / parameters	2292 / 0 / 175	5369 / 259 / 323
Goodness-of-fit on F ²	1.016	1.046
Final R indices [I > 2σ(I)]	R1 = 0.0561 wR2 = 0.1211	R1 = 0.0296 wR2 = 0.0699
R indices (all data)	R1 = 0.0926 wR2 = 0.1352	R1 = 0.0316 wR2 = 0.0708
Largest diff. peak and hole [e nm ⁻³]	497 and -335	363 and -162
g1 / g2	0.064 / 3.995	0.047 / 0.000

Table 9-2: Crystal data and structure refinement for compounds **3** and **4**

Compound	3	4
Identification code	Soffi	Teufelstein
Formula	C ₁₆ H ₁₄ AlN ₂ PS ₂	C ₄₀ H ₅₂ N ₆ P ₂ S ₄ Si ₄ Zn ₂ •2THF
M _r [g mol ⁻¹]	356.36	1194.36
T [K]	100(2)	173(2)
Crystal system	monoclinic	triclinic
Space group	P2 ₁ /c	P $\bar{1}$
<i>a</i> [pm]	970.76(18)	1301.62(7)
<i>b</i> [pm]	2332.27(5)	1496.66(8)
<i>c</i> [pm]	734.29(14)	1584.01(8)
α [°]	90	73.2730(10)
β [°]	99.271(4)	89.9230(10)
γ [°]	90	83.4230(10)
V [nm ³]	1.6411(5)	2.9341(3)
Z	4	2
ρ_{calc} [Mgm ⁻³]	1.442	1.352
μ [mm ⁻¹]	0.472	1.137
F(000)	736	1248
Crystal size [mm]	0.4 x 0.2 x 0.02	0.4 x 0.3 x 0.3
θ range [°]	2.30 to 25.34	1.34 to 26.40
Reflections collected	17553	63406
Unique reflections	3007	11984
R _{int}	0.0795	0.0244
Absorption correction	empirical	empirical
Max. and min. transmission	1.000 and 0.746	1.000 and 0.882
Data / restraints / parameters	3007 / 0 / 201	11984 / 54 / 618
Goodness-of-fit on F ²	1.022	1.082
Final R indices [<i>I</i> > 2 σ (<i>I</i>)]	R1 = 0.0750 wR2 = 0.1811	R1 = 0.0355 wR2 0.0965
R indices (all data)	R1 = 0.0978 wR2 0.1914	R1 = 0.0384 wR2 = 0.1014
Largest diff. peak and hole [e nm ⁻³]	1034 and -698	1428 and -395
g1 / g2	0.131 / 0.000	0.054 / 2.599

Table 9-3: Crystal data and structure refinement for compounds **5** and **6**

Compound	5	6
Identification code	Maulkuppe	Kleinsassen
Formula	C ₂₀ H ₂₆ CdN ₃ PS ₂ Si ₂ •THF	C ₂₀ H ₂₆ N ₃ PS ₂ Si ₂ Sn•Et ₂ O
M _r [g mol ⁻¹]	644.21	614.14
T [K]	173(2)	100(2)
Crystal system	triclinic	monoclinic
Space group	P $\bar{1}$	C2/c
<i>a</i> [pm]	897.79(7)	3755.8(11)
<i>b</i> [pm]	1234.02(9)	905.8(3)
<i>c</i> [pm]	1329.27(10)	1704.9(5)
α [°]	91.6350(10)	90
β [°]	97.7540(10)	110.257(4)
γ [°]	99.8220(10)	90
V [nm ³]	1.43583(19)	5.441(3)
Z	2	8
ρ_{calc} [Mgm ⁻³]	1.490	1.499
μ [mm ⁻¹]	1.067	1.257
F(000)	660	2498
Crystal size [mm]	0.4 x 0.4 x 0.05	0.4 x 0.3 x 0.06
θ range [°]	1.68 to 26.44	3.14 to 26.05
Reflections collected	30950	84657
Unique reflections	5904	5352
R _{int}	0.0241	0.0361
Absorption correction	empirical	empirical
Max. and min. transmission	1.000 and 0.852	1.000 and 0.826
Data / restraints / parameters	5904 / 0 / 313	5352 / 104 / 359
Goodness-of-fit on F ²	1.070	1.232
Final R indices [<i>I</i> > 2 σ (<i>I</i>)]	R1 = 0.0235 wR2 = 0.0588	R1 = 0.0378 wR2 = 0.0868
R indices (all data)	R1 = 0.0247 wR2 = 0.0595	R1 = 0.0425 wR2 = 0.0884
Largest diff. peak and hole [e nm ⁻³]	693 and -202	1475 and -1028
g1 / g2	0.033 / 0.750	0.034 / 21.28

Table 9-4: Crystal data and structure refinement for compounds **7** and **8**

Compound	7	8
Identification code	Steinwand	Schackau
Formula	C ₅₆ H ₃₂ Fe ₂ N ₈ P ₄ S ₈ •tol	C ₁₄ H ₈ CsN ₂ PS ₂
M _r [g mol ⁻¹]	1401.09	432.22
T [K]	100(2)	173(2)
Crystal system	triclinic	orthorhombic
Space group	P $\bar{1}$	Cmc2 ₁
<i>a</i> [pm]	1090.59(5)	2579.61(15)
<i>b</i> [pm]	1574.71(8)	732.46(4)
<i>c</i> [pm]	1834.11(9)	806.45(5)
α [°]	81.0860(10)	90
β [°]	80.9210(10)	90
γ [°]	89.2160(10)	90
V [nm ³]	3.0726(3)	1.52376(15)
Z	2	4
ρ_{calc} [Mgm ⁻³]	1.514	1.884
μ [mm ⁻¹]	0.897	2.798
F(000)	1428	832
Crystal size [mm]	0.4 x 0.3 x 0.2	0.4 x 0.03 x 0.02
θ range [°]	1.14 to 26.40	2.89 to 26.37
Reflections collected	61389	6839
Unique reflections	12582	1719
R _{int}	0.0339	0.0312
Absorption correction	empirical	empirical
Max. and min. transmission	1.000 and 0.939	1.000 and 0.822
Data / restraints / parameters	12582 / 0 / 767	1587 / 1 / 94
Goodness-of-fit on F ²	1.089	1.168
Final R indices [<i>I</i> > 2 σ (<i>I</i>)]	R1 = 0.0320 wR2 = 0.0789	R1 = 0.0262 wR2 = 0.0570
R indices (all data)	R1 = 0.0395 wR2 = 0.0852	R1 = 0.0285 wR2 = 0.0577
Largest diff. peak and hole [e nm ⁻³]	595 and -271	758 and -493
g1 / g2	0.045 / 1.404	0.029 / 0.000

Table 9-5: *Crystal data and structure refinement for compounds 9 and 10*

Compound	9	10
Identification code	Schafstein	Heidelstein
Formula	C ₂₈ H ₁₈ LiMn ₂ N ₂ O ₄ PS ₂	C ₂₃ H ₉ N ₂ O ₉ PS ₂ W ₂ •C ₆ D ₆
M _r [g mol ⁻¹]	888.69	998.22
T [K]	173(2)	173(2)
Crystal system	monoclinic	monoclinic
Space group	C2/c	P2 ₁ /n
a [pm]	2795.7(12)	1402.41(10)
b [pm]	1639.7(7)	1479.63(10)
c [pm]	2161.2(9)	1495(11)
α [°]	90	90
β [°]	120.372(8)	90.0160(10)
γ [°]	90	90
V [nm ³]	8.55(1)	3.1039(4)
Z	8	4
ρ _{calc} [Mg m ⁻³]	1.381	2.136
μ [mm ⁻¹]	0.771	7.648
F(000)	3656	1880
Crystal size [mm]	0.3 x 0.3 x 0.2	0.4 x 0.3 x 0.2
θ range [°]	1.59 to 26.53	1.94 to 25.35
Reflections collected	29568	53238
Unique reflections	8630	5682
R _{int}	0.0626	0.0380
Absorption correction	empirical	empirical
Max. and min. transmission	1.000 and 0.716	1.000 and 0.432
Data / restraints / parameters	8630 / 18 / 496	5682 / 134 / 468
Goodness-of-fit on F ²	0.961	1.088
Final R indices [I > 2σ(I)]	R1 = 0.0616 wR2 = 0.1664	R1 = 0.0207 wR2 = 0.0508
R indices (all data)	R1 = 0.0895 wR2 = 0.1752	R1 = 0.0231 wR2 = 0.0519
Largest diff. peak and hole [e nm ⁻³]	1213 and -830	1062 and -336
g1 / g2	0.113 / 0.000000	0.029 / 2.315

Table 9-6: Crystal data and structure refinement for compounds **11** and **12**

Compound	11	12
Identification code	Pferdskopf	Milseburg
Formula	C ₁₉ H ₁₄ NPS	C ₂₅ H ₃₃ LiNO ₃ PS
M _r [g mol ⁻¹]	319.34	465.49
T [K]	100(2)	173(2)
Crystal system	orthorhombic	monoclinic
Space group	Pbca	P2 ₁ /c
<i>a</i> [pm]	1107.51(11)	1164.26(6)
<i>b</i> [pm]	1150.77(11)	2197.38(12)
<i>c</i> [pm]	2429.0(3)	1948.50(11)
α [°]	90	90
β [°]	90	90.7090(10)
γ [°]	90	90
V [nm ³]	3.0957(5)	4.9845(5)
Z	8	8
ρ _{calc} [Mgm ⁻³]	1.370	1.241
μ [mm ⁻¹]	0.307	0.220
F(000)	1328	1984
Crystal size [mm]	0.4 x 0.2 x 0.1	0.4 x 0.3 x 0.2
θ range [°]	3.057 to 24.9605	1.40 to 25.03
Reflections collected	11682	48156
Unique reflections	3077	8781
R _{int}	0.0380	0.0363
Absorption correction	empirical	empirical
Max. and min. transmission	1.000 and 0.759	1.000 and 0.932
Data / restraints / parameters	2688 / 0 / 199	8781 / 0 / 577
Goodness-of-fit on F ²	1.016	1.028
Final R indices [I > 2σ(I)]	R1 = 0.0362 wR2 = 0.0866	R1 = 0.0409 wR2 = 0.0989
R indices (all data)	R1 = 0.0450 wR2 = 0.0914	R1 = 0.0532 wR2 = 0.1064
Largest diff. peak and hole [e nm ⁻³]	444 and -215	397 and -180
g1 / g2	0.049 / 1.338	0.057 / 1.361

Table 9-7: *Crystal data and structure refinement for compounds 13 and 14*

Compound	13	14
Identification code	Wasserkuppe	Ziegenkopf
Formula	C ₁₅ H ₁₀ N ₂ S ₂	C ₄₆ H ₄₉ Cl ₂ Li ₂ N ₄ O ₄ S ₄
M _r [g mol ⁻¹]	282.37	934.91
T [K]	173(2)	173(2)
Crystal system	monoclinic	monoclinic
Space group	C2/c	Cc
<i>a</i> [pm]	2545.5(2)	1469.02(8)
<i>b</i> [pm]	453.59(4)	1864.58(10)
<i>c</i> [pm]	1120.65(11)	1728.07(9)
α [°]	90	90
β [°]	102.943(2)	90.4960(10)
γ [°]	90	90
V [nm ³]	1.2610(2)	4.7332(4)
Z	4	4
ρ _{calc} [Mgm ⁻³]	1.487	1.312
μ [mm ⁻¹]	0.407	0.360
F(000)	584	1956
Crystal size [mm]	0.4 x 0.4 x 0.3	0.4 x 0.2 x 0.2
θ range [°]	1.64 to 26.37	1.76 to 25.03
Reflections collected	3336	45614
Unique reflections	1280	6783
R _{int}	0.0358	0.0380
Absorption correction	none	empirical
Max. and min. transmission		1.000 and 0.801
Data / restraints / parameters	1280 / 0 / 87	6783 / 23 / 520
Goodness-of-fit on F ²	1.226	1.077
Final R indices [I > 2σ(I)]	R1 = 0.0321 wR2 = 0.0934	R1 = 0.0722 wR2 = 0.2032
R indices (all data)	R1 = 0.0365 wR2 = 0.1114	R1 = 0.0773 wR2 = 0.2061
Largest diff. peak and hole [e nm ⁻³]	362 and -280	466 and -454
g1 / g2	0.066 / 0.753	0.127 / 9.983

10 Literature

- [1] A. E. Martell, *Advances in Chemistry Series* **1967**, 62, 272.
- [2] G. van Koten, *Pure Appl. Chem.* **1989**, 61, 1681.
- [3] M. Albrecht, G. van Koten, *Angew. Chem.* **2001**, 113, 3866; *Angew. Chem. Int. Ed.* **2001**, 40, 3750.
- [4] S. Gründemann, M. Albrecht, J. A. Loch, J. W. Faller, R. H. Crabtree, *Organometallics* **2001**, 20, 5485.
- [5] a) I. G. Jung, S. U. Son, K. H. Park, K.-C. Chung, J. W. Lee, Y. K. Chung, *Organometallics* **2003**, 22, 4715; b) M. Q. Slagt, R. J. M. Klein Gebbink, M. Lutz, A. L. Spek, G. van Koten, *J. Chem. Soc., Dalton Trans.* **2002**, 2591; c) H. P. Dijkstra, M. D. Meijer, J. Patel, R. Kreiter, G. P. M. van Klink, M. Lutz, L. A. Spek, A. J. Canty, G. van Koten, *Organometallics* **2001**, 20, 3159; d) A. W. Kleij, R. A. Gossage, R. J. M. Klein Gebbink, N. Brinkmann, E. J. Reijerse, U. Kragl, M. Lutz, L. A. Spek, G. van Koten, *J. Am. Chem. Soc.* **2000**, 122, 12112.
- [6] M. Mehring, M. Schürmann, K. Jurkschat, *Organometallics* **1998**, 17, 1227.
- [7] a) D. Morales-Morales, R. E. Cramer, C. M. Jensen, *J. Organomet. Chem.* **2002**, 654, 44; b) R. P. Hughes, A. Williamson, C. D. Incarvito, A. L. Rheingold, *Organometallics* **2001**, 20, 4741.
- [8] a) T. Kanbara, K. Okada, T. Yamamoto, H. Ogawa, T. Inoue, *J. Organomet. Chem.* **2004**, 689, 1860; b) M. D. Meijer, B. Mulder, G. P. M. van Klink, G. van Koten, *Inorg. Chim. Acta* **2003**, 352, 247; c) T. Kanbara, T. Yamamoto, *J. Organomet. Chem.* **2003**, 688, 15.
- [9] E. Peris, J. A. Loch, J. Mata, R. H. Crabtree, *Chem. Commun.* **2001**, 201.
- [10] J. R. Miecznikowski, S. Gründemann, M. Albrecht, C. Mégret, E. Clot, J. W. Faller, O. Eisenstein, R. H. Crabtree, *J. Chem. Soc., Dalton Trans.* **2003**, 831.
- [11] L. Fan, B. M. Foxman, O. V. Ozerov, *Organometallics* **2004**, 23, 326.
- [12] G. Chessa, L. Canovese, L. Gemelli, F. Visentin, R. Seraglia, *Tetrahedron* **2001**, 57, 8875.
- [13] W. D. Kerber, J. H. Koh, M. R. Gagne, *Org. Lett.* **2004**, 6, 3013.
- [14] a) M. Doux, N. Mézailles, L. Ricard, P. Le Floch, *Organometallics* **2003**, 22, 4624; b) M. Doux, N. Mézailles, L. Ricard, P. Le Floch, *Eur. J. Inorg. Chem.* **2003**, 3878.
- [15] a) A. Amoedo, M. Grana, J. Martinez, T. Pereira, M. Lopez-Torres, A. Fernández, J. J. Fernández, J. M. Vila, *Eur. J. Inorg. Chem.* **2002**, 613; b) A. Sundermann, O. Uzan, J. M. L. Martin, *Organometallics* **2001**, 20, 1783.

- [16] M. Gupta, C. Hagen, R. J. Flesher, C. K. William, C. M. Jensen, *Chem. Commun.* **1996**, 2083 and *Chem. Commun.* **1996**, 2687.
- [17] a) M. Gerisch, J. R. Krumper, R. G. Bergmann, T. D. Tilley, *J. Am. Chem. Soc.* **2001**, *123*, 5818; b) P. Steenwinkel, R. A. Gossage, G. van Koten, *Chem. Eur. J.* **1998**, *4*, 759; c) J. Errington, W. S. McDonald, B. L. Shaw, *J. Chem. Soc.* **1980**, 2312.
- [18] a) H. Nakai, S. Ogo, Y. Watanabe, *Organometallics* **2002**, *21*, 1674; b) D. E. Bergbreiter, P. L. Osburn, A. Wilson, E. M. Sink, *J. Am. Chem. Soc.* **2000**, *122*, 9058.
- [19] G. Rodriguez, M. Albrecht, J. Schoenmaker, A. Ford, M. Lutz, A. L. Spek, G. van Koten, *J. Am. Chem. Soc.* **2002**, *124*, 5127.
- [20] D. E. Bergbreiter, P. L. Osburn, J. D. Frels, *J. Am. Chem. Soc.* **2001**, *123*, 11105.
- [21] A. Melaiye, R. S. Simons, A. Milsted, F. Pingitore, C. Wesdemiotis, C. A. Tessier, W. J. Youngs, *J. Med. Chem.* **2004**, *47*, 973.
- [22] a) W. Lu, B.-X. Mi, M. C. W. Chan, Z. Hui, N. Zhu, S.-T. Lee C.-M. Che, *Chem. Commun.* **2002**, 206; b) S.-W. Lai, M. C.-W. Chan, K.-K. Cheung, C.-M. Che, *Organometallics* **1999**, *18*, 3327; c) S.-W. Lai, M. C.-W. Chan, T.-C. Cheung, S.-M. Peng, C.-M. Che, *Inorg. Chem.* **1999**, *38*, 4046; d) T.-C. Cheung, K.-K. Cheung, S.-M. Peng, C.-M. Che, *J. Chem. Soc., Dalton Trans.* **1996**, 1645.
- [23] a) R. G. Pearson, *J. Am. Chem. Soc.* **1985**, *107*, 6801; b) R. G. Parr, R. G. Pearson, *J. Am. Chem. Soc.* **1983**, *105*, 7512.
- [24] J. J. Schneider, *Nachrichten aus der Chemie* **2000**, *48*, 614.
- [25] a) U. Schubert, J. Pfeiffer, F. Stöhr, D. Sturmayer, S. Thompson, *J. Organomet. Chem.* **2002**, *646*, 53; b) C. S. Slone, D. A. Weinberger, C. A. Mirkin, *Prog. Inorg. Chem.* **1999**, *48*, 233; c) P. Braunstein, F. Naud, *Angew. Chem.* **2001**, *113*, 702; *Angew. Chem. Int. Ed.* **2001**, *40*, 680; d) A. Bader, E. Lindner, *Coord. Chem. Rev.* **1991**, *108*, 27.; d) A. Bader, E. Lindner, *Coord. Chem. Rev.* **1991**, *108*, 27.
- [26] P. Jutzi, T. Redeker, *Eur. J. Inorg. Chem.* **1998**, 663.
- [27] P. Braunstein, Y. Chauvin, S. Mercier, L. Saussine, A. De Cian, J. Fischer, *J. Chem. Soc., Chem. Commun.* **1994**, 2203.
- [28] H. Sinn, W. Kaminsky, H. J. Vollmer, R. Woldt, *Angew. Chem.* **1980**, *92*, 396; *Angew. Chem., Int. Ed. Engl.* **1980**, *18*, 390.
- [29] a) E. Zurek, T. Ziegler, *Prog. Polym. Sci.* **2004**, *29*, 107; b) H. Cramail, K. Radhakrishnan, A. Deffieux, *C. R. Chimie* **2002**, *5*, 49; c) S. J. Obrey, A. R. Barron, *J. Chem. Soc., Dalton Trans.* **2001**, *17*, 2456; d) M. Watanabe, N. C. Mahon, C. J. Harlan, A. R. Barron, *Organometallics*

- 2001**, 20, 460; e) W. Kaminsky, *Catalysis Today* **2000**, 62, 23; f) E. Y.-X. Chen, T. J. Marks, *Chem. Rev.* **2000**, 100, 1391.
- [30] G. A. Olah in *Lewis Acids in Organic Synthesis* (Ed. H. Yamamoto), Wiley-VCH, New York, **2000**.
- [31] A. Fukuoka, M. Ichikawa, J. A. Hriljac, D. F. Shriver, *Inorg. Chem.* **1987**, 26, 3643.
- [32] a) S. Velmathi, S. Swanalakshmi, S. Narasimhan, *Tetrahedron: Asymmetry* **2003**, 14, 113; b) N. Yamagiwa, S. Matsunaga, M. Shibasaki, *J. Am. Chem. Soc.* **2003**, 125, 16178.
- [33] D. Prim, B. Andrioletti, F. Rose-Munch, E. Rose, F. Couty, *Tetrahedron* **2004**, 60, 3325.
- [34] a) C. Darnault, A. Volbeda, E. J. Kim, P. Legrand, X. Vernède, P. A. Lindahl, J. C. Fontecilla-Camps, *Nat. Struct. Biol.* **2003**, 10, 271; b) T. I. Doukov, T. M. Iverson, J. Seravalli, S. W. Ragsdale, C. L. Drennan, *Science* **2002**, 298, 567; c) S. W. Ragsdale, M. Kumar, *Chem. Rev.* **1996**, 96, 2515.
- [35] N. Sträter, T. Klabunde, P. Tucker, H. Witzel, B. Krebs, *Science* **1995**, 268, 1489.
- [36] J. A. Tainer, E. D. Getzoff, J. S. Richardson, D. C. Richardson, *Nature* **1983**, 306, 284.
- [37] Edward Tripp in *Crowell's Handbook of Classical Mythology*, Thomas Y. Crowell Company, New York **1970**.
- [38] M. Pfeiffer, T. Stey, H. Jehle, B. Klüpfel, W. Malisch, V. Chandrasekhar, D. Stalke, *Chem. Commun.* **2001**, 337.
- [39] N. Kocher, D. Leusser, A. Murso, D. Stalke, *Chem. Eur. J.* **2004**, 10, 3622.
- [40] a) M. F. M. Al-Dulaymmi, P. B. Hitchcock, R. L. Richards, *J. Organomet. Chem.* **1988**, 338, C31; b) M. F. M. Al-Dulaymmi, A. Hills, P. B. Hitchcock, D. L. Hughes, R. L. Richards, *J. Chem. Soc., Dalton Trans.* **1992**, 241.
- [41] M. F. M. Al-Dulaymmi, D. L. Hughes, R. L. Richards, *J. Organomet. Chem.* **1992**, 424, 79.
- [42] S. S. Moore, G. M. Whitesides, *J. Org. Chem.* **1982**, 47, 1489.
- [43] A. Steiner, D. Stalke, *J. Chem. Soc., Chem. Commun.* **1993**, 444.
- [44] a) K. Issleib, A. Brack, *Z. Anorg. Allg. Chem.* **1957**, 292, 245; b) D. Redmore, *Chem. Rev.* **1971**, 71, 317; c) N. J. Curtis, R. S. Brown, *J. Org. Chem.* **1980**, 45, 4038.
- [45] Y. Uchida, Y. Takaya, S. Oae, *Heterocycles* **1990**, 30, 347.
- [46] F. H. Pinkerton, S. F. Thames, *Organosilicon Compounds* **1971**, 257.
- [47] G. Sheldrick in *SHELX-97 manual*, Göttingen **1997**.
- [48] R. S. Rowland, R. Taylor, *J. Phys. Chem.* **1996**, 100, 7384.

- [49] a) G. Becker, M. Schmidt, W. Schwarz, M. Westerhausen, *Z. Anorg. Allg. Chem.* **1992**, *33*, 608; b) G. Becker, W. Becker, M. Schmidt, W. Scharz, M. Westerhausen, *Z. Anorg. Allg. Chem.* **1991**, *7*, 605; c) G. Becker, H. P. Beck, *Z. Anorg. Allg. Chem.* **1977**, *430*, 77.
- [50] P. Rademacher in *Strukturen organischer Moleküle*, VCH, Weinheim **1987**.
- [51] M. Pfeiffer in *Reaktivität und Koordinationsverhalten ambidenter Ligandensysteme*, dissertation, Würzburg **2000**.
- [52] a) D. Leusser, J. Henn, N. Kocher, D. Stalke, B. Engels, *J. Am. Chem. Soc.* **2004**, *126*, 1781; b) N. Kocher, D. Leusser, A. Murso, D. Stalke, *Chem. Eur. J.* **2004**, *10*, 3622; c) D. Leusser, B. Walfort, D. Stalke, *Angew. Chem.* **2002**, *114*, 2183; *Angew. Chem. Int. Ed.* **2002**, *41*, 2079.
- [53] Dr. J. Henn, Würzburg, *private communication*, **2004**.
- [54] R. F. W. Bader in *Atoms In Molecules: A Quantum Theory*, Oxford University Press, Oxford, **1990**.
- [55] T. Steiner, *Angew. Chem.* **2002**, *114*, 50; *Angew. Chem. Int. Ed.* **2002**, *41*, 48.
- [56] J. Kroon, J. A. Kanters, *Nature* **1974**, *248*, 667.
- [57] A. L. Llamas-Saiz, C. Foces-Foces, O. Mo, M. Yañez, J. Elguero, *Acta Crystallogr.* **1992**, *48 B*, 700.
- [58] a) H. Gornitzka, D. Stalke, *Eur. J. Inorg. Chem.* **1998**, 311; b) A. Steiner, D. Stalke, *Organometallics* **1995**, *14*, 2422; c) A. Steiner, D. Stalke, *Chem. Commun.* **1993**, 444.
- [59] a) J. D. Hoefelmeyer, F. P. Gabbai, *Organometallics* **2002**, *21*, 982; b) P. C. Andrews, P. J. Duggan, M. Maguire, P. J. Nichols, *Chem. Commun.* **2001**, 53; c) W. Clegg, L. Horsburgh, S. T. Liddle, F. M. Mackenzie, R. E. Mulvey, A. Robertson, *J. Chem. Soc., Dalton Trans.* **2000**, 1225; d) K. Hensen, A. Lemke, T. Stumpf, M. Bolte, H. Fleischer, C. R. Pulham, R. O. Gould, S. Harris, *Inorg. Chem.* **1999**, *38*, 4700; e) T. Seifert, W. Storch, M. Vosteen, *Eur. J. Inorg. Chem.* **1998**, 1343; f) S. Harvey, J. D. Kildea, B. W. Skelton, A. H. White, *Aust. J. Chem.* **1992**, *45*, 135; g) C. L. Raston, W. T. Robinson, B. W. Skelton, C. R. Whitaker, A. H. White, *Aust. J. Chem.* **1990**, *43*, 1163; h) C. L. Raston, C. R. Whitaker, A. H. White, *J. Chem. Soc., Dalton Trans.* **1988**, 991; i) P. C. Blake, M. F. Lappert, J. L. Atwood, H. Zhang, *Chem. Commun.* **1988**, 1436; j) A. J. Banister, W. Clegg, W. R. Gill, *Chem. Commun.* **1987**, 850.
- [60] a) P. C. Andrews, P. J. Duggan, M. Maguire, P. J. Nichols, *Chem. Commun.* **2001**, 53; b) P. B. Hitchcock, M. F. Lappert, W.-P. Leung, D.-S. Liu, T. C. W. Mak, Z.-X. Wang, *J. Chem. Soc., Dalton Trans.* **1999**, 1263; c) M. Nieger, N. Poetschke, E. Niecke, K. Airola, *Z. Kristallogr.-New Cryst. Struct* **1997**, *212*, 247; d) K. W. Henderson, A. E. Dorigo, Q.-L. Liu, P. G. Williard, *J. Am. Chem. Soc.* **1997**, *119*, 11855; e) H. Chen, R. A. Bartlett, H. V. R. Dias, M. M. Olmstead,

- P. P. Power, *J. Am. Chem. Soc.* **1989**, *111*, 4338; f) D. Stalke, U. Klingebiel, G. M. Sheldrick, *Chem. Ber.* **1988**, *121*, 1457; g) D. Barr, W. Clegg, R. E. Mulvey, R. Snaith, D. S. Wright, *Chem. Commun.* **1987**, 716; h) R. A. Bartlett, H. V. R. Dias, H. Hope, B. D. Murray, M. M. Olmstead, P. P. Power, *J. Am. Chem. Soc.* **1986**, *108*, 6921; i) T. Fjeldberg, P. B. Hitchcock, M. F. Lappert, A. J. Thorne, *Chem. Commun.* **1984**, 822.
- [61] a) H. Gornitzka, D. Stalke, *Angew. Chem.* **1994**, *106*, 695; *Angew. Chem., Int. Ed. Engl.* **1994**, *33*, 693; b) H. Gornitzka, D. Stalke, *Organometallics* **1994**, *13*, 4398.
- [62] a) J. S. Bradley, F. Cheng, S. J. Archibald, R. Supplit, R. Rovai, C. W. Lehmann, C. Krüger, F. Lefebvre, *Dalton Trans.* **2003**, 1846; b) M.-A. Munoz-Hernandez, T. S. Keizer, P. Wie, S. Parkin, D. A. Atwood, *Inorg. Chem.* **2001**, *40*, 6782; c) J. S. Silveira, C. D. Abernethy, R. A. Jones, A. H. Cowley, *Chem. Commun.* **1999**, 1645; d) J. Niesmann, U. Klingebiel, C. Ropken, M. Noltemeyer, R. Herbst-Irmer, *Main Group Chem.* **1998**, *2*, 297; e) J. F. Janik, R. L. Wells, A. L. Rheingold, I. A. Guzei, *Polyhedron* **1998**, *17*, 4101; f) R. J. Wemshulte, P. P. Power, *Inorg. Chem.* **1998**, *37*, 2106; g) J. Niesmann, U. Klingebiel, M. Noltemeyer, R. Boese, *Chem. Commun.* **1997**, 365; h) M. G. Gardiner, G. A. Koutsantonis, S. M. Lawrence, F.-U. Lee, C. L. Raston, *Chem. Ber.* **1996**, *129*, 545; i) D. A. Atwood, D. Rutherford, *Main Group Chem.* **1996**, *1*, 431; j) P. J. Brothers, R. J. Wehmschulte, M. M. Olmstead, K. Ruhlandt-Senge, S. R. Parkin, P. P. Power, *Organometallics* **1994**, *13*, 2792; k) M. A. Petrie, K. Ruhlandt-Senge, P. P. Power, *Inorg. Chem.* **1993**, *32*, 1135; l) K. M. Waggoner, M. M. Olmstead, P. P. Power, *Polyhedron* **1990**, *9*, 257; m) G. M. Sheldrick, W. S. Sheldrick, *J. Chem. Soc. A* **1969**, 2279.
- [63] a) M. Pfeifer, A. Murso, L. Mahalakshmi, D. Moigno, W. Kiefer, D. Stalke, *Eur. J. Inorg. Chem.* **2002**, 3222; b) F. Thomas, S. Schulz, M. Nieger, *Eur. J. Inorg. Chem.* **2001**, 161; c) L. Miinea, S. Suh, S. G. Bot, J.-R. Liu, W.-K. Chu, D. M. Hoffman, *J. Mater. Chem.* **1999**, *9*, 929; d) J. Lewinski, P. Gos, T. Kopeck, J. Lipkowski, R. Luboradzki, *Inorg. Chem. Commun.* **1999**, *2*, 374; e) L. M. Engelhardt, P. C. Junk, C. L. Raston, B. W. Skelton, A. H. White, *J. Chem. Soc., Dalton Trans.* **1996**, 3297; f) M. R. Mason, J. M. Smith, S. G. Bott, A. R. Barron, *J. Am. Chem. Soc.* **1993**, *115*, 4971; g) M. D. Healy, J. W. Ziller, A. R. Barron, *J. Am. Chem. Soc.* **1990**, *112*, 2949; h) P. Pullmann, K. Hensen, J. W. Bats, *Z. Naturforsch.*, **1982**, *37B*, 1312.
- [64] M. Pfeiffer, F. Baier, T. Stey, D. Leusser, D. Stalke, B. Engels, D. Moigno, W. Kiefer, *J. Mol. Model.* **2000**, *6*, 299
- [65] U. Wannagat, H. Niederprüm, *Chem. Ber.* **1961**, *94*, 1540.

- [66] a) M. Westerhausen, *Inorg. Chem.* **1991**, *30*, 96; b) D. C. Bradley, M. B. Hursthouse, A. A. Ibrahim, K. M. A. Malik, M. Montevalli, R. Mösele, H. Powell, J. D. Runnacles, A. C. Sullivan, *Polyhedron* **1990**, *9*, 2959.
- [67] a) S. Neander, U. Behrens, *Z. Anorg. Allg. Chem.* **1999**, *625*, 1429; b) W. S. Rees Junior, O. Just, D. S. Van Derveer, *J. Mater. Chem.* **1999**, *9*, 249; c) J. L. Stewart, R. A. Andersen, *Polyhedron* **1998**, *17*, 953; d) S. Kühner, R. Kuhnle, H.-D. Hausen, J. Weidlein, *Z. Anorg. Allg. Chem.* **1997**, *623*, 25; e) M. A. Putzer, J. Magull, H. Goesmann, B. Neumüller, K. Dehnicke, *Chem. Ber.* **1996**, *129*, 1401; f) P. Miele, J. D. Foulon, N. Hovnanian, J. Durand, L. Cot, *Eur. J. Solid State Inorg. Chem.* **1992**, *29*, 573; g) P. B. Hitchcock, M. F. Lappert, L. J.-M. Pierssens, *Chem. Commun.* **1996**, 1189; h) M. A. Petrie, K. Ruhlandt-Senge, H. Hope, P. P. Power, *Bul. Soc. Chim. Fr.* **1993**, *130*, 851; i) P. Miele, J. D. Foulon, N. Hovnanian, J. Durand, L. Cot, *Eur. J. Solid State Inorg. Chem.* **1992**, *29*, 573; j) R. W. Chorley, P. B. Hitchcock, M. F. Lappert, W.-P. Leung, P. P. Power, M. M. Olmstead, *Inorg. Chim. Acta* **1992**, *198*, 203; k) J. J. Ellison, P. P. Power, S. C. Shoner, *J. Am. Chem. Soc.* **1989**, *111*, 8044; l) B. D. Murray, P. P. Power, *Inorg. Chem.* **1984**, *23*, 4584; m) T. Fjeldberg, H. Hope, M. F. Lappert, P. P. Power, A. J. Thorne, *Chem. Commun.* **1983**, 639; n) J. S. Gothra, M. B. Hursthouse, A. J. Welch, *Chem. Commun.* **1973**, 669.
- [68] H. C. Aspinall, P. A. Williams, J. Gaskell, A. C. Jones, J. L. Roberts, L. M. Smith, P. R. Chalker, G.-W. Critchlow, *Chem. Vap. Deposition* **2003**, *9*, 7.
- [69] R. L. LaDuca, P. T. Wolczanski, *Inorg. Chem.* **1992**, *31*, 1311.
- [70] a) P. W. Roesky, *Z. Anorg. Allg. Chem.* **2003**, *629*, 1881; b) M. R. Gagné, C. L. Stern, T. J. Marks, *J. Am. Chem. Soc.* **1992**, *11*, 275.
- [71] H. Bürger, W. Sawodny, U. Wannagat, *J. Organomet. Chem.* **1965**, *3*, 113.
- [72] Chemical Structural Database, release 5.25, January 2004.
- [73] a) D. R. Armstrong, G. C. Forbes, R. E. Mulvey, W. Clegg, D. M. Tocke, *J. Chem. Soc., Dalton Trans.* **2002**, 1656; b) M. H. Chisholm, J. Gallucci, K. Phomphrai, *Inorg. Chem.* **2002**, *41*, 2785; c) S. D. Bunge, O. Just, W. S. Rees Junior, *Polyhedron* **2001**, *20*, 823; d) X. Shen, X. Shi, B. Kang, Y. Liu, Y. Tong, H. Jiang, K. Chen, *Polyhedron* **1998**, *17*, 4049; e) M. A. Putzer, A. Dashti-Mommertz, B. Neumüller, K. Dehnicke, *Z. Anorg. Allg. Chem.* **1998**, *624*, 263; f) H. Schuhmann, J. Gottfriedsen, F. Girgsdies, *Z. Anorg. Allg. Chem.* **1997**, *623*, 1881.
- [74] a) E. Sahin, S. Die, A. Atac, S. Yurdakul, *J. Mol. Struct.* **2002**, *616*, 253; b) E. Katsoulakou, N. Lalioti, C. P. Raptopoulou, A. Terzis, E. Manessi-Zoupa, S. P. Perlepes, *Inorg. Chem. Commun.* **2002**, *5*, 719; c) J. Pang, E. J.-P. Marcotte, C. Seward, R. S. Brown, S. Wang,

- Angew. Chem.* **2001**, *113*, 4166; *Angew. Chem. Int. Ed.* **2001**, *40*, 4042; d) K.-Y. Ho, W.-Y. Yu, K.-K. Cheung, C.-M. Che, *J. Chem. Soc., Dalton Trans.* **1999**, 1581; e) C. A. Grapperhaus, T. Tuntulani, J. H. Reibenspies, M. Y. Darensbourg, *Inorg. Chem.* **1998**, *37*, 4052; f) J. Behm, S. D. Lotz, W. A. Herrmann, *Z. Anorg. Allg. Chem.* **1993**, *619*, 849; g) M. P. Byrn, C. J. Curtis, Y. Hsiou, S. I. Khan, P. A. Sawin, S. K. Tendick, A. Terzis, C. E. Strouse, *J. Am. Chem. Soc.* **1993**, *115*, 9480; h) R. Baggio, M. T. Garland, M. Perec, *J. Chem. Soc., Dalton Trans.* **1993**, 3367; i) M. A. Khan, D. G. Tuck, *Acta Crystallogr.* **1984**, *40C*, 60; j) W. S. Sheldrick, *Z. Naturforsch.* **1982**, *37B*, 653; k) H. Lynton, M. C. Sears, *Can. J. Chem.* **1971**, *49*, 3418.
- [75] R. D. Shannon, *Acta Crystallogr.* **1976**, *32A*, 751.
- [76] CRC Handbook of Chemistry and Physics, (ed. D. R. Lide), 75th Edition, CRC press, Boca Raton **1995**.
- [77] a) M. Fettouhi, B. E. Ali, A. M. El-Ghanam, S. Golhen, L. Ouahab, N. Daro, J.-P. Sutter, *Inorg. Chem.* **2002**, *41*, 3705; b) H. Zhu, M. Strobele, Z. Yu, Z. Wang, H. J. Meyer, X. You, *Inorg. Chem. Commun.* **2001**, *4*, 577; c) R. E. Marsh, *Acta Crystallogr.* **1995**, *51B*, 897; d) R. Baggio, A. Frigerio, E. B. Halac, D. Vega, M. Perec, *J. Chem. Soc., Dalton Trans.* **1992**, 549; e) P. F. Rodesiler, R. W. Turner, N. G. Charles, E. A. H. Griffith, E. L. Amma, *Inorg. Chem.* **1984**, *23*, 999; f) J. Dilen, A. T. H. Lenstra, J. G. Haasnoot, J. Reedijk, *Polyhedron* **1983**, *2*, 195; g) M. Cannas, G. Carta, A. Cristini, G. Marongiu, *J. Chem. Soc., Dalton Trans.* **1976**, 210.
- [78] a) A. Amoedo-Portela, R. Carballo, J. S. Casas, E. Garcia-Martinez, A. Sanchez-Gonzalez, J. Sordo, E. M. Vazquez-Lopez, *Polyhedron* **2003**, *22*, 1077; b) W. F. Wacholtz, J. T. Mague, *Acta Crystallogr.* **2001**, *57C*, 1400; c) J. Pickardt, B. Staub, *Z. Naturforsch.* **1999**, *54B*, 329; d) P. O'Brien, M. B. Hursthouse, M. Motevalli, J. R. Walsh, A. C. Jones, *J. Organomet. Chem.* **1993**, *449*, 1; e) M. J. Almond, M. P. Beer, M. G. B. Drew, D. A. Rice, *Organometallics* **1991**, *10*, 2072; f) R. A. Santos, E. S. Gruff, S. A. Koch, G. S. Harbison, *J. Am. Chem. Soc.* **1990**, *112*, 9257; g) G. W. Bushnell, S. R. Stobart, *Can. J. Chem.* **1980**, *58*, 574; h) R. Zannetti, *Gazz. Chim. Ital.* **1960**, *90*, 1428.
- [79] J. Emsley in *Die Elemente*, Walter de Gruyter, Berlin, New York **1994**.
- [80] M. J. S. Gynane, D. H. Harries, M. F. Lappert, P. P. Power, P. Rivière, M. Revière-Baudet, *J. Chem. Soc., Dalton Trans.* **1977**, 2004.
- [81] a) W.-P. Leung, H. L. Hou, H. Cheng, Q.-C. Yang, H.-W. Li, T. C. Mak, *J. Chem. Soc., Dalton Trans.* **2003**, 1505; b) M. Westerhausen, T. Bollwein, N. Makropoulos, S. Schneiderbauer, M. Suter, H. Nöth, M. Mayer, H. Piotrowski, K. Polborn, A. Pfitzner, *Eur. J. Inorg. Chem.* **2002**,

- 389; c) K. B. Aubrecht, M. A. Hillmyer, W. B. Tolman, *Macromolecules* **2002**, *35*, 644; d) Y. Ding, H. W. Roesky, M. Noltemeyer, H.-G. Schmidt, P. P. Power, *Organometallics* **2001**, *20*, 1190; e) A. E. Ayers, T. M. Klapötke, H. V. R. Dias, *Inorg. Chem.* **2001**, *40*, 1000; f) A. Akkari, J. J. Byrne, I. Saur, G. Rima, H. Gornitzka, J. Barrau, *J. Organomet. Chem.* **2001**, *622*, 190;
- g) C. J. Cardin, D. J. Cardin, S. P. Constantine, M. G. B. Drew, H. Rashid, M. A. Convery, D. Fenske, *J. Chem. Soc., Dalton Trans.* **1998**, 2749.
- [82] a) S. R. Foley, Y. Zhou, G. P. A. Yap, D. S. Richeson, *Inorg. Chem.* **2000**, *39*, 924; b) R. Fleischer, D. Stalke, *Organometallics* **1998**, *17*, 832; c) G. Ossig, A. Meller, S. Freitag, R. Herbst-Irmer, *Chem. Commun.* **1993**, 497; d) M. A. Paver, C. A. Russel, D. Stalke, D. S. Wright, *Chem. Commun.* **1993**, 1349; e) B. S. Jolly, M. F. Lappert, L. M. Engelhardt, A. H. White, C. L. Raston, *J. Chem. Soc., Dalton Trans.* **1993**, 2653; f) M. J. McGeary, K. Folting, K. G. Caulton, *Inorg. Chem.* **1989**, *28*, 4051; g) T. A. K. Al-Allaf, C. Eaborn, P. B. Hitchcock, M. F. Lappert, A. Pidcock, *Chem. Commun.* **1985**, 548; h) P. B. Hitchcock, M. F. Lappert, M. C. Misra, *Chem. Commun.* **1985**, 863.
- [83] a) O. Q. Munro, P. S. Madalla, R. A. F. Warby, T. B. Seda, G. Hearne, *Inorg. Chem.* **1999**, *38*, 4724; b) L. Chen, G.-B. Yi, L.-S. Wang, U. R. Dharmawardana, A. C. Dart, M. A. Khan, G. B. Richer-Addo, *Inorg. Chem.* **1998**, *37*, 4677; c) M. Mylrajan, L. A. Andersson, J. Sun, T. M. Loehr, C. S. Thomas, E. P. Sullivan Junior, M. A. Thomas, K. M. Long, O. P. Anderson, S. H. Strauss, *Inorg. Chem.* **1995**, *34*, 3953; d) L. Toupet, P. Sodano, G. Simenneaux, *Acta Crystallogr.* **1990**, *46C*, 1631; e) N. Li, P. Coppens, J. Landrum, *Inorg. Chem.* **1988**, *27*, 482; f) P. Sodano, G. Simenneaux, L. Toupet, *J. Chem. Soc., Dalton Trans.* **1988**, 2615; g) C. Lecomte, P. Coppens, R. Blessing, L. Li, *Acta Crystallogr.* **1984**, *40A*, C168; h) M. P. Byrn, B. A. Katz, N. L. Keder, K. R. Levan, C. J. Magurany, K. M. Miller, J. W. Pritt, C. E. Strouse, *J. Am. Chem. Soc.* **1983**, *105*, 4916; i) M. E. Kastner, W. R. Scheidt, T. Mashiko, C. A. Reed, *J. Am. Chem. Soc.* **1978**, *10*, 666; j) J. L. Hoard, G. H. Cohen, M. D. Glick, *J. Am. Chem. Soc.* **1967**, *89*, 1992.
- [84] a) Y. Ohgo, T. Ikeue, M. Nakamura, *Acta Crystallogr.* **1999**, *55C*, 1817; b) A. Haryono, K. Oyaizu, K. Yamamoto, J. Natori, E. Tschuchida, *Chem. Lett.* **1998**, 233; c) M. P. Byrn, C. E. Strouse, *J. Am. Chem. Soc.* **1991**, *113*, 2501; d) K. M. Miller, C. E. Strouse, *Acta Cryst.* **1984**, *40C*, 1324; e) K. M. Miller, C. E. Strouse, *Inorg. Chem.* **1982**, *23*, 2395; f) K. Anzai, K. Hatano, Y. J. Lee, W. R. Scheidt, *Inorg. Chem.* **1981**, *20*, 2337.

- [85] a) R. A. Ghiladi, R. M. Kretzer, I. Guzei, A. L. Rheingold, Y.-M. Neuhold, K. R. Hatwell, A. D. Zuberbuhler, K. D. Karlin, *Inorg. Chem.* **2001**, *40*, 5754; b) N. Li, Z. Su, P. Coppens, J. Landrum, *J. Am. Chem. Soc.* **1990**, *112*, 7294; c) S. H. Strauss, M. E. Silver, K. M. Long, R. G. Thompson, R. A. Hudgens, K. Spartalian, J. A. Ibers, *J. Am. Chem. Soc.* **1985**, *107*, 4207; d) J. P. Collman, J. L. Hoard, N. Kim, G. Lang, C. A. Reed, *J. Am. Chem. Soc.* **1975**, *97*, 2676.
- [86] a) T. Chishiro, Y. Shimazaki, F. Tani, Y. Tachi, Y. Naruta, S. Karasawa, S. Hayami, Y. Maeda, *Angew. Chem.* **2003**, *115*, 2894; *Angew. Chem. Int. Ed.* **2003**, *42*, 2788; b) L. Cheng, M. A. Khan, D. R. Powell, R. W. Taylor, G. B. Richter-Addo, *Chem. Commun.* **1999**, 1941; c) O. Q. Munro, W. R. Scheidt, *Inorg. Chem.* **1998**, *37*, 2308; d) G.-B. Yi, M. A. Khan, G. B. Richter-Addo, *Inorg. Chem.* **1995**, *34*, 5703; e) M. A. Phillippi, N. C. Baenziger, H. M. Goff, *Inorg. Chem.* **1981**, *20*, 3904.
- [87] B. M. L. Chen, A. Tullinsky, *J. Am. Chem. Soc.* **1972**, *94*, 4144.
- [88] M. Sono, M. P. Roach, E. D. Coulter, J. H. Dawson, *Chem. Rev.* **1996**, *96*, 2841.
- [89] S. D. Kinzie, M. Thevis, K. Ngo, J. Whitelegge, J. A. Loo, M. M. Abu-Omar, *J. Am. Chem. Soc.* **2003**, *125*, 4710.
- [90] R. N. Austin, H.-K. Chang, G. J. Zylstra, J. T. Groves, *J. Am. Chem. Soc.* **2000**, *122*, 11747.
- [91] E. I. Solomon, T. C. Brunold, M. I. Davis, J. N. Kemsley, S.-K. Lee, N. Lehnert, F. Neese, A. J. Skulan, Y.-S. Yang, J. Zhou, *Chem. Rev.* **2000**, *100*, 235.
- [92] W. Weiss, R. Schlögel, *Topics in Catalysis* **2000**, *13*, 75.
- [93] J. Palágyi, L. Markó, *J. Organomet. Chem.* **1982**, *236*, 343.
- [94] M. L. Kantam, B. Kavita, F. Figueras, *Catal. Lett.* **1998**, *51*, 113.
- [95] Y. Yamashita, M. Ueno, Y. Kuriyama, S. Kobayashi, *Adv. Synth. Catal.* **2002**, *344*, 929.
- [96] G. A. Olah, S. J. Kuhn, B. A. Hardie, *J. Am. Chem. Soc.* **1964**, *6*, 1055.
- [97] a) H. Roussel, B. Mehlomakulu, F. Belhadj, E. van Stehen, J. M. M. Miller, *J. Catal.* **2002**, *205*, 97; b) M. D. Allen, G. J. Hutchings, M. Bowker, *Appl. Catal.*, **2001**, *217A*, 33.
- [98] R. B. King, *J. Organomet. Chem.* **1999**, *586*, 2.
- [99] K.-D. Jung, O.-S. Joo, S.-H. Cho, S.-H. Han, *Appl. Catal.*, **2003**, *240A*, 235.
- [100] M. M. Olmstead, P. P. Power, S. C. Shoner, *Inorg. Chem.* **1991**, *30*, 2547.
- [101] a) M.-S. Zhou, S.-P. Huang, L.-H. Wenig, W.-H. Sun, D.-S. Liu, *J. Organomet. Chem.* **2003**, *665*, 237; b) A. Panda, M. Stender, R. J. Wright, M. M. Olmstead, P. Klavins, P. P. Power, *Inorg. Chem.* **2002**, *41*, 3909; c) B. Vendemiati, G. Prini, A. Meetsma, B. Hessen, J. H. Teuben, O. Traverso, *Eur. J. Inorg. Chem.* **2001**, 707; d) R. W. Saalfrank, O. Struck, K. Nun,

- C.-J. Lurz, R. Harbig, K. Peters, H. G. von Schnering, E. Bill, A. X. Trautwein, *Chem. Ber.* **1992**, *125*, 2331.
- [102] a) M.-S. Zhou, S.-P. Huang, L.-H. Wenig, W.-H. Sun, D.-S. Liu, *J. Organomet. Chem.* **2003**, *665*, 237; b) K. Rachlewicz, L. Latos-Grazynski, E. Vogel, Z. Ciunik, L. B. Jerzykiewicz, *Inorg. Chem.* **2002**, *41*, 1979; c) C. Da Silva, L. Bonomo, E. Solari, R. Scopelliti, C. Floriani, N. Re, *Chem. Eur. J.* **2000**, *6*, 4518; d) C. Weymann, A. A. Danopoulos, G. Wilkinson, T. K. N. Sweet, M. B. Hursthouse, *Polyhedron* **1996**, *15*, 3605; e) R. W. Saalfrank, O. Struck, K. Nunn, C.-J. Lurz, R. Harbig, K. Peters, H. G. von Schnering, E. Bil, A. X. Trautwein, *Chem. Ber.* **1992**, *125*, 2331; f) M. P. Byrn, C. J. Curtis, I. Goldberg, Y. Hsiou, S. I. Khan, P. A. Sawin, S. K. Tendick, C. E. Strouse, *J. Am. Chem. Soc.* **1991**, *113*, 6549; g) M. Tahiri, P. Doppelt, J. Fischer, R. Weiss, *Inorg. Chim. Acta* **1987**, *127*, L1; h) J. F. Kimer, W. Dow, W. R. Scheidt, *Inorg. Chem.* **1976**, *15*, 1685.
- [103] K. F. Tesh, B. D. Jones, T. P. Hanusa, J. C. Huffmann, *J. Am. Chem. Soc.* **1992**, *114*, 6590.
- [104] S. Wingerter, M. Pfeiffer, F. Baier, T. Stey, D. Stalke, *Z. Anorg. Allg. Chem.* **2000**, *626*, 1121.
- [105] F. T. Edelmann, F. Pauer, M. Wedler, D. Stalke, *Inorg. Chem.* **1992**, *31*.
- [106] G. Rabe, H. Heise, G. P. A. Yap, L. M. Liable-Sands, I. A. Guzei, A. L. Rheingold, *Inorg. Chem.* **1998**, *37*, 4235.
- [107] a) S. Kato, N. Kitaoka, O. Niyomura, Y. Kitoh, T. Kanda, M. Ebihara, *Inorg. Chem.* **1999**, *38*, 496; b) M. Niemeyer, P. P. Power, *Inorg. Chem.* **1996**, *35*, 7264.
- [108] a) T. Rottgers, W. S. Sheldrick, *Z. Anorg. Allg. Chem.* **2002**, *628*, 1305; b) M. Arca, F. Demartin, F. A. Devillanova, A. Garau, F. Isaia, V. Lippolis, G. Verani, *Inorg. Chem.* **1998**, *37*, 4164; c) H.-J. Drexler, H. Reinke, H.-J. Holdt, *Z. Anorg. Allg. Chem.* **1998**, *624*, 1376.
- [109] a) B. H. Weiller, *J. Am. Chem. Soc.* **1992**, *114*, 10910; b) R. N. Perutz, J. J. Turner, *J. Am. Chem. Soc.* **1975**, *97*, 4791.
- [110] a) W. Strohmeier, *Angew. Chem.* **1964**, *76*, 873; *Angew. Chem., Int. Ed. Engl.* **1964**, *3*, 730; b) W. Strohmeier, C. Barbeau, *Z. Naturforsch.* **1962**, *17B*, 848.
- [111] a) J. E. Coleman, K. E. Dulaney, A. A. Bengali, *J. Organomet. Chem.* **1999**, *572*, 65; b) P.-F. Yang, G. K. Yang, *J. Am. Chem. Soc.* **1992**, *114*, 6937.
- [112] a) B. Crocock, C. Long, R. A. Howie, *Acta Crystallogr.* **1992**, *48C*, 1004; b) H. G. Alt, H. E. Engelhardt, E. Steinlein, R. D. Rogers, *Organometallics* **1988**, *344*, 321; c) W. A. Herrmann, B. Koumbouris, E. Herdtweck, M. L. Ziegler, P. Weber, *Chem. Ber.* **1987**, *120*, 931; d) H. Lang, G. Mohr, O. Scheidesteger, G. Huttner, *Chem. Ber.* **1985**, *118*, 574; e) D. Wormsbächer, F. Edelmann, U. Behrens, *Chem. Ber.* **1982**, *115*, 1332; f) S. Hoehne, E.

- Lindner, J.-P. Gumz, *Chem. Ber.* **1978**, *111*, 3818; g) C. Barbeau, R. J. Dubey, *Can. J. Chem.* **1973**, *51*, 3684; h) C. Barbeau, K. S. Dichmann, L. Ricard, *Can. J. Chem.* **1973**, *51*, 3027.
- [113] J. Cowie, E. J. M. Hamilton, J. C. V. Laurie, A. J. Welch, *J. Organomet. Chem.* **1990**, *394*, 1.
- [114] a) B. Ahrens, J. M. Cole, J. P. Hickey, J. N. Martin, M. J. Mays, P. R. Raithby, S. J. Teat, A. D. Woods; *J. Chem. Soc., Dalton Trans.* **2003**, 1389; b) Y. Ortin, A. Sournia-Saquet, N. Lugan, R. Mathieu, *Chem. Commun.* **2003**, 1060; c) D. Gorz, H. Pritzkow, W. Siebert, *Eur. J. Inorg. Chem.* **2003**, 2783; d) W.-Y. Wong, W.-K. Wong, C. Sun, W.-T. Wong, *J. Organomet. Chem.* **2000**, *612*, 160; e) J. Grobe, W. Gola, D. Le Van, B. Krebs, M. Lage, *Organometallics* **1998**, *17*, 5717; f) B. Schiemenz, G. Huttner, L. Zsolnai, P. Kircher, T. Diercks, *Chem. Ber.* **1995**, *128*, 187; g) C. M. Lukehart, G. P. Torrence, J. V. Zeile, *J. Am. Chem. Soc.* **1975**, *97*, 6903; h) A. Mawby, G. E. Pringle, *J. Inorg. Nucl. Chem.* **1972**, *34*, 877.
- [115] a) F. Hartl, T. Mahabiersing, P. Le Floch, F. Mathey, L. Ricard, P. Rosa, S. Zalis, *Inorg. Chem.* **2003**, *42*, 4442; b) F. Liang, H. W. Schmalte, T. Fox, H. Berke, *Organometallics* **2003**, *22*, 3382; c) J. C. Röder, F. Meyer, E. Kaifer, *Angew. Chem.* **2002**, *114*, 2414; *Angew. Chem. Int. Ed.* **2002**, *41*, 2304; d) G. Kong, G. N. Harakas, B. R. Whittlesey, *J. Am. Chem. Soc.* **1995**, *117*, 3502; e) A. Alvanipour, H. Zhang, J. L. Atwood, *J. Organomet. Chem.* **1988**, *358*, 295; f) J. M. Boncella, R. A. Andersen, *Inorg. Chem.* **1984**, *23*, 432.
- [116]a) M. Herberhold, W. Milius, A. Pfeifer, *Z. Naturforsch.* **2003**, *58B*, 1; b) G. Renner, G. Huttner, P. Rutsch, *Z. Naturforsch.* **2001**, *56B*, 1328; c) T. Groer, M. Scheer, *Z. Anorg. Allg. Chem.* **2000**, *626*, 1211; d) J.-A. Kim, T.-M. Chung, Y. K. Chung, J.-H. Jung, S. W. Lee, *J. Organomet. Chem.* **1995**, *486*, 211; e) H. Werner, M. A. Tena, N. Mahr, K. Peters, H.-G. von Schnering, *Chem. Ber.* **1995**, *128*, 41; f) M. E. Bar, S. K. Smith, B. Spencer, L. F. Dahl, *Organometallics* **1991**, *10*, 3983; g) R. C. Hynes, K. F. Preston, J. J. Springs, A. J. Williams, *Organometallics* **1990**, *9*, 2298.
- [117] a) K. Müller-Buschbaum, G. B. Deacon, C. M. Forsyth, *Eur. J. Inorg. Chem.* **2002**, 3172; b) K. P. C. Vollhardt, J. K. Cammack, A. J. Matzger, A. Bauer, K. B. Capps, C. D. Hoff, *Inorg. Chem.* **1999**, *38*, 2624; c) Z.-Z. Zhang, J.-K. Zhang, W.-D. Zhang, H.-P. Xi, H. Cheng, H. G. Wang, *J. Organomet. Chem.* **1996**, *515*, 1; d) A. Recknagel, A. Steiner, S. Brooker, D. Stalke, F. T. Edelman, *Chem. Ber.* **1991**, *124*, 1373; e) J. S. Merola, R. A. Gentile, G. B. Ansell, M. A. Modrick, S. Zentz, *Organometallics* **1982**, *1*, 1731; f) D. M. Hamilton Junior, W. S. Willis, G. D. Stucky, *J. Am. Chem. Soc.* **1981**, *103*, 4255; g) A. J. Conway, G. J. Gainsford, R. R. Schrieke, J. D. Smith, *J. Chem. Soc., Dalton Trans.* **1975**, 2499.

- [118] a) E. Leiner, O. Hampe, M. Scheer, *Eur. J. Inorg. Chem.* **2002**, 584; b) B. Neumüller, W. Petz, *Organometallics* **2001**, 20, 163; c) A. Fretzen, A. Ripa, R. Liu, G. Bernardinelli, E. P. Kundig, *Chem. Eur. J.* **1998**, 4, 251; d) V. Balema, H. Goesmann, E. Matern, G. Fritz, *Z. Anorg. Allg. Chem.* **1996**, 622, 35; e) W.-T. Wong, W.-K. Wong, *Acta Crystallogr.* **1994**, 50C, 1404; f) R. H. Heyn, J. C. Huffmann, K. G. Caulton, *New. J. Chem.* **1993**, 17, 797; g) S.-G. Shyu, M. Calligaris, G. Nardin, A. Wojcicki, *J. Am. Chem. Soc.* **1987**, 109, 3617.
- [119] W. A. Schenk, *J. Organomet. Chem.* **1979**, 179, 253.
- [120] a) B. Hoge, T. Herrmann, C. Thosen, I. Pantenburg, *Inorg. Chem.* **2003**, 42, 3623; b) G. Manzoni de Oliveira, M. Horner, M. Seiffert, A. J. Bortoluzzi, *J. Chem. Cryst.* **1999**, 29, 193; c) T. Campbell, A. M. Gibson, H. Hart, S. D. Orchard, S. J. J. A. Pope, G. Reid, *J. Organomet. Chem.* **1999**, 592, 296; d) J. E. Davis, M. J. Mays, P. R. Raithby, G. P. Shields, P. K. Tomkin, *Chem. Commun.* **1996**, 2051; e) M. G. Davidson, A. J. Edwards, M. A. Paver, P. R. Raithby, C. A. Russel, A. Steiner, K. L. Verhorevoort, D. S. Wright, *Chem. Commun.* **1995**, 1989; f) D. Dou, M. Westerhausen, G. L. Wood, G. Linti, E. N. Duesler, H. Nöth, R. T. Paine, *Chem. Ber.* **1993**, 126, 379; g) G. L. Geoffroy, W. C. Mercer, R. R. Whittle, L. Marko, S. Vastag, *Inorg. Chem.* **1985**, 24, 3771; h) D. A. DuBois, E. N. Duesler, R. T. Paine, *Organometallics* **1984**, 3, 1913.
- [121] J. H. Reibenspies, D. Darensbourg, E. Atnip, *Z. Kristallogr.* **1994**, 209, 759.
- [122] a) N. H. T. Huy, C. Compain, L. Ricard, F. Mathey, *J. Organomet. Chem.* **2002**, 650, 57; b) N. Hofmann, C. Wismach, P. G. Jones, R. Streubel, N. H. T. Huy, F. Mathey, *Chem. Commun.* **2002**, 454; c) R. Streubel, S. Priemer, F. Ruthe, P. G. Jones, *Eur. J. Inorg. Chem.* **2000**, 1253; d) H. Wilkens, O. Ostrowski, J. Jeske, F. Ruthe, P. G. Jones, R. Streubel, *Organometallics* **1999**, 18, 5627; e) R. Streubel, A. Ostrowski, H. Wilkens, F. Ruthe, J. Jeske, P. G. Jones, *Angew. Chem.* **1997**, 109, 409; *Angew. Chem. Int. Ed. Engl.* **1997**, 36, 378; f) H. Westermann, M. Nieger, E. Niecke, J.-P. Majoral, A.-M. Caminade, R. Mathieu, E. Irmer, *Organometallics* **1989**, 8, 244.
- [123] a) A. O. Youssef, M. M. H. Khalil, R. M. Ramadan, A. A. Soliman, *Transition Met. Chem.* **2003**, 28, 331; b) L.-F. Tang, W.-L. Jia, X.-M. Zhao, P. Yang, J.-T. Wang, *J. Organomet. Chem.* **2002**, 658, 198; c) L.-F. Tang, Z.-H. Wang, J.-F. Chai, X.-B. Leng, J.-T. Wang, H.-G. Wang, *J. Organomet. Chem.* **2002**, 642, 179; d) S. Benet, S. M. Brown, G. Conole, M. Kessler, S. Rowling, E. Sinn, S. Woodward, *J. Chem. Soc., Dalton Trans.* **1995**, 367; e) P. N. W. Baxter, J. A. Connor, J. D. Wallis, D. C. Povey, A. K. Powell, *Polyhedron* **1992**, 11, 1771;

- f) N. S. Magomedova, G. K.-I. Magomedov, *Metallorg. Khim. (Russ.)* **1990**, 3, 129; g) R. A. Howie, G. Izquierdo, G. P. McQuillan, *Inorg. Chim. Acta* **1983**, 72, 165.
- [124] P. J. Walsh, F. J. Hollander, R. G. Bergmann, *J. Am. Chem. Soc.* **1988**, 110, 8729.
- [125] a) S. Blair, K. Izod, R. W. Harrington, W. Clegg, *Organometallics* **2003**, 22, 302; b) G. W. Rabe, I. A. Guzei, A. L. Rheingold, *Inorg. Chim. Acta* **2001**, 315, 254; c) G. Becker, E. Eschbach, O. Mundt, M. Reti, E. Niecke, K. Issbemer, M. Nieger, V. Thelen, H. Nöth, R. Waldhor, M. Schmidt, *Z. Anorg. Allg. Chem.* **1998**, 624, 469; d) M. Driess, H. Pritzkow, *Z. Anorg. Allg. Chem.* **1996**, 622, 1524; e) M. Andrianarison, D. Stalke, U. Klingebiel, *J. Organomet. Chem.* **1990**, 381, C38; f) M. Andrianarison, U. Klingebiel, D. Stalke, G. M. Sheldrick, *Phosphorus, Sulfur, Silicon, Relat. Elem.* **1989**, 46, 183; g) E. Hey, C. L. Raston, B. W. Skelton, A. H. White, *J. Organomet. Chem.* **1989**, 362, 1; h) R. E. Mulvey, K. Wade, D. R. Armstrong, G. T. Walker, R. Snaith, W. Clegg, D. Reed, *Polyhedron* **1987**, 6, 987; i) R. A. Bartlett, M. M. Olmstead, P. P. Power, G. A. Sigel, *Inorg. Chem.* **1987**, 26, 1941.
- [126] a) G. Müller, H.-P. Abicht, M. Waldkirchner, J. Lachmann, M. Lutz, M. Winkler, *J. Organomet. Chem.* **2001**, 622, 121; b) A. Pape, M. Lutz, G. Müller, *Angew. Chem.* **1994**, 106, 2375; *Angew. Chem. Int. Ed. Engl.* **1994**, 33, 2281; c) H. H. Karsch, K. Zellner, S. Gamper, G. Müller, *J. Organomet. Chem.* **1991**, 414, C39; d) H. H. Karsch, K. Zellner, P. Mikulcik, J. Lachmann, G. Müller, *Organometallics* **1990**, 9, 190; e) L. T. Byrne, L. M. Engelhardt, G. E. Jacobsen, W.-P. Leung, R. I. Papasergio, C. L. Raston, B. W. Skelton, P. Twiss, A. H. White, *J. Chem. Soc., Dalton Trans.* **1989**, 105; f) H. H. Karsch, A. Appelt, B. Deubelly, K. Zellner, J. Riede, G. Müller, *Z. Naturforsch.* **1988**, 43B, 1416; g) L. M. Engelhardt, J. McB. Harrowfield, M. F. Lappert, I. A. MacKinnon, B. H. Newton, C. L. Raston, B. W. Skelton, A. H. White, *Chem. Commun.* **1986**, 846.
- [127] A. Murso in *Electronic response of phosphorus and nitrogen based ligands on metal coordination*, dissertation, Würzburg **2004**.
- [128] C. Boga, A. C. Bonamartini, L. Forlanui, E. Mezzina, A. Pompa, P. Sgarabotto, D. Spinelli, P. E. Todesco, *J. Chem. Res. (M)* **1999**, 1737.
- [129] D. Stalke, *Chem. Soc. Rev.* **1998**, 27, 171.
- [130] a) H. Hope, *Acta Crystallogr.* **1988**, 44B, 22; b) T. Kottke, D. Stalke, *J. Appl. Crystallogr.* **1993**, 26, 615; c) T. Kottke, R. J. Lagow, D. Stalke, *J. Appl. Crystallogr.* **1996**, 29, 465.
- [131] Bruker, SMART-NT, Data Collection Software, Version 5.6, Bruker Analytical X-ray Instruments Inc., Madison, Wisconsin (USA), **2000**.

-
- [132] Bruker, SAINT-NT, Data Reduction Software, Version 6.045, Bruker Analytical X-ray Instruments Inc., Madison, Wisconsin (USA), 1999.
- [133] G. M. Sheldrick, SADABS 2.06 and 2.10, Empirical Absorption Correction Program, University of Göttingen (Germany), **2001**.
- [134] Bruker, SHELX-TL; Version 6, Bruker Analytical X-ray Instruments Inc., Madison, Wisconsin (USA), **2000**.
- [135] a) H. D. Flack, *Acta Cryst.* **1983**, 39A, 876. b) G. Bernadinelli, H. D. Flack, *Acta Cryst.* **1985**, 41A, 500.

Publications

1. R. v. Bülow, S. Deuerlein, T. Stey, R. Herbst-Irmer, H. Gornitzka, D. Stalke: **N-Aryl Anions: Half way between Amides and Carbanions**, *Z. Naturforsch.* **2004**, *59B*, 1471-1479.
2. L. Lameyer, O. A. Salah, S. Deuerlein, T. Stey, D. Stalke: **Structural Variances in the Homologous Series of Alkaline Earth Metallated Octamethylcyclotetrasilazandiides**, *Z. Anorg. Allg. Chem.* **2004**, *630*, 1801-1806.
3. J. F. Bickley, M. C. Copey, J. C. Jeffery, A. P. Leedham, C. A. Russell, D. Stalke, A. Steiner, T. Stey, S. Zacchini: **From the tetra(amino) phosphonium cation, $[P(NHPh)_4]^+$, to the tetra(imino) phosphate trianion, $[P(NPh)_4]^{3-}$, two-faced ligands that bind anions and cations**, *Dalton Trans.* **2004**, *7*, 989-995.
4. M. Bolboaca, T. Stey, A. Murso, D. Stalke, W. Kiefer: **P-N Bond Length Alterations Monitored by Infrared Absorption and Fourier Transform Raman Spectroscopy in Combination with Density Functional Theory Calculations**, *Appl. Spectros.* **2003**, *57*, 970-976.
5. V. Singh, S. Lahiri, V. V. Kane, T. Stey, D. Stalke: **Efficient Stereoselective Synthesis of Novel Steroid-Polyquinane Hybrids**, *Organic Letters* **2003**, *5*, 2199-2202.
6. F. Baier, Z. Fei, H. Gornitzka, A. Murso, S. Neufeld, M. Pfeiffer, I. Rüdener, A. Steiner, T. Stey, D. Stalke: **Phosphane- and phosphorane Janus Head ligands in metal coordination**, *J. Organomet. Chem.* **2002**, *661*, 111-127.
7. S. Wingerter, M. Pfeiffer, T. Stey, M. Bolboaca, W. Kiefer, V. Chandrasekhar, D. Stalke: **The Iminophosphorane $Ph_3P:NSiMe_3$ as a Synthone for M-Caryl σ Bonds (M = In, Fe, Ge) Implementing Imino Sidearm Donation**, *Organometallics* **2001**, *20*, 2730-2735.

8. M. Pfeiffer, T. Stey, H. Jehle, B. Klüpfel, W. Malisch, D. Stalke, V. Chandrasekhar: **Site-selective coordination behavior of the Py₂P⁻-anion: the N-C-P-allylic system as σ - and π -donor in [(PMDETA)Cs{(μ -PPy)Py}]₂ and as a μ^2 - σ -phosphorus-donor in [Cp(CO)₂Fe]₂{(μ -P)Py₂}[BMe₄], *Chem. Commun.* **2001**, 4, 337-338.**
9. S. Wingerter, M. Pfeiffer, A. Murso, C. Lustig, T. Stey, V. Chandrasekhar, D. Stalke: **Phosphorus-Based Ambidentate Chelating Ligands: Pyridyl-N- and Imido-N-Metal Coordination in the Py₂P(NSiMe₃)₂ Anion, *J. Am. Chem. Soc.* **2001**, 123, 1381-1388.**
10. M. Pfeiffer, F. Baier, T. Stey, D. Leusser, D. Stalke, B. Engels, D. Moigno, W. Kiefer: **Di(2-pyridyl)-Amides and -Phosphides: Syntheses, Reactivity, Structures, Raman-Experiments and Calculations, *J. Mol. Mod.* **2000**, 6, 299-311.**
11. S. Wingerter, M. Pfeiffer, F. Baier, T. Stey, D. Stalke: **Synthese and Reaktivität von Diphenylphosphanyltrimethylsilylamin Ph₂PN(H)SiMe₃, *Z. Anorg. Allg. Chem.* **2000**, 626, 1121-1130.**

Book contribution

T. Stey, D. Stalke: **Lead structures in lithium organic chemistry** in *The Chemistry of Organolithium Compounds* (Eds. Rappaport, Zvi; Marek, Ilan) John Wiley and Sons, Chichester, **2004**.

Lebenslauf

Persönliche Daten

Name Thomas Josef Stey
Geburtsdatum 11. Mai 1975
Geburtsort Fulda
Familienstand ledig

Schulbildung

1981-1985 Grundschule Eichenzell
1985-1994 Freiherr-vom-Stein-Schule Fulda; Gymnasium der Stadt Fulda
Abschluss: Allgemeine Hochschulreife

1994-1995 Grundwehrdienst

Studium

WS 1995-Ws 2000 Studium der Biologie und Chemie für das Lehramt an Gymnasien
1999 - 2000 Schriftliche Hausarbeit im Arbeitskreis Prof. Dr. D. Stalke am Institut für Anorganische Chemie der Universität Würzburg mit dem Titel:
„Reaktivität und Koordinationsverhalten von Diphénylphosphanyltrimethylsilylamin und Di(2-pyridyl)phosphan“

Herbst 2000 Studienabschluss: Erstes Staatsexamen

Januar – Februar 2001 nebenberuflicher wissenschaftlicher Mitarbeiter am Institut für Anorganische Chemie der Universität Würzburg

seit März 2001 Arbeiten an der Dissertation mit dem Thema:
“Di(benzothiazol-2-yl)phosphane – Studies on a *Janus Head* Ligand“
seit März 2001 wissenschaftlicher Mitarbeiter am Institut für Anorganische Chemie der Universität Würzburg

Erklärung

Hiermit erkläre ich an Eides statt, dass ich die Dissertation „Di(benzothiazol-2-yl)phosphane – Studies on a *Janus Head* Ligand“ selbständig angefertigt habe und keine anderen als die von mir angegebenen Quellen und Hilfsmittel benutzt habe.

Ich erkläre außerdem, dass diese Dissertation weder in gleicher oder anderer Form bereits in einem anderen Prüfungsverfahren vorgelegen hat.

Ich habe früher außer den mit dem Zulassungsgesuch urkundlich vorgelegten Graden keine weiteren akademischen Grade erworben oder zu erwerben versucht.

Würzburg, 23.12.2004

(Thomas Stey)